

Molecular mechanisms of chronic experimental inflammatory renal diseases

PhD dissertation

Gábor Kökény M.D.

Semmelweis University
PhD School of Basic Medical Sciences



Supervisors: László Rosivall M.D., Ph.D., Med. habil., D.Sc. Med.
Péter Hamar M.D., Ph.D.

Official opponents: Ágnes Haris M.D., Ph.D., head physician
Attila Szabó M.D., Ph.D., assistant professor

Chair of the Exam Committee: György Reusz M.D., Ph.D., Med. habil.,
D.Sc. Med.

Members of the Exam Committee: András Szabó M.D., Ph.D., D.Sc. Med.
József Balla M.D., Ph.D., Med. habil.,
D.Sc. Med.

Budapest
2007

TABLE OF CONTENT

TABLE OF CONTENT	2
ABBREVIATIONS	4
1. INTRODUCTION	6
1.1 INTRODUCTION A (RENAL FIBROSIS).....	6
1.1.1 Hemodynamic factors in glomerulosclerosis	7
1.1.2 Podocytes play a key role in the progression	7
1.1.3 Oxidative stress in chronic renal disease	10
1.1.4 The role of RAS on progression – more complex than we thought?	10
1.1.5 Kidney damage activates the sympathetic nervous system.....	12
1.1.6 Therapeutical possibilities to halt progression	13
1.2. INTRODUCTION B (LUPUS NEPHRITIS)	14
1.2.1. Epidemiology of lupus	14
1.2.2. Clinical and histological features of lupus nephritis	15
1.2.3. Experimental model of SLE	16
1.2.4. Pathogenesis of lupus nephritis	17
1.2.5. Does pregnancy increase the risk for flares in lupus patients?	18
2. HYPOTHESIS AND SPECIFIC AIMS	20
2.1 HYPOTHESIS AND SPECIFIC AIMS A (RENAL FIBROSIS)	20
2.2 HYPOTHESIS AND SPECIFIC AIMS B (LUPUS NEPHRITIS).....	21
3. MATERIALS AND METHODS	22
3.1 EXPERIMENTAL DESIGN A (RENAL FIBROSIS).....	22
3.1.1 Animal model	22
3.1.2 Operative procedures	23
3.1.3 Measurement of albuminuria and blood pressure.....	24
3.1.4 Perfusion harvest and tissue preparation.....	25
3.1.5 Immunohistological methods	26
3.1.6. Semiquantitative examination of the kidney - indices of renal damage	27
3.1.7 Glomerular morphometry and stereology	29
3.1.8 Real-Time RT-PCR.....	32
3.1.9 Data analysis	32

3.2 EXPERIMENTAL DESIGN B (LUPUS NEPHRITIS)	34
3.2.1. <i>MRL/lpr lupus prone mice</i>	34
3.2.2. <i>Assesment of kidney function and blood pressure</i>	35
3.2.3. <i>Flow cytometry</i>	36
3.2.4. <i>ELISA of plasma INF-γ and anti-dsDNA autoantibody levels</i>	36
3.2.5. <i>Histology of the kidneys</i>	37
3.2.6. <i>Renal IgG and C3 deposition, and CD3⁺ infiltration</i>	37
3.2.7. <i>Real-time RT-PCR</i>	38
3.2.8. <i>Data analysis</i>	39
4. RESULTS	40
4.1 RESULTS A (RENAL FIBROSIS)	40
4.1.1. <i>Animal data</i>	40
4.1.2. <i>Albuminuria and blood pressure</i>	41
4.1.3. <i>Indices of renal damage</i>	41
4.1.4. <i>Stereologic measurements</i>	44
4.1.5. <i>Cellular analysis of the glomerulus</i>	45
4.1.6. <i>Immunohistochemistry and real-time PCR analysis of the kidneys</i>	46
4.2 RESULTS B (LUPUS NEPHRITIS)	50
4.2.1. <i>Survival and kidney function</i>	50
4.2.2. <i>Lymphoproliferation and anti-dsDNA levels</i>	54
4.2.3. <i>IFN-γ production in the blood and the kidney</i>	54
5. DISCUSSION	56
5.1 DISCUSSION A (RENAL FIBROSIS)	56
5.2 DISCUSSION B (LUPUS NEPHRITIS)	62
6. CONCLUSIONS	68
6.1 CONCLUSIONS A (RENAL FIBROSIS)	68
6.2 CONCLUSIONS B (LUPUS NEPHRITIS)	68
7. ABSTRACT	69
8. MAGYAR NYELVŰ ÖSSZEFOGLALÓ	70
9. REFERENCES	71
10. LIST OF PUBLICATIONS	91
11. ACKNOWLEDGEMENTS	94

ABBREVIATIONS

ACE	angiotensin converting enzyme
ACEI	angiotensin converting enzyme inhibitor
AngII	angiotensin II
ANOVA	analysis of variance
AT1	angiotensin receptor type-1
BUN	blood urea nitrogen
BW	body weight
C3	complement-3
CRF	chronic renal failure
ECM	extracellular matrix
eNOS	endothelial nitric oxide synthase (NOS-3)
ESRD	end-stage renal disease
dsDNA	double-stranded DNA
IFN- γ	interferon gamma
IgG	immunoglobulin-gamma
IDI	interstitial damage index
IL-4	interleukin-4
IL-10	interleukin-10
GAPDH	glyceraldehyde 3-phosphate dehydrogenase
GN	glomerulonephritis
GS	glomerulosclerosis
GSI	glomerosclerosis index
H&E	hematoxylin-eosin
KW	kidney weight
M	multiparous
mV_{Glom}	mean glomerular volume
NO	nitric oxide
nNOS	neuronal nitric oxide synthase (NOS-1)
N_{Glom}	total number of glomeruli per kidney
Q	Quinapril

PAS	Periodic-acid Schiff
R	Rhizotomy
RAS	renin-angiotensin system
ROS	reactive oxygen species
RT-PCR	reverse transcriptase polymerase chain reaction
SD	standard deviation
SLE	systemic lupus erythematoses
SNS	sympathetic nervous system
SNX	subtotal nephrectomy
ssDNA	single-stranded DNA
TGF- β	transforming growth factor-beta
Th1	T-helper type 1
Th2	T-helper type 2
TDI	tubular damage index
VDI	vascular damage index
V	virgin
V_{Matrix}	volume of mesangial matrix relative to glomerular tuft volume
V_{Tuft}	glomerular tuft volume

1. INTRODUCTION

End-stage renal disease (ESRD) is a major and increasing health care problem worldwide [1]. ESRD develops secondary to various renal diseases such as diabetes mellitus, essential hypertension, or systemic lupus erythematosus (SLE). The number of ESRD patients is growing exponentially, and the average annual incidence of ESRD reached about 135 new patients per million of population in Europe [2], but even higher in the United States [3].

1.1 INTRODUCTION A (RENAL FIBROSIS)

Progressive renal fibrosis is the final common pathway of chronic renal diseases of different etiologies, being one of the major challenges in nephrology. This nonspecific process continues even when the initial insult is no longer present. Regardless of the primary cause, the common underlying histological lesions comprise tubulointerstitial fibrosis, tubular atrophy and glomerulosclerosis (GS). Although many details of GS were revealed in the last decades, and several molecular mechanisms have been proven to play a major role in the development and progression, its pathogenesis is still poorly understood and successful, curative therapies are still not available.

Glomerulosclerosis consists of the uncontrolled accumulation of extracellular matrix (including type IV collagen and fibronectin) in glomeruli and tubulointerstitium, and obliteration of the capillary filter that contribute to the loss of renal function [4, 5]. Factors known to promote sclerosis include high intraglomerular capillary pressure [6, 7], mechanical stress and glomerular hypertrophy [8, 9] and the excessive passage of plasma proteins through the glomerular capillary filter [10].

During the process of GS and renal scarring, infiltrating inflammatory cells seem to play a major pathogenic role, by producing transforming growth factor- β (TGF- β , a major pro-fibrogenic growth factor) and inducing oxidative stress. Furthermore, elevation of angiotensin II (AngII) aggravates inflammation through stimulating cytokine synthesis and oxidative stress.

1.1.1 Hemodynamic factors in glomerulosclerosis

Shear stress induced by elevated intraglomerular capillary pressure leads to injury, activation, and dysfunction of the glomerular endothelium, which in turn initiates glomerular microinflammation, activating macrophages and mesangial cells with proliferation and dysfunction of mesangial cells. Communication between cells depends on the release of a wide range of cytokines and growth factors [11]. Transforming growth factor β_1 (TGF- β_1) is a profibrotic growth factor that lies in a final common pathway for multiple causes of GS. Under the influence of TGF- β_1 , mesangial cells regress to an embryonic mesenchymal phenotype (mesangioblasts) capable of excessive production of extracellular matrix (ECM) leading to mesangial expansion, an early sign of glomerulosclerosis [12].

1.1.2 Podocytes play a key role in the progression

Podocytes are the most differentiated cells within the glomerulus. Synthesizing various components of the glomerular basement membrane and the slit diaphragm, they are crucially involved in the maintenance of the glomerular filtration barrier [13]. Mechanical damage to the podocytes may be a key factor in the initiation and progression of GS (for a schematic diagram, see Figure 1), either as a result from direct injury or from the reduction in the cell density due to compensatory glomerular hypertrophy [8, 10, 14]. Podocytes are stretched in progressive GS which leaves areas of denuded glomerular basement membrane and favours the formation of adhesion to the Bowman's capsule [13].

It has been recently demonstrated that mechanical stress increases AngII synthesis in cultured podocytes [15]. Activation of podocytes and elevated AngII levels trigger mesangial cells to further express TGF- β_1 . Moreover, it has been shown that TGF- β_1 synthesis by podocytes is stimulated by protein overload [16].

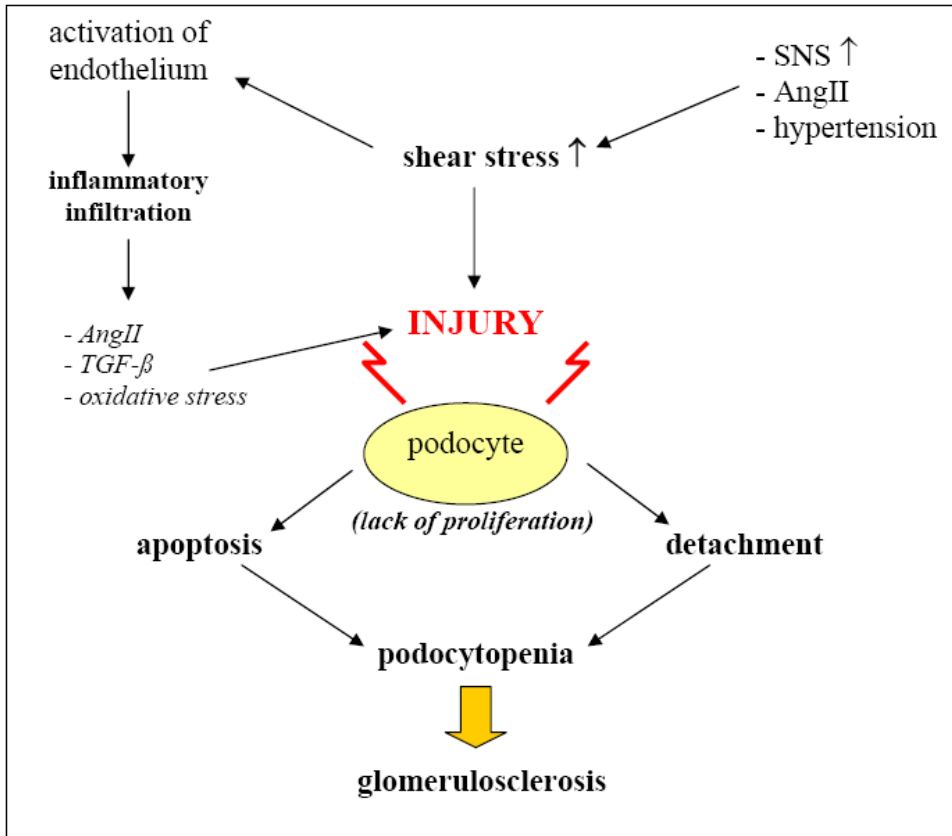


Figure 1. The contribution of podocyte injury to glomerulosclerosis. After shear stress injury due to overactivation of the sympathetic nervous system (SNS), AngII or hypertension, podocytes undergo apoptosis and/or detachment. These events lead to a decrease in podocyte number (podocytopenia), which contributes to the development of progressive glomerulosclerosis. Apoptosis results from increased TGF- β , AngII and oxidative stress. In contrast to other glomerular cells, podocytes are highly differentiated cells and do not typically proliferate in response to injury, therefore they cannot replace those podocytes lost by apoptosis and detachment.

After experimental renal mass reduction, proteinuria leads to the loss of podocyte architecture and fusion of foot processes, then cells undergo effacement of foot processes, cell detachment from the basement membrane and tuft adhesion to the Bowman capsule (Figure 2.) [17, 18]. Low protein diet is proven to retard glomerular damage after subtotal nephrectomy (SNX) [19], supporting the deteriorating effects of protein overload. These factors altogether result in excessive synthesis of glomerular extracellular matrix and eventual GS [20-22]

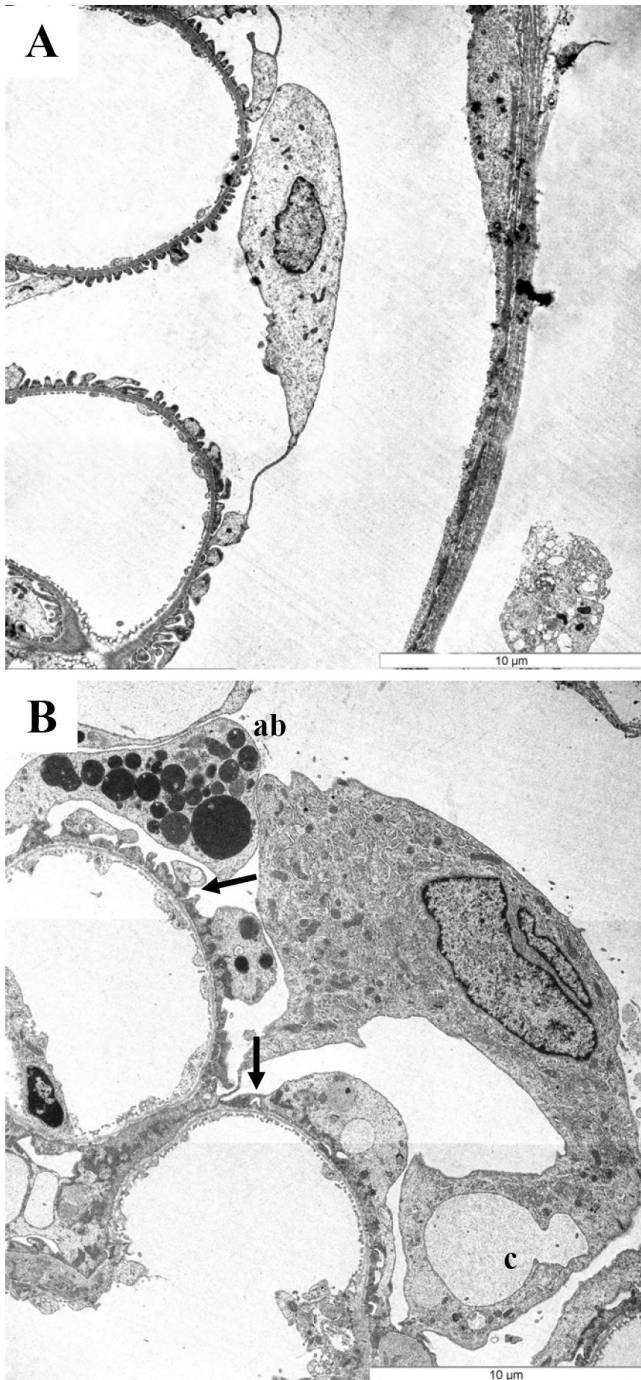


Figure 2. Typical electronmicroscopic findings of podocyte ultrastructure in healthy and damaged podocytes. Ultrathin slides from our experiment, stained with uranyl acetate and lead citrate. Magnifications x4000 (bar: 10 μ m). A: Podocytes of sham operated rat have normal size and ultrastructure. B: SNX rat, showing enlarged podocyte, fusion of foot processes (arrows), and signs of degeneration (formation of apoptotic bodies (ab) and pseudocysts (c)).

1.1.3 Oxidative stress in chronic renal disease

Evidence of increased oxidative stress have also been documented in several animal models of renal failure [23-25]. Interstitial recruitment of inflammatory leukocytes and myofibroblasts occur early in renal fibrosis, and recruited macrophages secrete many pro-fibrogenic molecules. The generation of free radicals (reactive oxygen and nitrogen species) is considered to be an initiator of inflammatory response in the kidney [26]. Reactive oxygen species (ROS) generated in uremia avidly react with nitric oxide (NO), and its widespread sequestration as nitrated proteins (nitrotyrosine) [27] necessarily limits the bioavailability of NO in animals with chronic renal failure (CRF). In this regard, several studies have pointed to the possible reduction of NO production in CRF. For instance, renal insufficiency has been shown to cause accumulation of endogenous NOS inhibitors (methylated L-arginine derivatives and guanidino compounds), which can potentially depress NO production in CRF [28, 29]. In addition, rats with renal mass reduction show reduced urinary excretion of NO metabolites (total nitrates + nitrites) and diminished histochemically detectable NOS in the remnant kidney, suggesting reduced renal NO production [30].

1.1.4 The role of RAS on progression – more complex than we thought?

The blood pressure-independent role of the renin-angiotensin system (RAS) in progressive deterioration of renal function has been firmly established in animal experiments [31, 32]. The RAS is a coordinated hormonal cascade leading to the production of angiotensin II, controlling cardiovascular, renal, and adrenal function that governs fluid and electrolyte balance, and arterial pressure [33]. The classical RAS begins with the biosynthesis of renin, a 340-amino-acid glycoprotein, in juxtaglomerular cells [34]. Following its release, renin cleaves the decapeptide angiotensin I from the circulating glycoprotein angiotensinogen. Angiotensinogen synthesized in the liver provides the majority of systemic circulating angiotensin peptides, but angiotensinogen is also synthesized and constitutively released in other tissues including the heart, vasculature, kidneys, and adipose tissue. Angiotensin converting enzyme (ACE) cleaves a dipeptide sequence from angiotensin I to yield the octapeptide angiotensin II (AngII) [34]. Ang II mediates most of its effects via binding to G-protein-coupled AT1 receptors. In the kidney, angiotensin II binding to AT1

receptors (present in nephron segments, interstitial cells, and the vasculature) stimulates vasoconstriction, sodium and water retention, and several non-hemodynamic responses. Within the glomerulus, AngII reduces the ultrafiltration coefficient and modulates glomerular capillary permselectivity leading to proteinuria, initiating and increasing subsequent tubulointerstitial injury [31, 35]. AngII is a growth factor of glomerular mesangial and endothelial cells, tubular epithelial cells and fibroblasts [36, 37]. Ang II causes cellular hypertrophy [37], induces apoptosis [38], increases the expression of TGF- β and stimulates synthesis of extracellular matrix proteins such as collagen type IV [36, 37]. Ang II also acts as proinflammatory cytokine and promotes oxidative stress [37, 39].

Accumulating evidence suggest that local renin-angiotensin systems (RAS) exist in various tissues, among others in the kidney. A complete RAS has been localized in proximal tubular cells [40]. It has been recently suggested that local RAS may play an important role in the progression of kidney fibrosis, as renal injury activates the local RAS directly or indirectly [37]. Moreover, differentiated human podocytes express all RAS components required to generate AngII [41]. This RAS appears to be involved not only in physiological mechanisms, but also in pathological responses [15, 42]. For example, AngII blockade reduces experimentally induced tubulointerstitial fibrosis [43]. Moreover, AngII itself can induce the apoptosis of podocytes [44]. Therefore, inhibition of AngII effects in podocytes might lower podocyte tonus, decrease the rate of apoptosis, and increase glomerular permselectivity [45]. Indeed, a recent study demonstrated that ACE inhibition had a protective effect in a mouse model of focal segmental GS, when started early after podocyte injury [46].

In renal injury, the induction of RAS leads to the aggravation of kidney disease, therefore RAS was early recognized as a potential therapeutical target. The angiotensin converting enzyme (ACE) inhibitors have been available for use in the blockade of the renin-angiotensin system for two decades [47]. Both clinical and experimental studies have proven the beneficial effect of ACE inhibition (ACEI) or angiotensin receptor blockade on the progression of chronic kidney disease [48-52]. It has been recently shown that ACEI treatment prevents the early onset of proteinuria in experimental diabetes, independently of systemic or glomerular hemodynamic changes [53]. Clinical studies have impressively demonstrated markedly reduced proteinuria and progression

of glomerular disease [48, 51, 52, 54] in patients treated with ACEI. Moreover, limited evidence from experimental and clinical studies show, that ACEI may even cause regression of renal disease [55].

1.1.5 Kidney damage activates the sympathetic nervous system

An influence of sympathetic innervation on renal function was first recognized in 1859 when Claude Bernard observed that in anaesthetized anuric dogs urine flow resumed when splanchnic nerves were cut [56]. The kidney is also a source of signals that modulate the activity of the sympathetic nervous system (SNS). The effects can be broadly categorized into: (1) effects on renal haemodynamics, i.e. alpha-1-adrenergic receptor mediated vasoconstriction [57], (2) stimulation of renin release from the juxtaglomerular granular cells mediated via beta-1-adrenergic mechanisms [58], and (3) direct stimulation of transtubular sodium reabsorption mediated by alpha-2- and alpha-1-adrenergic receptors located in the peritubular membranes [59]. There is also experimental evidence that the SNS modulates extracellular matrix production of mesangial cells via alpha-1-adrenergic receptors [60].

Renal chemoreceptors [61], and mechanoreceptors are known to mediate, at least in part, the blood pressure increase in response to elevated pressures in the renal vein, the ureter and interlobular arteries [62]. Such afferent signals may be important in the diseased kidney, which activates the sympathetic nervous system (SNS) via afferent signals [63].

The first clinical study showing sympathetic overactivity in kidney disease in diabetic patients was provided by the microneurographic study of Converse and colleagues in 1992 [64]. Campese and colleagues [65, 66] documented activation of the SNS in models of renal damage. Dorsal rhizotomy abrogated ascending stimulatory signals emanating from the kidney. This intervention reduced elevation of blood pressure and attenuated renal disease progression. In addition, blockade of sympathetic activity either by a central sympathetic inhibitor [67] or a beta-blocker [68] attenuated progression independently of blood pressure both in the remnant kidney model and in clinical studies [69]. However, it has remained undecided whether the beneficial effect of reduced sympathetic activity is mediated via reducing renin secretion from juxtaglomerular apparatus or whether the effect is renin-independent. The systemic

inhibition of SNS may lead to confounding effects, as inhibition of the efferent renal sympathetic nerves may increase renal resistance [70] and cause denervation natriuresis [71] leading to a rebound activation of RAS. Thus, the selective inhibition of renal afferent sympathetic signals by rhizotomy was preferred as a clearer experimental alternative.

Recently, several studies have emphasized the role of the SNS in progressive kidney disease. Hendel and colleagues demonstrated that renal denervation attenuated the hypertensive effects of AngII infusion in the rat [72]. In CRF patients, blockade of AngII also reduced the sympathetic overactivity [73]. Moreover, a cross-sectional study concluded that elevated adrenergic activity correlates with albuminuria, independent of blood pressure [74].

1.1.6 Therapeutical possibilities to halt progression

It has recently been emphasized that none of the current interventions including blockade of the RAS and of the SNS is completely effective in constantly abrogating progression [75]. On one hand, the activity of systemic and local RAS does not change in parallel. Acute, systemic administration of ACEI results in almost complete inhibition of systemic AngII formation, but affects intrarenal AngII production little or not at all [76]. On the other hand, although acute ACEI treatment markedly decrease circulating AngII levels [77], a rebound rise in AngII in patients taking ACE inhibitors over long periods is often observed [78, 79]. A recent experiment showed the beneficial effect of locally delivering angiotensin receptor blockers in rat kidneys [42] but this interesting therapeutical approach is definitely not suitable in the everyday treatment of CRF patients.

Moreover, other enzymes in the kidney, such as chymases, convert angiotensin I to AngII. Chymases are serine proteases which were first described in cardiovascular tissues [80]. ACE inhibitors does not inhibit chymase activity, and recent clinical data demonstrate that the expression of chymases in kidneys of diabetic patients correlated with ECM deposition [81].

It has therefore been argued that the interventional strategies of the future will presumably be combined interventions, e.g. RAS plus SNS or aldosterone receptor blockade [82, 83].

1.2. INTRODUCTION B (LUPUS NEPHRITIS)

Systemic lupus erythematosus (SLE or lupus) is a chronic, generalized autoimmune disease characterized by pathogenic autoantibody overproduction [84]. The autoantibodies are produced against a variety of self components (ssDNA, dsDNA, nucleoproteins, etc) [85]. It is a complex disease with very heterogenous manifestations, affecting several organs, primarily the kidneys, skin, joints and the cardiovascular system.

The first known descriptions of SLE originate in the middle ages. The term “lupus” is attributed to the 12th century physician Rogerius, who used it to describe the classic malar rash. It was Móric Kaposi who recognized the systemic manifestations of the disease in 1872. In 1894, quinine was first reported to be an effective therapy for the disease. Four years later, the combination of salicylates with quinine was noted to have a superior effect. This was the best available treatment to patients until the middle of the twentieth century, when Hench discovered the efficacy of corticosteroids in the treatment of SLE.

1.2.1. Epidemiology of lupus

The reported prevalence of SLE in the population varies between 20-130 cases per 100,000 in recent studies (reviewed in reference [86]). Due to improved detection of mild disease, the incidence has nearly tripled in the last 40 years [87]. Estimated incidence rates in USA and Europe range from about 2 to 5 per 100,000 per year [88]. Lupus can occur at any age, but 65% of patients with SLE have disease onset between the ages of 16 and 55 and it is rare before puberty. There is an increased frequency of SLE among women that is thought to be due to an estrogen hormonal effect [89]. This estrogen effect is reflected by the female:male ratio of SLE in different age groups. The ratio rises from 3:1 in children up to 10-15:1 in adults but falls back to approximately 8:1 in patients over 60 years of age [90]. These data are in accordance with murine models of lupus, in which estrogens are precipitating factors in the development of the disease.

The course of SLE is unpredictable, with periods of illness (called flares) alternating with remission. The progressive deterioration of kidney function and cardiovascular complications [91] are the most common cause of death among SLE patients. Lupus nephritis is a serious disease whose prognosis can usually be improved dramatically by treatment, but for which the treatment is potentially toxic (mainly corticosteroids and other immunosuppressants), prolonged, complex and difficult to carry out. Thus, renal involvement is associated with significant mortality and morbidity.

1.2.2. Clinical and histological features of lupus nephritis

Among SLE patients, up to 60% of adults and 80% of children may develop overt renal abnormalities. The dominant feature of renal lupus is proteinuria, present in almost every patient. This can be accompanied by microscopic hematuria in about 80% of the cases, while hypertension occurs in only 20-50% of the patients [92].

Glomerular histology shows mononuclear cell infiltration, and lesions vary from focal segmental glomerulonephritis to diffuse membranous glomerulonephritis (see Figure 3), accompanied by glomerular IgG deposition.

Tubulointerstitial damage accompanies glomerular lesions, characterized by cellular infiltrates of monocytes and T-cells which may also invade the tubules ("tubulitis") contributing to the impairment of renal function. Immune complexes in the tubular basement membrane are present in about 50% of patients with nephritis [92].

Lupus nephritis is a severe disease, but now only 10-15% of patients develop end-stage kidney failure [93]. The overall five-year survival of patients with lupus nephritis increased to 82% in the 90's compared to 44% between 1950-1969 [92].

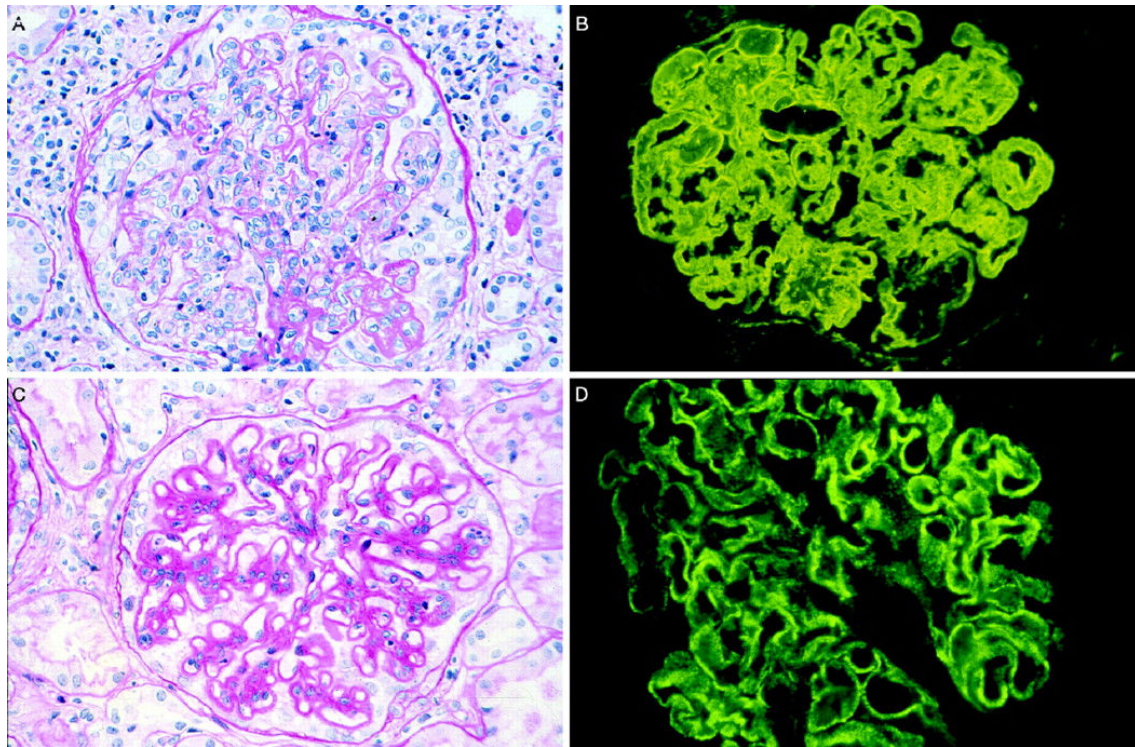


Figure 3. Photomicrograph of human kidney biopsies with A: focal segmental GN and C: diffuse membranous GN (PAS, 200x), B, D: immunofluorescence micrograph illustrating massive glomerular IgG deposition (260x). Source: ref. [92]

1.2.3. Experimental model of SLE

Mouse models of SLE have been studied over 3 decades. Spontaneous SLE in murine models is characterized by high levels of serum autoantibodies (eg. against double-stranded DNA (dsDNA)). The mice also develop severe, progressive glomerulonephritis with glomerular immune complex deposits, mesangial expansion, glomerulosclerosis, interstitial fibrosis and fatal renal failure. The MRL/MpJ-*Fas*^{lpr} mouse strain (lpr) is a well known model of murine systemic autoimmunity [94]. MRL/lpr mice spontaneously develop a severe autoimmune disease, which shares most clinical signs and symptoms of human lupus. The lpr mutation is characterized by the insertion of an endogenous retrovirus, a 5.3 kb early transposone element (ETn) into the second intron of the TNF-R superfamily Fas gene, causing a defective Fas molecule [95]. As the mutant Fas molecule cause a severe defect in apoptosis, lpr mice have severe lymphoproliferation characterized mainly by CD4⁻ CD8⁻ B220⁺ double negative (DN) T-lymphocytes of thymic origin [96]. The abnormal DN cells are proposed to be self-reactive, accompanied by abnormalities in lymphocyte function [97]. LPR mice

suffer from massive autoantibody production starting at 8 weeks of age [98-100]. Lymphoproliferation of DN cells leads to generalized lymphadenomegalia, splenomegalia and organ infiltrates, which include kidneys [101], lacrimal glands [102], salivary glands [103, 104], thyroid gland [105] and skin [106]. Apart from cell infiltrates, the autoantibody production starts at 8 weeks of age, leading to systemic autoimmunity, with rheuma factor (RF), anti-dsDNA, anti-Sm titers rising with age [98, 107]. The resulting systemic autoimmunity cause severe glomerulonephritis at 5-7 months of age, pathologically characterized by IgG deposition (IgG2a, IgG2b, IgG3) and mononuclear cell infiltrates [101, 108]. Joint lesions also develop similarly to human rheumatoid arthritis [109]. Skin pathology is characterized by immunoglobulin deposition and cellular infiltration [110]. Skin lesions mimic those in human lupus [106].

1.2.4. Pathogenesis of lupus nephritis

Despite an increasing amount of experimental and clinical data on SLE, the pathogenesis of lupus nephritis is still poorly understood. As DNA was one of the earliest identified autoantigens in human SLE [111, 112] and immunoglobulins eluted from diseased human kidneys were shown to react with DNA, this led to the hypothesis that deposition of immune complexes and the subsequent inflammatory response are the pathologic basis of kidney injury. Immune complexes directly activate resident renal cells through Toll-like receptors to produce inflammatory mediators. Cytokines can induce endothelial cells to express adhesion molecules, recruiting inflammatory cells after immune complex deposition [113].

Although autoantibody deposition in the kidneys is an important pathogenic component of SLE nephritis, it is increasingly recognized that cellular immunity also contributes to renal disease. Some data suggest that not anti-dsDNA antibodies, but kidney reactive T-cells are required for the pathology of lupus nephritis. Indeed, T-cell infiltration in kidneys of mouse models correlates with the severity of nephritis [114]. Chan and colleagues demonstrated that MRL/lpr mice develop glomerulosclerosis and interstitial nephritis even in the absence of immunoglobulins [115], showing that deposition of immune complexes are not required for the development of chronic kidney disease. In another study, deletion of kidney reactive T-cells protected MRL/lpr

mice from fatal glomerulonephritis [116]. Moreover, some SLE patients develop a non-inflammatory podocyte damage (“lupus podocytopathy”) mediated by soluble inflammatory mediators [117]. All these data provide a growing evidence that kidney reactive T-cells and signals from the innate immune system may contribute to the pathogenesis of lupus nephritis. This hypothesis may explain the heterogeneity of renal manifestations in lupus patients.

Cytokines may play a major role in the regulation of SLE. Murine as well as human lupus is associated with a predominant proinflammatory cytokine response. In MRL/lpr mice IFN- γ may play a dominant role in the pathogenesis of kidney disease [118]. In this model elevated IFN- γ and significant reduction in IL-4 and IL-10 cytokine production of CD4⁺ lymphocytes has been demonstrated [118]. IFN- γ gene deficiency in MRL/lpr mice dramatically reduced glomerulonephritis [119], thus increased their survival period. Recent data indicate that human lupus nephritis is also associated with IFN- γ upregulation and IL-4, IL-10 downregulation [120, 121].

IL-10 is a major cytokine with a strong stimulatory effect on B-lymphocyte functions [122] and a major anti-inflammatory / immunosuppressive cytokine inhibiting cellular infiltration [123, 124]. IL-10 overproduction has been demonstrated to be associated with autoantibody production in lupus patients [125] while IL-10 serum level has been correlated to the activity of the disease [126]. However, in the MRL/lpr model, IL-10 had suppressive effects against T-lymphocyte driven autoimmunity [127].

1.2.5. Does pregnancy increase the risk for flares in lupus patients?

The majority of SLE patients are female in childbearing age [128]. Thus, understanding the role of pregnancy in SLE is of high relevance and would help to elaborate therapeutic strategies for women suffering from autoimmunity and who have still a desire to procreate.

Although there has been some debate in published works as to whether flares in lupus activity actually occur during pregnancy, the present consensus is that pregnancy could exacerbate lupus activity [129]. Flares arise in about 30–60% of pregnant patients with lupus, 11% suffering a major reactivation requiring hospitalization and high doses of prednisone [130, 131]. Flares in renal disease activity are more common in those who had active disease at conception than in those in remission [131]. However, literature

data are still controversial, as some reports describe an adverse effect of gestation on disease progression [132, 133], while others claim that pregnancy have no effect on lupus nephritis [134-136]. Latter clinical reports are supported by studies on the NZB/W F1 mouse model of lupus, where only mild or no increase of disease activity was shown due to pregnancy [137, 138].

Pregnancy induces a complex and only a partially understood change in cytokine production. Both murine and human pregnancies are proposed to be associated with a shift towards anti-inflammatory cytokine predominance [139-141], with decreased proinflammatory cytokine production [133, 142, 143]. Although this shift in cytokine balance inhibits some (cellular) immune functions, it may stimulate humoral immunity. It has been early shown that estrogens can augment the number of CD8⁺ cells [144] but high levels of estrogens enhance the production of IL-10 in CD4⁺ lymphocytes, thus shifting the balance toward anti-inflammatory cytokine production [145].

2. HYPOTHESIS AND SPECIFIC AIMS

2.1 HYPOTHESIS AND SPECIFIC AIMS A (RENAL FIBROSIS)

Blockade of the renin-angiotensin system or the sympathetic nervous system were shown to ameliorate progression in experimental models of kidney fibrosis. However, none of the monotherapies could constantly ameliorate the progression of chronic renal failure. Therefore, we hypothesized that the combination of ACE inhibition using quinapril and selective sympathetic denervation by dorsal rhizotomy is superior to the respective single interventions in the rat model of progressive glomerulosclerosis.

Our specific aims were:

- 1) analyze the progression of glomerulosclerosis using the model of renal mass reduction in rats treated with quinapril, rhizotomy, and both;
- 2) assess and compare the histological indices of renal damage (glomerulosclerosis index, tubulointerstitial and vascular damage);
- 3) using stereological techniques, investigate changes in glomerular capillarisation, glomerular cell density, and ultrastructure of podocytes, mesangial cells and endothelial cells;
- 4) analyze the expression of fibrosis-related molecules (TGF- β 1, collagen IV);
- 5) to investigate the role of nitros-oxidative stress (as a marker of inflammation) in our model, we aimed to assess the expression of nitric oxide synthase isoforms (eNOS and nNOS) and nitrotyrosine using molecular methods.

2.2 HYPOTHESIS AND SPECIFIC AIMS B (LUPUS NEPHRITIS)

Based on the observed shift to systemic anti-inflammatory immune response in pregnancy, it has been suggested that pregnancy may have a beneficial influence on systemic autoimmunity. We hypothesized that, due to the cytokine shift observed in normal mice, pregnancy may delay the progression of kidney disease in lupus prone MRL/lpr mice.

Our specific aims were:

- 1) as lupus is a chronic disease, we aimed to develop a model of long-term pregnancy-induced systemic cytokine shift, using MRL/lpr mice having 3 consecutive pregnancies (multiparous mice);
- 2) evaluate the progression of systemic autoimmunity (anti-dsDNA titers, lymphoproliferation and serum IFN- γ levels) in multiparous mice and age-matched non-pregnant (virgin) control females;
- 3) compare survival data of multiparous and virgin mice;
- 4) evaluate the progression of lupus nephritis by monthly determination of proteinuria (to estimate kidney function) and by standard histology after harvest;
- 5) compare the severity of immunocomplex mediated glomerular damage by immunohistochemistry for IgG and C3 deposits;
- 6) assess local pro-inflammatory and anti-inflammatory cytokine expression in the kidneys (IFN- γ , IL-4 and IL-10) using molecular methods.

3. MATERIALS AND METHODS

3.1 EXPERIMENTAL DESIGN A (RENAL FIBROSIS)

3.1.1 *Animal model*

We used subtotal (5/6) nephrectomy (SNX), a well established model of renal fibrosis. The process of renal fibrosis and CRF has been well characterized in that model, and the signs of renal injury develop in a relative short period of time [146].

Twenty-week-old male Sprague-Dawley rats (Charles River, Germany) weighing 350-400 g were used in our study. Sprague-Dawley strain was chosen as numerous studies demonstrated, that the results obtained with these rats correlated well with human results, whereas other strains (eg. Wistar-Furth) proved to be insensitive towards SNX induced renal fibrosis [147].

The animals were housed at the Central Animal Facility (Zentrales Tierlabor) at the Ruperto Carola University of Heidelberg under standard conditions: 12 hours dark-light cycle (light on 08:00-20:00 h), 55% relative humidity, $22 \pm 1^\circ\text{C}$. The rats had free access to water and laboratory chow (Altromin standard diet, Lage, Germany). The rats were housed in separate polycarbonate cages (Tecniplast, Buguggiate, Italy), and received drinking water from dark brown flasks to avoid light-induced dissociation of quinapril. All procedures were in accordance with the guidelines of the Institutional Animal Care and Use Committee.

After one week acclimatization period, rats were randomly divided into 8 groups (n=12-17/group, see Table 1): 4 groups of animals underwent SNX, and 4 groups were sham operated and served as controls (sham). In both SNX and sham groups, half of the animals were subjected to bilateral dorsal rhizotomy (see below) or sham rhizotomy. In the groups of SNX and sham-operated animals, with or without rhizotomy, half of the animals received 10 mg/kg body weight/day quinapril dissolved in drinking water for 16 weeks. This dose has been reported to cause effective suppression of the RAS. The control animals received tap water.

The amount of consumed water was controlled once a week and the drug concentration in the drinking fluid was adjusted accordingly.

Table 1. Experimental groups.

Group	Kidney operation	Quinapril (Q) or Rhizotomy (R) intervention
Sham	Sham	Water (-) -
Sham + R		+
Sham + Q		Quinapril (Q) -
Sham + R + Q		+
SNX	SNX	Water (-) -
SNX + R		+
SNX + Q		Quinapril (Q) -
SNX + R + Q		+

3.1.2 Operative procedures

Animals were anesthetized using a combination of ketamine and xylazine. Ketamine (Ketanest®, Parke-Davies, Germany) was administered at a dose of 100 mg/kg body weight, with xylazine (Rompun®, Bayer AG, Leverkusen, Germany) at 2 mg/kg body weight. The anesthetics were injected intramuscularly into conscious rats; the needed level of narcosis was achieved after 5-10 min, and lasted for about 60 min. All animals were weighed before narcosis.

SNX was performed as described previously [67, 68]. In brief, retroperitoneum and the right kidney was reached through a midline laparotomy. The right kidney was exposed and carefully decapsulated, avoiding damage to the adrenal. Then, the renal vein and artery and the ureter were carefully ligated together at the hilus using a 3-0 absorbable prolene suture (Ethicon, Johnson and Johnson, Germany), and the rat was uninephrectomized, i.e. the right kidney was removed and weighed. The muscle and skin were closed together using 3-0 Vicryl suture (Ethicon). Eight days later, 2/3 of the left kidney cortex (which undergone compensatory hypertrophy) was removed. After decapsulating the kidney, the upper and lower poles were removed by resecting 66% cortical tissue, leaving the pelvis and the hilus intact. The cut surfaces of the kidney were covered with Gelaspon® (Chauvin Ankerpharm, Rudolfstadt, Germany) for

hemostasis. During resection, the excised renal tissue was weighed on an analytic scale and the process was continued until an amount of 66% of the previously measured weight of the right kidney was removed. The muscle and skin were closed together using 3-0 Vicryl suture (Ethicon).

To eliminate the possibly confounding effects of different operating conditions, sham-operated control animals underwent anesthesia at the same day as SNX animals, but the kidneys were only decapsulated and the hilus manipulated.

Dorsal rhizotomy was performed during the preceding uninephrectomy as described by Campese and Kogosov [65]. Briefly, from a dorsal incision, above the left kidney, the lumbar vertebral column was exposed by gently pulling the muscle away from the vertebrae. The dorsal roots were visualized and cut with fine scissors. Rhizotomy was performed at T10-L2, which contain the greatest concentration of afferent fibers from the kidneys to the brainstem. Animals were only included in the study, if all 5 dorsal roots could be identified on either side of the spine.

The medication with Quinapril was started 48 hours after the second kidney operation.

3.1.3 Measurement of albuminuria and blood pressure

At the beginning and at the end of the study, rats were kept in metabolic cages (Tecniplast, Buguggiate, Italy) for 24 hours. Twenty microliters of penicillin were added to the collection tubes to prevent bacterial degradation of proteins, and urine samples were collected. Urinary albumin excretion was determined using a microplate solid phase sandwich ELISA [148] with slight modifications. Briefly, Nunc® Maxisorb 96-well plates (Sigma-Aldrich GmbH, Deisenhofen, Germany) were coated with 100 µl coating solution (0.2 µg / ml rat serum albumin (RSA, A6414, Sigma) in 0.1 M NaHCO₃), incubated at 37 °C for 3 hours then at 4 °C overnight and washed four times with washing buffer (containing 0.5% gelatine, 2 mM diethyl malonic acid, 0.3 M NaCl, 0.1 mM EDTA and 0.1% Tween-20). Standards were then prepared from RSA stock (1 mg / ml RSA in 0.1 M NaHCO₃) and 50 µl from each was added to the plate. Urine samples were first centrifuged at 2000 g for 10 min, at 4 °C, and supernatants were taken and diluted 1:100, 1:500 and 1:1000 with washing buffer. Finally, 50 µl of each

sample dilution was added in duplicate to the plate. Fifty microliters of peroxidase conjugated rabbit anti-rat albumin (55776, ICN Biochemicals, USA) antibody solution (1:100, diluted in washing buffer) were then added to each well. Plates were incubated at 37 °C for 1 hour. Substrate solution containing 0.02% H₂O₂ was prepared dissolving tetramethylbenzidine tablets (T3405, Sigma) in 1:1 volume of washing buffer and dH₂O. Plates were washed 3 times with washing buffer and 200 µl of substrate solution was added to each well. Plates were finally read with an MRX 1.2 microplate reader (Dynex Technologies GmbH, Denkendorf, Germany) [149] and the albumin concentration was determined as the arithmetic mean of duplicates.

At the end of the study, systolic blood pressure was measured in all rats while conscious by tail-cuff electrospigmomanometry (TSE, Bad Homburg, Germany)[150] at an ambient temperature of 40 degrees to assure venous dilatation in the tails. In addition, in 2 animals per group telemetric blood pressure was measured using the system of Data Sciences International (St. Paul, Minn., USA). Transmitters (TA11PA-C40) were implanted into the abdominal aorta at the uninephrectomy operation. Implantation of the transmitters was performed as described elsewhere [67]. Briefly, the abdominal aorta was ligated and, through an approximately 1mm incision made with microsurgery scissors (Aesculap, Germany), the measuring catheter was introduced into the aortic lumen. Finally, the incision area was closed with “tissue glue” and the ligature was released. The body of the transmitters were placed in the abdominal cavity and immobilized using 3 sutures to the abdominal wall. Receivers (RPC1) were placed underneath the cage, as the maximal range of the transmitters is 40 cm. Mean, systolic, and diastolic arterial blood pressure and heart rate derived from the peak systolic blood pressure signal were recorded. Results are given as the mean of 150-min readings on 3 consecutive days.

3.1.4 Perfusion harvest and tissue preparation

At week 16 the experiment was terminated and rats were harvested by retrograde perfusion via the abdominal aorta as described previously [149]. All animals were perfused under the same conditions and on the same day. Briefly, the animals were first anesthetized with ketamine+xylazine (for details, see operating procedures), then rats

were mounted on a cork plate and immobilized at their extremities. The abdomen was opened by midline laparotomy, the vena cava inferior and the aorta abdominalis were exposed, and the latter was clamped proximal and distal to the incision site. After a 2 mm wide incision was made, the aorta was cannulated with a modified 20G catheter, attached to a 15 ml collection tube, and the proximal clamp was then released. Approx. 6 ml of blood was taken for chemistry, and then perfusion was started with Dextran 40 (Rheomacrodex®) containing 0.5% procainhydrochloride, for 2 minutes. After 10 seconds, the v. cava was cut to avoid excessive venous pressure. As hyperosmolar solution, Dextran 40 protects from the development of interstitial edema and the aggregation of erythrocytes and thrombocytes, which would lead to thrombosis and inadequate perfusion in the kidneys. Procain acts as a vasodilatator in the microcirculation, which enables better perfusion of the organs. Finally, the organs were perfused with fixation solutions. For morphometric analysis, 3% glutaraldehyde in 0.2 molar phosphatebuffer (Sørensen solution, pH 7.4) was used as fixative in 7 animals per group, for approximately 12 minutes at 110 Hgmm perfusion pressure [67, 68, 149]. For immunohistochemical analysis, 10 animals per group were perfused with ice-cold 0.9% NaCl.

The glutar-perfused left remnants (or in sham-operated animals, the intact left kidneys) were harvested for morphometric and stereologic measurements. The kidneys were sectioned in a plane perpendicular to the interpolar axis, yielding slices of 1.5-2 mm width. From these slices, ten small (2x2x2 mm) pieces were cut by area-weighted sampling and embedded in Epon-Araldite. Semithin (1 µm) and ultrathin sections (0.08 µm) were prepared and stained with methylene blue/basic fuchsine or lead citrate/uranyl acetate, respectively. The remaining tissue slices were embedded in paraffin; 4-µm sections were stained with periodic acid-Schiff (PAS).

Half of the saline-perfused kidneys were immersion fixed in 4% buffered formaldehyde, embedded in paraffin, and cut into 4-µm-thick sections. The other half of the kidneys were snap-frozen in liquid nitrogen for mRNA expression analysis.

3.1.5 Immunohistological methods

Paraffin sections were prepared and incubated with antibodies, using the avidin-biotin method [149]. Briefly, after 10 min rehydration in dH2O and TBS, samples were

blocked with 10% goat serum for 20 min, then slides were incubated with the respective primary antibodies for 60 min at room temperature. After washing in TBS for 10 min, one drop of the respective biotinylated secondary antibody (SuperSensitive Link, Biogenex, USA) was applied for 20 min at room temperature. After the next washing in TBS, one drop of streptavidine-conjugated alkaline phosphatase (Biogenex) was applied for 20 min. Staining was developed with Fast red substrate (DAKO) for 5 min. Slides were counterstained with Mayer's haemalaun and finally coated with Aquatex (Merck, Germany).

Antibodies against the following epitopes were used:

- TGF- β_1 (anti-TGF- β_1 rabbit IgG polyclonal antibody, 1:50; Santa Cruz Biotechnology, Santa Cruz, Calif., USA),
- collagen IV (anti-collagen IV rabbit polyclonal antibody, 1:40, Biotrend Chemikalien, Cologne, Germany),
- endothelial nitric oxide synthase [eNOS (NOS-3), anti-eNOS rabbit polyclonal antibody, 1:400; ABR-Affinity BioReagents, Golden, Colo., USA],
- neuronal nitric oxide synthase [nNOS (NOS-1), anti-nNOS rabbit polyclonal antibody, 1:50, BD Pharmingen, Heidelberg, Germany],
- nitrotyrosine (sheep polyclonal antibody, 1:400, Oxis Research, USA).

Immunohistochemical reactivity was examined in a blinded manner with light microscopy. To evaluate glomerular staining, 50 glomeruli were counted per sample, while staining of the tubulointerstitium was evaluated in the whole sample. We used a semiquantitative score system. Briefly, glomeruli were scored at a magnification of $\times 400$ as follows: 0 = no staining, 1 = weak staining, 2 = moderate staining in $\sim 50\%$ of glomerular tuft, 3 = moderate staining in $> 50\%$ of glomerular tuft, 4 = strong staining of the entire glomerulus. Tubulointerstitium was scored at a magnification of $\times 200$ as follows: 0 = no staining, 1 = weak, 2 = mild, 3 = strong, 4 = very strong staining.

3.1.6. Semiquantitative examination of the kidney - indices of renal damage

To evaluate pathologic alterations on PAS-stained paraffin sections, the following methods were used as described [67], according to el Nahas [151] and Veniant et al [152]: glomerulosclerosis index (GSI), tubular and interstitial damage index (TDI, IDI), and vascular damage index (VDI).

The histological signs of glomerular damage are: hypertrophy and proliferation of the mesangial cells accompanied by excessive production of ECM (mesangial matrix), hyalinosis of the capillaries, podocyte hypertrophy and degeneration. Sclerosis may lead to complete obliteration of the glomerulus with consecutive loss of function.

Glomerulosclerosis index (GSI):

Slides were evaluated using light microscopy at 400x magnification, and the glomerulosclerosis index of each animal was derived as the arithmetic mean of 100 randomly sampled individual glomeruli according to el Nahas [151], using grades 0-4 as follows: 0) normal glomerulus; 1) beginning mesangial expansion / thickening of the basement membrane and/or irregular lumina of the capillaries, sclerosis in less than 25% of the glomerular tuft; 2) mild/moderate segmental hyalinosis/sclerosis involving less than 50% of the glomerular tuft; 3) diffuse glomerular hyalinosis/sclerosis involving 50-75% of glomerular tuft; 4) diffuse glomerulosclerosis with total tuft obliteration and collapse.

Tubular and interstitial damage index:

Determination of tubular and interstitial damage was performed using a modified method described by Veniant et al [152], as here we evaluated tubular and interstitial damage separately. The PAS-stained slides were counted using 100x magnification in 20 fields of view. The intensity of inflammation (mononuclear cell infiltration), interstitial fibrosis and tubular atrophy (grade 0-3) were evaluated as follows:

Tubular damage (TDI): 0) normal tubuli; 1) tubular atrophy in less than 25% of the field of view; 2) tubular atrophy and dilatation and/or hyalin deposition in 25%-50% of the field of view; 3) the above mentioned alterations in more than 50% of the field of view.

Interstitial damage (IDI): 0) normal interstitium; 1) signs of interstitial inflammation and fibrosis in less than 25% of the field of view; 2) interstitial inflammation and fibrosis in 25%-50% of the field of view; 3) interstitial inflammation and fibrosis in more than 50% of the field of view.

Vascular damage index (VDI):

Quantification of vascular damage was performed according to Veniant et al [152] in PAS-stained slides, using 200x magnification in 20 fields of view, evaluating the thickening of vessel walls and fibrinoid necrosis of the afferent arterioles, interlobular vessels and small arteries of the kidney, as follows (grade 0-4): 0) normal vessels; 1) mild wall thickening; 2) moderate wall thickening; 3) severe wall thickening; 4) fibrinoid necrosis of the vascular wall.

3.1.7 Glomerular morphometry and stereology

Glomerular Geometry.

Area density of the glomerular tuft (A_{AT}) and volume density of glomeruli (V_V) were measured by the point counting method with point density = area density = volume density ($P_P = A_A = V_V$) using a 100-point Zeiss eyepiece (Integration-plate II; Zeiss, Oberkochen, Germany) at a magnification of x400 on PAS sections. In addition, the number of glomeruli per area (N_A) was counted (for detailed description of analysis of glomerular geometry, see [13]). Briefly, from the above data the number of glomeruli per volume [$N_V = (1/1.382) \times (N_A^{1.5} \times V_V^{0.5})$] (corrected for tissue shrinkage: 45%) and total cortex volume was calculated from kidney mass (KW), specific weight of the kidney (SW_K), and volume density of the cortex according to $V_{Cortex} = KW/SW_K \times V_{VCortex}$ ($V_{VCortex} = (1/1.382) \times (N_A^{1.5} \times V_V^{0.5})$). From these parameters the total number of glomeruli was derived ($N_{Glom} = N_V \times V_{Cortex}$). Finally, the mean glomerular tuft volume: $mV_{Glom} = (1/1.382) \times A_T^{1.5}$ was calculated from the total area of the glomerular tuft and cortex area ($A_T = A_{AT} \times A_{Cortex}$). The number of glomeruli (N_{Glom}) per kidney was used to estimate the extent of surgical nephron reduction and the mean glomerular tuft volume (mV_{Glom}) was used to estimate the extent of glomerular enlargement. Glomerular mesangial matrix volume (V_{Matrix}) was calculated as the fractional mesangial matrix volume of the glomerular capillary tuft (points on the matrix/points on the whole glomerular tuft) and is given as percent.

Glomerular Cellularity.

The number per glomerulus and mean volume of glomerular cells (podocytes, mesangial and endothelial cells) was analyzed in 15 glomeruli per animal (Figure 4). The mean cell number/glomerulus (N_C) was calculated from cell density per volume (N_{c_v}) and volume density of the respective cell type (V_{c_v}) according to the equation: $N_{c_v} = k/\beta \times N_{c_A}^{1.5}/V_{c_v}^{0.5}$ with $k=1$ and $\beta=1.5$ for podocytes and 1.4 for mesangial and endothelial cells. The respective mean cell volumes were calculated according to the equation $mV_c = V_{c_v} \times mV_{glom}$ [146].

Glomerular Capillaries.

In 5 semithin sections per animal glomerular cell number and volume were analyzed using an eyepiece for point counting (see above) at a magnification of x1,000 (oil immersion). Briefly, the length density of glomerular capillaries (L_V : mm capillary/mm³ glomerular tuft volume) was determined according to the standard stereologic formula ($L_V = 2Q_A$: the number of capillary transects per area of the capillary tuft). This parameter gives the average capillary length normalized to glomerular volume to exclude the effect of hypertrophy; thus it is a marker of glomerular capillary obliteration. Furthermore, glomerular capillary length for the whole kidney (L_c), i.e. total capillary length, was determined. Glomerular capillary tuft volume (V_{Tuft}) was calculated as the fractional capillary tuft volume of the whole glomerulus (points on the tuft/points on the whole glomerulus) and is given as percentage.

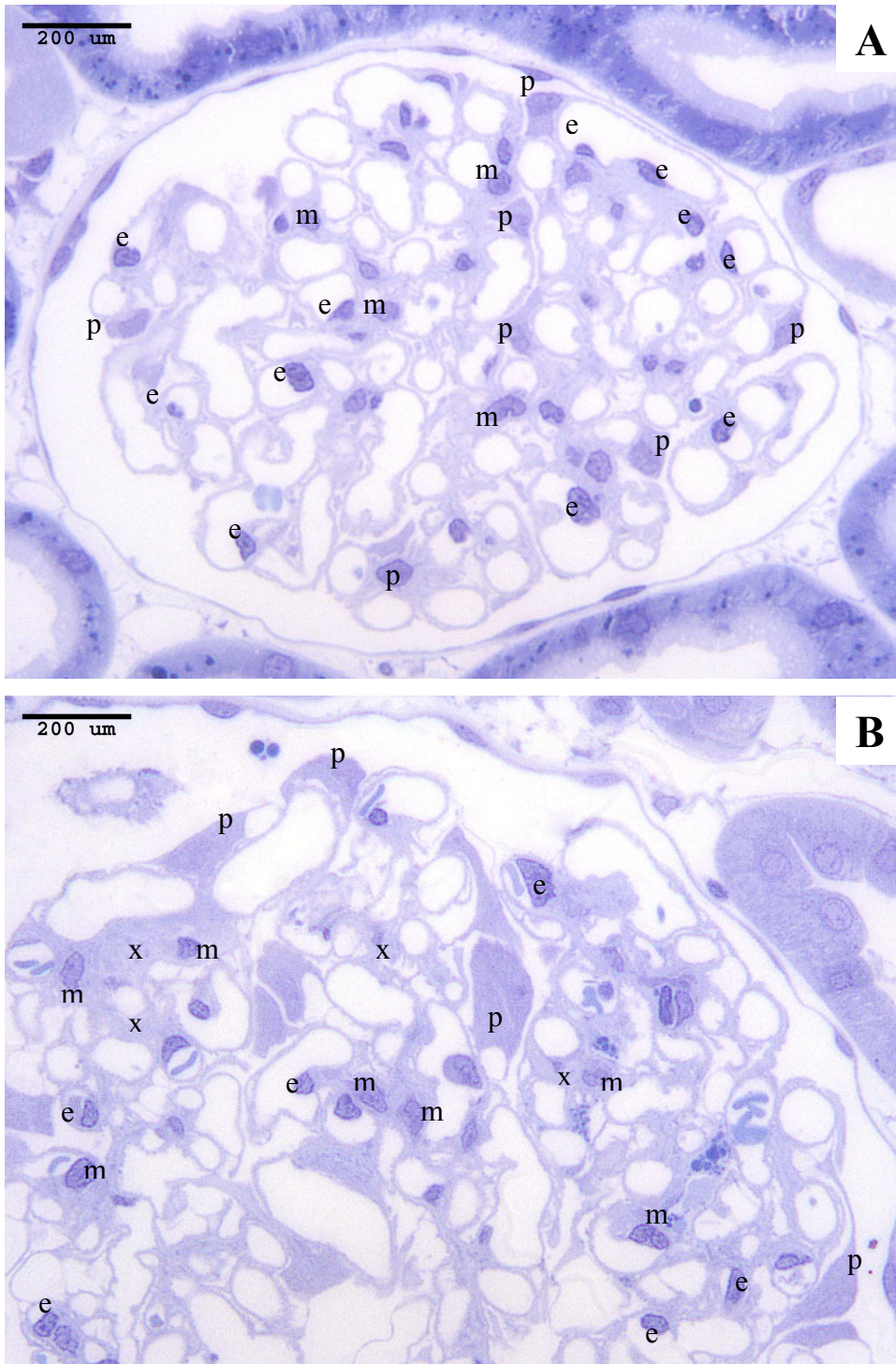


Figure 4. Glomerular cell structure in the kidneys of sham operated (A) and SNX rats (B). Semithin slides of our experimental animals, stained with toluidine-blue, magnification x1000). Glomeruli are cut in the equatorial plane as shown by the narrow Bowman's space. Note the significantly enlarged glomerulus in SNX kidney, with, increased number of mesangial cells, enlarged podocytes and excessive mesangial matrix deposition (e: endothelial cell, m: mesangial cell, p: podocyte, x: matrix).

3.1.8 Real-Time RT-PCR

Total RNA was isolated from whole kidneys using SV Total RNA Isolation System (Promega, Mannheim, Germany) according to the manufacturer's instructions. RNA concentration was determined photometrically at 260nm, RNA purity was determined with the A260/A280 ratio (samples between 1.5-1.9 were just taken for examination). RNA integrity was visualized after 1% agarose gel electrophoresis (1 µg RNA of each sample was loaded) under UV-light.

Reverse transcription was performed on a Promega thermal cycler with the 1st Strand cDNA Synthesis Kit (AMV) from Roche (Roche Diagnostics, Mannheim, Germany) using 1 µg RNA and random primers (final concentration: 3.2 µg) as follows: 10 min at 25 °C, 30 min at 55 °C and 5 min at 85 °C.

All quantitative PCR reactions were performed on a LightCycler (Roche Diagnostics, Mannheim, Germany) using the LightCycler-Faststart DNA Master SYBR Green I Kit (Roche). The samples were quantified normalizing to glyceraldehyde-3-phosphate dehydrogenase (GAPDH) expression. Primer sequences were as follows:

GAPDH forward 5'-CAATGACCCCTTCATTGACC-3',

GAPDH reverse 5'-CGCCAGTAGACTCCACAACA-3';

TGF-β₁ forward 5'-CACCATCCATGACATGAACC-3',

TGF-β₁ reverse 5'-TCATGTTGGACAACCTGCTCC-3';

eNOS forward 5'-TGACCCTCACCGATAACAACA-3',

eNOS reverse 5'-CTGGCCTTCTGCTCATTTTC-3'.

The PCR conditions were as follows: GAPDH: 95 °C for 10 sec, 57 °C for 10 sec, 72 °C for 20 sec; TGF-β₁: 95 °C for 10 sec, 54 °C for 10 sec, 72 °C for 18 sec; eNOS: 95 °C for 10 sec, 62 °C for 10 sec, 72 °C for 12 sec. Specificity of the PCR reaction was confirmed with melting curve analysis. Every sample was quantified using a gene-specific standard curve, and the mean value of three different PCR runs was taken for statistical evaluation.

3.1.9 Data analysis

Data are presented as mean ± standard deviation (SD). Randomly selected animals (n = 7) were used for morphometric analysis. Statistical analyses were performed using SPSS 13 for Windows (SPSS Inc, USA). Data were tested for normal

distribution using the Kolmogorov-Smirnov test. For data with normal distribution, one-way ANOVA was used to compare the groups. Otherwise, Kruskal-Wallis test was chosen for analysis of variance, followed by Duncan's multiple range test, to test for differences between groups. The zero hypothesis was rejected if the probability of error (p) was less than 0.05.

3.2 EXPERIMENTAL DESIGN B (LUPUS NEPHRITIS)

3.2.1. MRL/lpr lupus prone mice

MRL/lpr (MRL/MpJ-*fas*^{Tnfrsrlpr}, MHC haplotype: H2:k) female mice (Jackson Laboratories, USA) were housed in our animal facility in an individually ventilated cage system (Charles River Ltd, Hungary), had access to standard rodent chow (Altromin, Germany) and water ad libitum. Mice were divided randomly into two groups at 7 weeks of age and were accommodated for 10 days. The multiparous (M) group females were mated three times consecutively with NMRI males (Charles River, Hungary) and weaned immediately after parturition to exclude the possible immunomodulatory effects of lactation as described by Ratkay et al [153].

NMRI males (outbred strain originally developed in the Naval Medical Research Institute, MHC haplotype: H2:q, see www.taconic.com) were used for allo-mating. Non-syngeneic matings were performed to model allogenic human pregnancies. Pregnancy duration was 21 days. After parturition, males were removed for 5 days to allow the females to rest and were then placed back with the females for the next mating. MRL/lpr females were always paired with the same NMRI male (see Figure 5 for study design). Mice of the second virgin (V) group were housed apart, two virgin females were kept per cage to provide the same social environment in both groups.

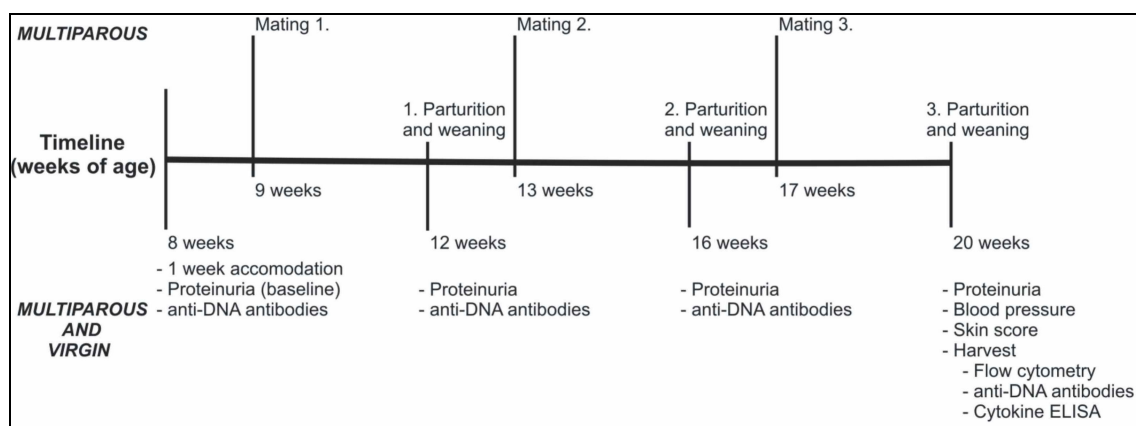


Figure 5. Study design and timeline of the experiments. Upper half: interventions on multiparous mice only; lower half: interventions on both multiparous and virgin mice.

The experiments were carried out in 4 parts. The first experiment (n=12/group) was a survival experiment; to determine time of harvest for tissue collection and to measure proteinuria. Molecular, histological and functional measurements were performed in a second experiment (n=6/group), which was terminated at 20 weeks of age. The third experiment (n=6/group) was carried out to increase the number of samples for histological and molecular measurements. The fourth (n=5/group) experiment was carried out to re-confirm changes in skin pathology and survival.

All animal experiments were carried out according to the institutional regulations and the Hungarian law on animal care and protection (1998/XVIII, 243/1998(XII.31)).

3.2.2. Assessment of kidney function and blood pressure

Twenty-four hour urine samples were collected from all animals in diuresis cages (Tecniplast, Buguggiate, Italy) at specific time points (8, 12, 16, 20 weeks of age, right after parturition, n=5-8/group). Blood samples were obtained with heparinized capillaries by retro-orbital puncture under ether anesthesia and the blood was anticoagulated in the collecting tubes with 1:10 volume of heparin. Blood urea nitrogen (mmol/l, n=4-8/group and preterminal uremic animals) levels were evaluated in a Reflotron Plus laboratory machine with enzymatic reagents (Boehringer Mannheim, Germany). Proteinuria (mg protein/24h) was measured photometrically using the Bradford method with Bio-Rad Protein Assay (Bio-Rad, USA) at 595 nm following the instructions by the manufacturer.

To assess blood pressure at the time of harvest (V:n=6, M:n=4), a non-invasive tail cuff blood pressure system (IITC Life Science, USA) was used. The IITC system has been shown to give comparable results to telemetry, and the high sensitivity allows to measure below 35 °C, minimizing the confounding factor of heat-induced stress. For optimal results, the environmental temperature was set to 30 °C and the animals were habituated for the procedure 3 times before measurement. All values were determined as mean value of three consecutive measurements.

3.2.3. Flow cytometry

Blood lymphocytes were used to evaluate the immune state of the animals by analyzing the percentage of CD4⁺, CD8⁺ (DN) CD3⁺(TCR), B220⁺ (DN B220⁺) cells by flow cytometry (V:n=9, M:n=5). The following anti-mouse mAbs were purchased from BD PharMingen (Soft-Flow, Hungary): PE-conjugated anti-CD3-complex (17A2), FITC-conjugated anti-CD4 (GK 1.5), APC-conjugated anti-CD8 (53-6.72) and PerCP-conjugated anti-CD45/B220 (RA3-6B2). For B-cell staining, anti-CD19-FITC and PerCP-conjugated anti-CD45/B220 (RA3-6B2) antibodies were used. For biotinylated antibodies, a streptavidin-APC complex (BD PharMingen) was used as second step reagent. Surface antigen expression was analysed using a BD FACSCalibur® flow cytometer (Becton Dickinson Immunocytometry, Mountain View, CA). Briefly, 30 µl peripheral blood sample was incubated with mAbs in the dark at room temperature for 20 min and then with 1 ml erythrocyte lysing solution (BD) in the dark at room temperature for 10 minutes. To remove unbound antibodies, samples were washed in 2 ml PBS, then fixed in 350 µl cold 2% paraformaldehyde and resuspended in FACS buffer before being analysed. Data were evaluated with CellQest software (BD).

3.2.4. ELISA of plasma INF- γ and anti-dsDNA autoantibody levels

Plasma IFN- γ levels were measured using a supersensitive IFN- γ ELISA kit (Bender MedSystems, Austria) following the manufacturer's instructions (n=4/group).

The levels of anti-dsDNA antibodies were evaluated from plasma samples at specific time points (8, 12, 16, 20 weeks of age, n=10/group) using anti-dsDNA ELISA. Briefly, 96-well ELISA plates (Greiner, Budapest) were coated with 25 µg/ml double-stranded calf thymus DNA (Sigma, Sigma-Aldrich Kft, Budapest, Hungary) in 0.1 M ammonium acetate and incubated overnight at 4 °C. After washing with PBS-1% Tween 20 (PBS-T) following distilled water, sera diluted 1:200 in serum diluent (PBS-T) were added in duplicate and incubated for 1 h at 37 °C. After washing, horseradish peroxidase (HRP)-conjugated goat anti-mouse IgG (Sigma) was used as a conjugate antibody (1:1000 in PBS-T, 1 h at 37 °C) followed by the substrate, o-phenylenediamine dihydrochloride (Sigma). The OD was measured photometrically after 20 min at 450 nm (ref.= 690 nm).

3.2.5. Histology of the kidneys

Kidney samples were fixed in 10% buffered formalin for 16-24 hours, then kept in 75% ethanol before being embedded in paraffin within 5 days. Four μm sections were cut and were stained with H&E, periodic-acid Schiff (PAS) or Crossman's tri-chrome. Samples were all evaluated in a blinded manner.

Kidney lesions (n=9/group) were scored as follows: the glomerulosclerosis index and the tubular, interstitial and vascular damage scores were assessed on PAS stained paraffin sections as previously described (*chapter 3.1.6*).

Perivascular cell accumulation was determined semiquantitatively at 400x magnification by scoring the number of cell layers surrounding the medium-sized vessels as follows: 0) none; 1) <5 cell layers; 2) 5-10 cell layers; 3) >10 cell layers. Periglomerular infiltration was scored in a similar way, counting the infiltrating cell layers around the glomeruli: 0) none; 1) 1-3 cell layers; 2) 4 or more cell layers.

3.2.6. Renal IgG and C3 deposition, and CD3⁺ infiltration

Kidney samples (n=4/group) were evaluated for IgG deposition by direct immunofluorescence staining. Briefly, 8 μm cryostat sections were attached to SuperFrost slides at room temperature and fixed in cold acetone. Air-dried slides were then washed in PBS, blocked with 20% normal goat serum then stained with FITC-conjugated goat anti-mouse antibody (Sigma) in 1:100 dilution and incubated in a dark chamber at 37 °C for 60 minutes. After washing with PBS, samples were coated using Fluorescent Mounting Medium (DAKO, Hamburg, Germany) and analyzed in a fluorescent microscope (Leica DMR-HC, Leica, Germany). The fluorescence intensity within the peripheral glomerular capillary walls were analyzed using ImageJ software (NIH, Bethesda, Maryland, USA).

Complement-3 deposition was evaluated in cryostat kidney sections (n=4/group) using immunohistochemistry as described elsewhere [154]. We opted for immunohistochemistry as it has been shown to be more specific than immunofluorescence. Briefly, after rehydration in TBS, blocking was performed with 5% BSA, then slides were incubated with goat anti-mouse C3 antibody (Cappel, USA), diluted 1:200 for 60 min at room temperature. Endogen peroxidase was quenched with 3% H₂O₂ in methanol for 30 min after application of the primary antibody. After

washing, HRP-conjugated rabbit anti-goat antibody (Sigma) was applied 1:200 for 30 min and AEC (DAKO) substrate was added for 5 min. Slides were counterstained with Mayer's haemalaun and coated with Aquatex (Merck, Germany).

Glomerular staining was evaluated in a blinded manner counting 30 glomeruli per sample, with a semiquantitative score system: 0) no staining, 1) weak staining, 2) moderate staining in ~50% of glomerular tuft, 3) moderate staining in >50% of glomerular tuft, 4) strong staining of the entire glomerulus.

The infiltration of CD3 positive cells per kidney was determined on paraffin sections (n=8/group). Antibody mixture (mouse monoclonal anti-CD3, 1:50, DAKO) was prepared using a commercial mouse-on-mouse kit (Innogenex, Biogenex, Germany) following the manufacturer's protocol. After deparaffinization and rehydration of the slides, antigen retrieval was performed in citric buffer pH 6.0 for 20 min. After washing in TBS, slides were blocked with 5% goat serum for 15 min, followed by the incubation with the primary antibody mixture overnight at 4 °C. After washing, streptavidin-conjugated alkaline phosphatase (Biogenex) was applied for 20 min. Samples were washed again and Fast Red substrate (DAKO) was added for 3 min. Slides were counterstained with Mayer's haemalaun and coated with Aquatex (Merck). The immunostaining was analyzed by counting the positive cells in 10 randomly selected fields at 400x magnification using a 10x10 points Zeiss eyepiece (Integration-plate II; Zeiss Co., Germany). The results are expressed as CD3 positive cells per mm².

3.2.7. Real-time RT-PCR

100 mg of kidney samples (n=7-11/group) were treated with 1 ml Trizol (Gibco, Life Technologies, Germany) and disaggregated using a homogenizator (Ultra Turrax T8, Ika, Germany). The RNA was then extracted with chloroform, precipitated with isopropanol, washed with 75% ethanol and finally diluted in RNase-free-water. The RNA was quantified by reading ultraviolet absorbance at 260 nm.

Reverse transcription was performed as follows: 2 µg total RNA were placed for 2 min. on ice and supplemented with dNTPs (2.5 mM, Amersham Pharmacia), DNase I (2 U/ml, Stratagene) and RNase-inhibitor (40 U/ml, Promega) mixed in the reaction buffer. The mix was incubated for 30 min at 37°C and further heated to 75°C for 5min. Reverse transcription process commenced upon the addition of Reverse transcriptase

(200 U/ml, Amersham) and RNase- to the mixture. This reaction mixture was incubated at 42°C for 60 min followed by incubation at 94 °C for 5 min.

Amplification reactions (13 µl) for IFN- γ , IL-10, IL-4 and β -actin consisted of 2 µl cDNA, 6.25 µl mastermix containing PCR buffer, dNTPs, MgCl₂ and Ampli-Taq DNA Polymerase (Eurogentec, Berlin, Germany), 3 µl of the primer mix, 1.25 µl water and 0.5 µl of the fluorescent probes. PCR reaction was performed as follows: 2 min at 50 °C followed by an initial denaturation step of 10 min at 95 °C, followed by 15s at 95 °C and 1 min at the appropriate annealing temperature for 40 cycles. All samples were normalized regarding their β -actin content. Expression levels were calculated using the formula $2^{-\Delta Ct}$, where ΔCt is the difference of mean cytokine threshold cycle and mean beta-actin threshold cycle of triplicate measures. All reactions were performed on an ABI Prism 7700 Sequence Detection System (Perkin Elmer Applied Biosystems).

Primer and probe sequences were as follows:

IFN- γ forward: 5'- AGC AAC AGC AAG GCG AAA AA-3'
IFN- γ reverse: 5'-AGC TCA TTG AAT GCT TGG CG-3'
IFN- γ probe: 5'-ATT GCC AAG TTT GAG GTC AAC AAC CCA CA-3'
IL-10 forward: 5'- GAA GAC CCT CAG GAT GCG G-3'
IL-10 reverse: 5'- CCT GCT CCA CTG CCT TGC T-3'
IL-10 probe: 5'- CGC TGT CAT CGA TTT CTC CCC TGT GA-3'
IL-4 forward: 5'-CTC ATG GAG CTG CAG AGA CTC TTT-3'
IL-4 reverse: 5'- GTG ATG TGG ACT TGG ACT CAT TCA-3'
IL-4 probe: 5'-ATG CCT GGA TTC ATC GAT AAG CTG CAC CT-3'

3.2.8. Data analysis

Results are shown as medians \pm 75% quartiles (for non-parametric data) or means \pm SD (for parametric data). Data were analyzed statistically using SPSS for Windows (SPSS Inc.). Kaplan-Meier and log-rank test were made for survival analysis. The Kolmogorov-Smirnov test was performed to analyze distribution normality. Mann-Whitney-test was applied to analyze all non-parametric data (skin macroscopy scores, skin and kidney histology scores, IgG and C3 depositions, proteinuria). For normally distributed values of blood pressure, Student's t-test was employed.

4. RESULTS

4.1 RESULTS A (RENAL FIBROSIS)

4.1.1. Animal data

At the time of operation the body weight of the animals was comparable in all groups (table 2.). SNX rats had significantly higher serum creatinine and serum urea concentrations than sham operated animals. These values were significantly lower in the animals on combined intervention. Comparing the two single intervention groups, serum creatinine and serum urea tended to be lower in the rhizotomy animals vs. Quinapril monotherapy. In SNX animals the hematocrit values were significantly lower. Development of anemia was significantly inhibited by combined intervention.

Table 2. Laboratory values and body weight at the time of harvest. #p<0.01 vs sham+no intervention or respective control group; *p<0.05 vs SNX+no intervention.

Group	Creatinine [mg/dl]	Urea [mg/dl]	Hematocrit [%]	Initial body weight [g]	Body weight at harvest [g]
Sham	0.4±0.1	40.0±4.3	42.7±3.1	399±12.9	588±46.8
Sham + R	0.4±0.1	41.8±4.9	44.3±3.4	387±27.8	562±33.1
Sham + Q	0.4±0.0	51.6±9.1	44.6±3.4	385±14.6	548±21.6
Sham + R + Q	0.4±0.1	49.6±6.0	40.3±3.3	385±21.4	589±42.9
SNX	1.0±0.2 [#]	113.1±7.9 [#]	36.1±5.1 [#]	391±12.7	557±27.4
SNX + R	0.7±0.4 [*]	97.1±15.0 [*]	36.9±3.4	394±26.6	573±33.8
SNX + Q	0.9±0.01 [#]	123.4±13.9 [#]	37.0±1.5	394±10.3	546±18.6
SNX + R + Q	0.75±0.3 [*]	106.6±13.4 [*]	38.9±4.4 [*]	382±16.9	522±42.3
ANOVA	p<0.001	p<0.001	p<0.001	n.s.	n.s.

4.1.2. Albuminuria and blood pressure

At the end of the study albuminuria was strikingly higher in untreated SNX compared to sham, and significantly lower in SNX after rhizotomy alone compared to untreated SNX. It was also lower in SNX on Quinapril and lowest on combined intervention (Table 3).

Tail plethysmography overestimated blood pressure. Blood pressure was monitored by telemetry in a limited number of animals. The results (Figure 6) indicated higher blood pressure in untreated SNX and lower values in treated SNX.

Table 3. Values of albuminuria, systolic blood pressure and kidney weight relative to bodyweight at harvest. KW: kidney weight; BW: body weight; #p<0.05 vs Sham; *p<0.05 vs SNX; ** p<0.01 vs SNX; &p<0.05 vs SNX+Q; §ns: SNX+R+Q vs Sham+R+Q

Group	Albuminuria [mg/24h]	Systolic blood pressure (tail-cuff) [mmHg]	KW/BW[%]
Sham	4±2	129±12	0.36±0.02
Sham + R	2±1	125±30	0.41±0.04
Sham + Q	2±1	115±13	0.33±0.03
Sham + R + Q	1±1	114±10	0.39±0.03
SNX	169±75 [#]	162±13 [#]	0.49±0.1 [#]
SNX + R	86±45 [*]	138±28 [*]	0.45±0.07
SNX + Q	15±23 ^{**}	115±12 ^{**}	0.44±0.09
SNX + R + Q	5±4 ^{**,&§}	112±14 ^{**,&§}	0.42±0.05
ANOVA	p<0.001	p<0.001	p<0.001

4.1.3. Indices of renal damage

In untreated SNX, indices of glomerular (GSI), tubular (TDI), interstitial (IDI) and vascular damage (VDI) were all significantly higher than in sham (Table 4., Figure 7.). Rhizotomy had a marked effect on all indices except VDI. The effect of Quinapril monotherapy was even more striking (with the exception of VDI), but with exception of VDI combined intervention yielded the best outcome (p<0.05).

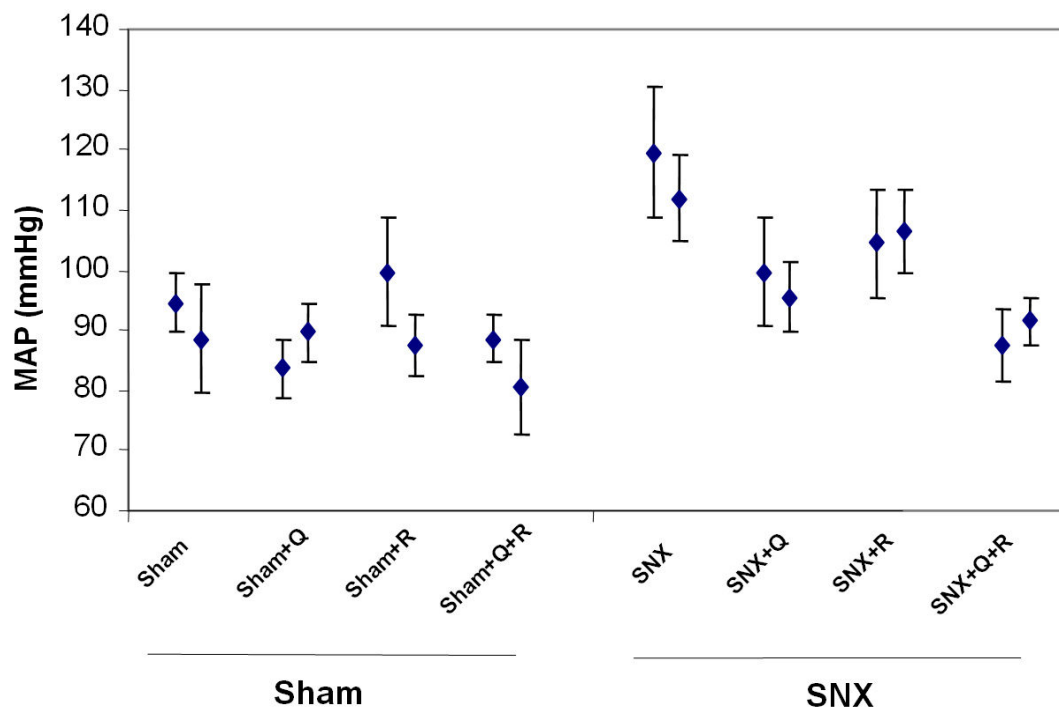


Figure 6: Telemetrically measured mean arterial pressure (MAP) in 2 animals per experimental group. Bars represent 15 measurements on 3 consecutive days by individual animals (mean ± SD of individual values).

Table 4. Morphologic-indices of renal damage. #p<0.05 vs Sham; *p<0.05 vs SNX; ** p<0.01 vs SNX; &p<0.05 vs SNX+Q; §ns: SNX+R+Q vs Sham+R+Q.

Group	GSI	TDI	IDI	VDI
Sham	0.14±0.04	0.55±0.31	0.11±0.14	0.20±0.28
Sham + R	0.13±0.04	0.26±0.12	0.16±0.17	0.07±0.15
Sham + Q	0.31±0.19	0.43±0.17	0.14±0.11	0.02±0.05
Sham + R + Q	0.36±0.17	0.29±0.16	0.08±0.10	0.10±0.14
SNX	1.40±0.6[#]	1.82±0.67[#]	1.78±0.60[#]	0.42±0.17[#]
SNX + R	0.80±0.23 [*]	1.46±0.13	0.75±0.25 [*]	0.40±0.29
SNX + Q	0.37±0.16 [*]	1.14±0.18 [*]	0.48±0.15 [*]	0.45±0.31
SNX + R + Q	0.31±0.15 ^{**,&§}	0.55±0.37 ^{**,&§}	0.15±0.13 ^{**,&§}	0.12±0.05 ^{*,§}
ANOVA	p<0.001	p<0.001	p<0.001	p<0.001

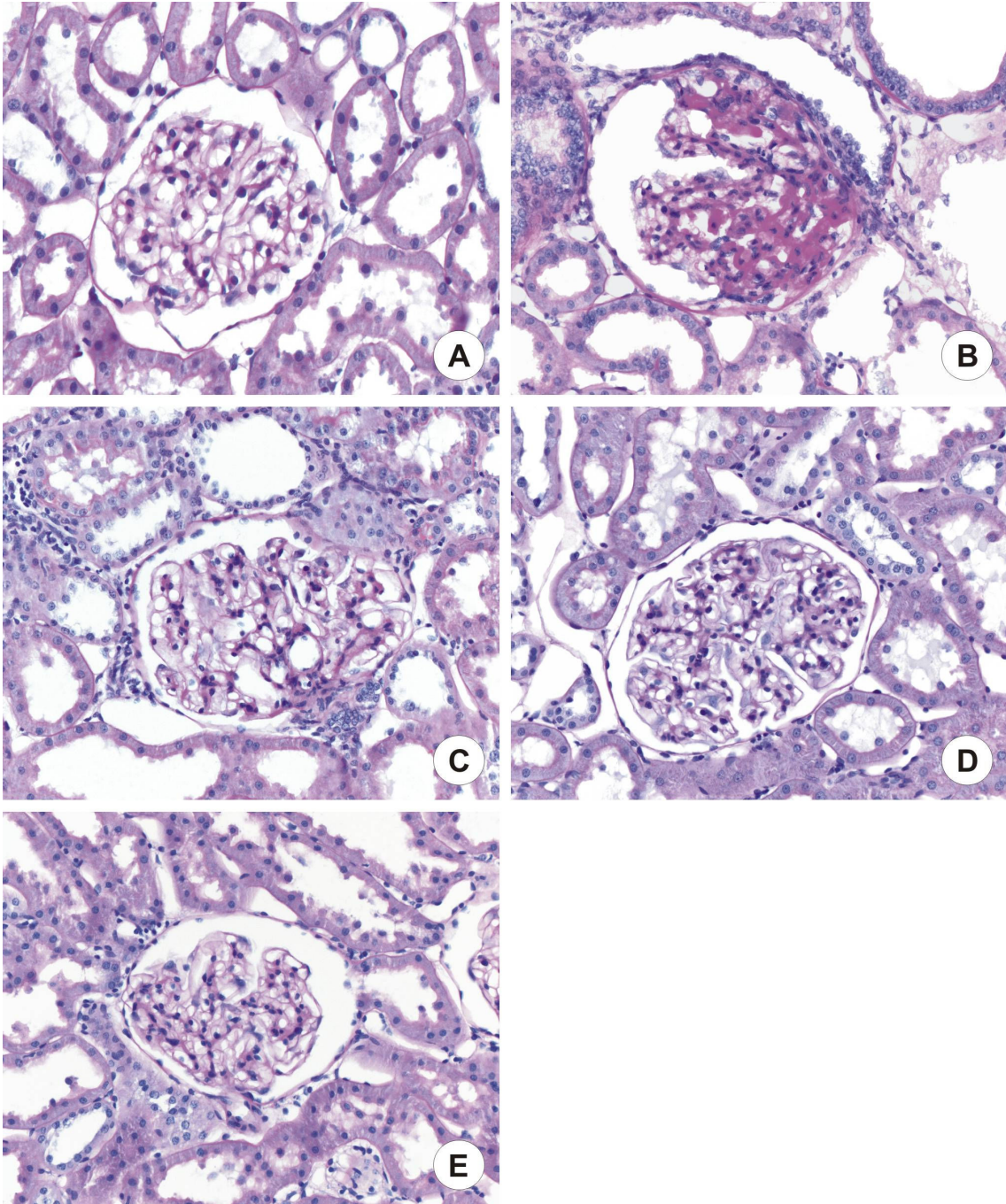


Figure 7. Representative photographs of glomeruli from a sham-nephrectomized animal (A) and SNX animals (B-E). B: SNX, C: SNX+Q, D: SNX+R, E: SNX+Q+R. PAS stain, magnification x400.

4.1.4. Stereologic measurements

SNX consistently reduced the number of glomeruli to a similar extent documenting the homogeneity of the SNX groups (Table 5.). In all SNX groups a compensatory increase in glomerular volume was noted which was significantly lower after Quinapril treatment. The length density of glomerular capillaries as well as the total length of capillaries per remnant kidney was significantly less after SNX reflecting capillary loss or obliteration as a result of glomerulosclerosis. Rhizotomy, but not Quinapril, almost normalized capillary length density. In SNX the matrix represented a significantly greater proportion of the tuft, reflecting glomerular extracellular matrix accumulation. The matrix/tuft ratio was significantly lower in Quinapril treated SNX, but was not affected by rhizotomy.

Table 5. Stereologic analysis of glomeruli. N_{Glom} : total number of glomeruli/kidney; mV_{Glom} : mean glomerular volume; # $p < 0.01$ vs Sham; * $p < 0.05$ vs SNX; §ns vs the respective control groups.

Group	Glomerular geometry		Glomerular capillaries		Glomerular matrix
	N_{Glom}	mV_{Glom} [$\times 10^6 \mu\text{m}^3$]	Length density [mm/mm ³]	Total length [m]	V_{Matrix} [% / V_{Tuft}]
Sham	45011±9939	2.6±2.2	6.3±1.3	6925±1964	13.7±0.8
Sham + R	49190±11343	3.0±1.9	6.5±1.0	7519±770	16.2±6.7
Sham + Q	45030±5389	2.8±2.5	5.5±1.2	6072±421	12.9±0.8
Sham + R + Q	62020±9826	2.7±2.3	6.4±0.5	7580±1401	13.4±1.2
SNX	18024±3290 [#]	7.3±1.6 [#]	4.3±0.2 [#]	3906±759 [#]	23.0±1.4 [#]
SNX + R	19136±5180	6.4±2.2	5.1±0.3 [*]	5302±1486 [*]	23.6±3.5 [#]
SNX + Q	23089±5959	5.0±3.2 [*]	4.5±0.4	3653±989	14.9±0.4 ^{*,§}
SNX + R + Q	19896±3704	4.5±1.7 [*]	5.0±0.7 [*]	5549±2208 [*]	14.1±0.8 ^{*,§}
ANOVA	$p < 0.001$	$p < 0.001$	$p < 0.001$	$p < 0.001$	$p < 0.001$

4.1.5. Cellular analysis of the glomerulus

In our model of renal damage, the number of podocytes per glomerulus remained unchanged, but the podocyte volume was strikingly increased in SNX (Table 6.). It was significantly lower in the Quinapril group and in rats on combination therapy, but not affected by rhizotomy

The number of endothelial cells was also strikingly increased in untreated SNX, but significantly lower in Quinapril treated SNX, but not in SNX with rhizotomy. There was no significant change in endothelial cell volume. Finally, in SNX a significant increase in mesangial cell number was noted which again was attenuated, but not normalized, by Quinapril. Rhizotomy did not affect this parameter. No significant changes of mesangial cell volume were noted.

Table 6. Cellular analysis of the glomerulus (number and volume of respective cells). #p<0.01 vs Sham; *p<0.05 vs SNX.

Group	Podocytes		Endothelial cells		Mesangial cells	
	Number/ glom.	Mean volume [mm ³]	Number/ glom.	Mean volume [mm ³]	Number/ glom.	Mean volume [mm ³]
Sham	109±6	796±71	446±76	181±43	364±84	210±51
Sham + R	106±10	810±41	500±62	166±50	356±42	291±118
Sham + Q	110±4	719±39	490±60	147±51	273±82	279±90
Sham + R + Q	106±2	806±59	511±58	132±11	342±28	258±48
SNX	123±3	2299±146 [#]	852±128 [#]	177±29	867±211 [#]	311±88
SNX + R	109±1	2217±149	1018±212	140±49	816±181	239±103
SNX + Q	112±6	1818±171 [*]	590±78 [*]	173±28	551±70 [*]	250±54
SNX + R + Q	106±3	1840±80 [*]	630±13 [*]	161±21	479±86 [*]	300±22
ANOVA	ns	p<0.001	P<0.001	ns	p<0.001	ns

4.1.6. Immunohistochemistry and real-time PCR analysis of the kidneys

Increased collagen was found in glomeruli (Table 7.) and was significantly reduced by Quinapril plus rhizotomy. Tubulointerstitial collagen deposition was prevented by all interventions. Interestingly, rhizotomy as a single intervention prevented tubulointerstitial collagen deposition significantly more effectively, than Quinapril monotherapy.

Glomerular TGF- β_1 expression (Figure 8) was only reduced by combined intervention, but not by Quinapril or rhizotomy (Table 7).

Table 7. Immunohistochemical analysis of fibrosis markers and TGF- β_1 real-time PCR results in the whole kidney. Data are presented as mean score \pm SD and mean relative expression level \pm SD, respectively. * $p < 0.05$ vs SNX; § $p < 0.05$ vs SNX+R; # $p < 0.05$ vs SNX+R+Q.

Group	Collagen IV		TGF- β_1		TGF- β_1 RT-PCR
	Glomeruli	Interstitialium	Glomeruli	Interstitialium	
Sham	0.07 \pm 0.05	0.21 \pm 0.12	0.08 \pm 0.03	0.20 \pm 0.05	1.02 \pm 0.37
Sham + R	0.07 \pm 0.05	0.24 \pm 0.10	0.08 \pm 0.02	0.14 \pm 0.02	0.80 \pm 0.25
Sham + Q	0.08 \pm 0.04	0.20 \pm 0.14	0.10 \pm 0.02	0.18 \pm 0.07	1.02 \pm 0.35
Sham + R + Q	0.07 \pm 0.04	0.30 \pm 0.10	0.11 \pm 0.03	0.22 \pm 0.05	1.12 \pm 0.37
SNX	0.6 \pm 0.07	0.92 \pm 0.17	0.57 \pm 0.04	0.49 \pm 0.09	3.00 \pm 0.60
SNX + R	0.57 \pm 0.07	0.36 \pm 0.10 [#]	0.48 \pm 0.08	0.45 \pm 0.10	1.88 \pm 0.70
SNX + Q	0.20 \pm 0.08 [§]	0.73 \pm 0.21 [*]	0.41 \pm 0.07	0.46 \pm 0.09	1.34 \pm 0.37
SNX + R + Q	0.25 \pm 0.06 [§]	0.45 \pm 0.14 [*]	0.32 \pm 0.08 [*]	0.42 \pm 0.17	1.04 \pm 0.30 [*]
ANOVA	$p < 0.05$	$p < 0.05$	$p < 0.05$	ns	$p < 0.05$

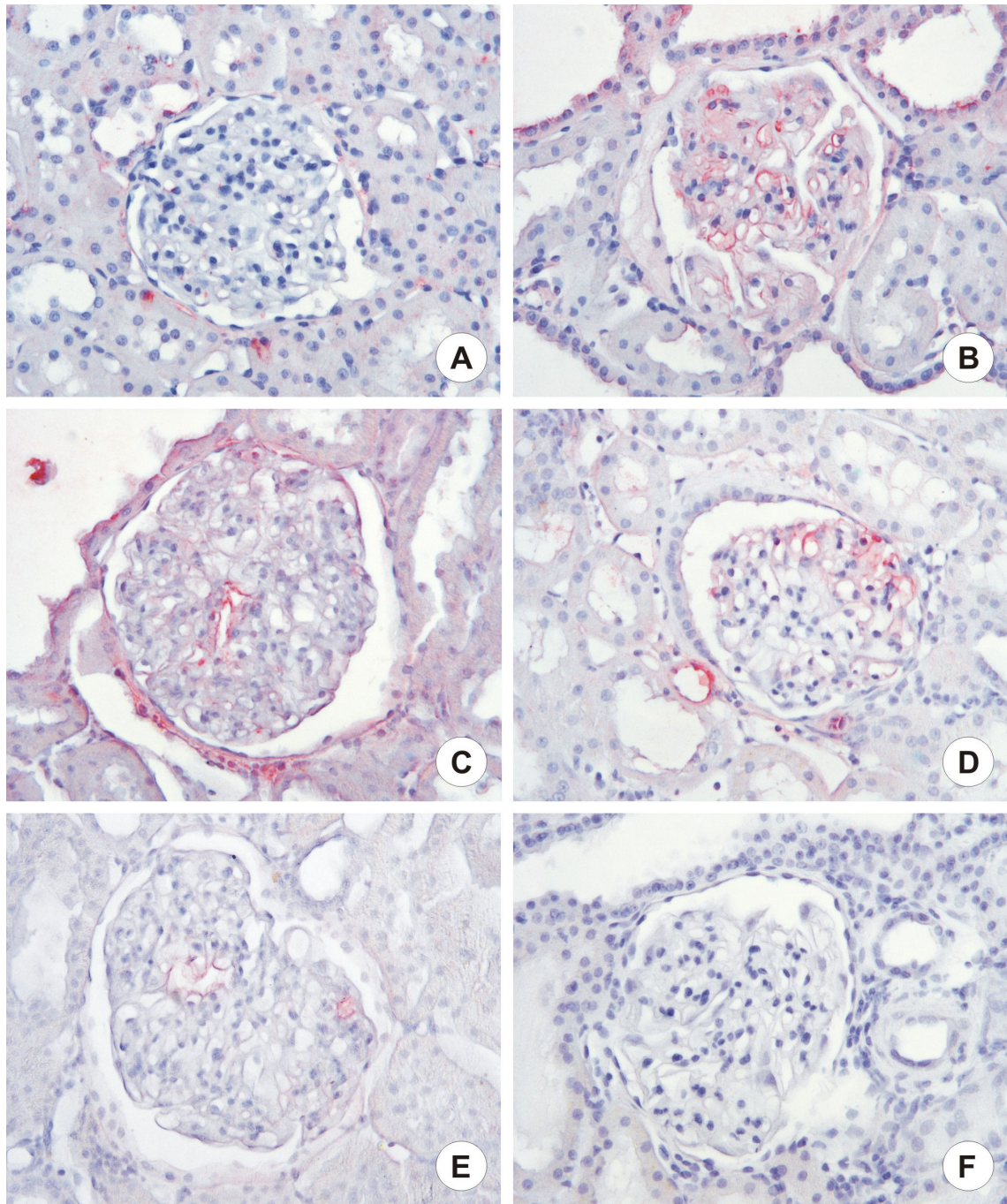


Figure 8. TGF- β_1 immunohistochemical staining of glomeruli. A: sham-nephrectomized animal, B: SNX, C: SNX+Q, D: SNX+R, E: SNX+Q+R, F: negative control. Magnification x400.

The protein expression of the nitric oxide (NO) producing enzyme NOS-3 (eNOS) in the glomeruli was mildly elevated in untreated SNX animals. Combined interventions, but not single interventions, normalized protein expression of NOS-3 (eNOS) in glomeruli (Table 8). A similar trend was seen with NOS-3 mRNA, but the differences between the groups were not significant.

The protein level expression of NOS-1 (nNOS, an other important NO producing enzyme in the kidney) in macula densa cells was reduced by 30% in SNX, compared to shams. It was unaffected by rhizotomy and Quinapril, but was normalized by combined intervention (Table 8).

Table 8. Immunohistochemical analysis of nitrosoxidative markers in the glomeruli and eNOS real-time PCR results in whole kidney samples. Data are presented as mean score \pm SD and mean relative expression level \pm SD, respectively. * $p < 0.05$ vs SNX; # $p < 0.05$ vs SNX+R+Q.

Group	nitrotyrosine	nNOS	eNOS	eNOS RT-PCR
Sham	0.14 \pm 0.04	0.73 \pm 0.13	0.58 \pm 0.11	0.88 \pm 0.16
Sham + R	0.17 \pm 0.09	0.76 \pm 0.09	0.72 \pm 0.27	0.91 \pm 0.14
Sham + Q	0.15 \pm 0.03	0.77 \pm 0.13	0.79 \pm 0.14	0.76 \pm 0.32
Sham + R + Q	0.11 \pm 0.04	0.79 \pm 0.03	0.67 \pm 0.36	0.95 \pm 0.17
SNX	0.98 \pm 0.18	0.46 \pm 0.09	1.33 \pm 0.09	1.33 \pm 0.39
SNX + R	0.89 \pm 0.11 [#]	0.47 \pm 0.18 [#]	0.84 \pm 0.09	0.93 \pm 0.12
SNX + Q	0.66 \pm 0.12	0.63 \pm 0.09	0.72 \pm 0.04	0.98 \pm 0.28
SNX + R + Q	0.50 \pm 0.11 [*]	0.80 \pm 0.11 [*]	0.65 \pm 0.15 [*]	1.00 \pm 0.13
ANOVA	$p < 0.005$	$p < 0.05$	$p < 0.005$	ns

Nitrotyrosine staining marked the oxidative stress of podocytes. The staining was more intense in untreated SNX rats compared to sham-operated rats (Table 8). It was not affected by rhizotomy, but reduced to some extent by quinapril and completely normalized by combined intervention (Figure 9).

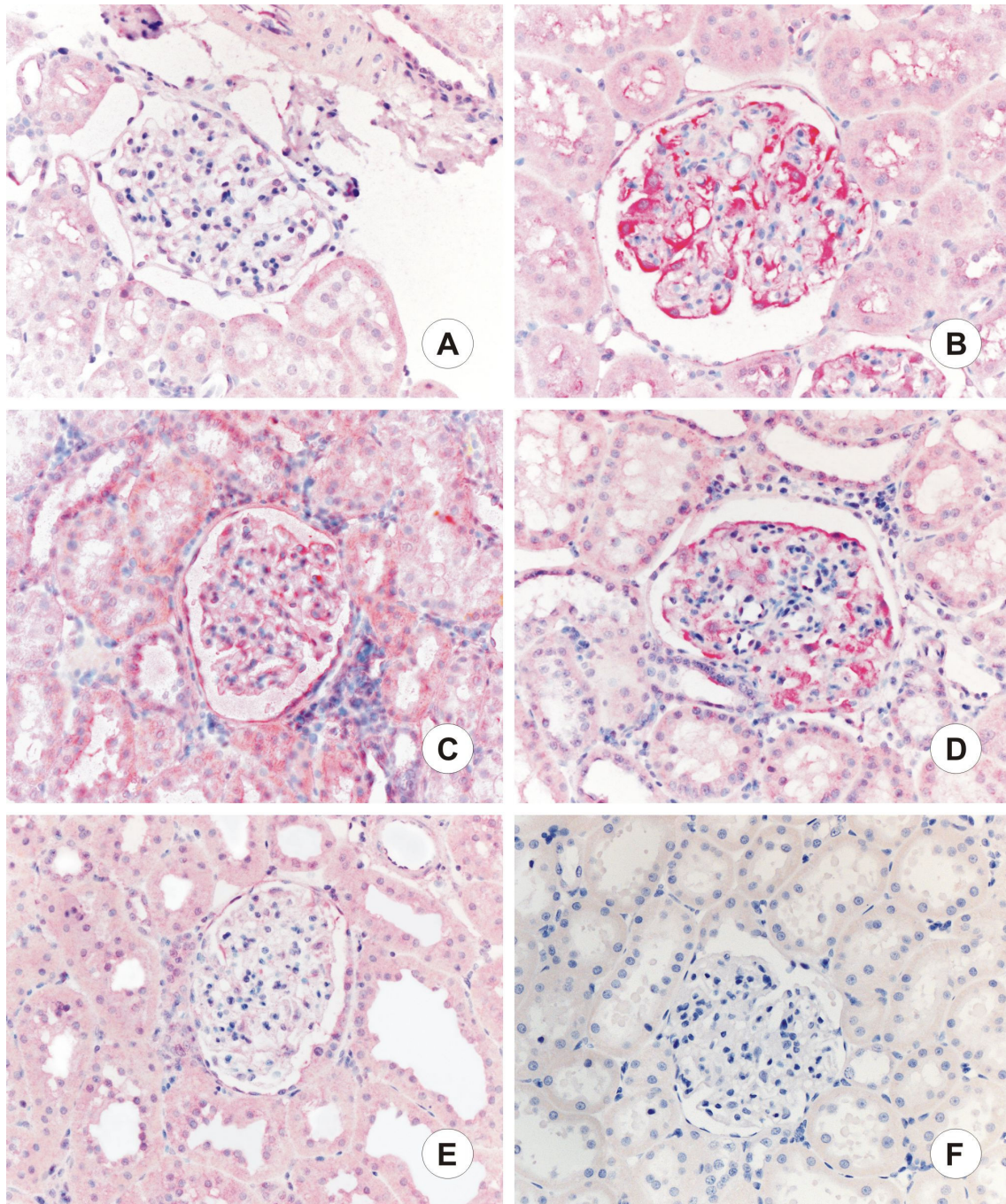


Figure 9. Nitrotyrosine immunohistochemistry of podocytes. A: sham-nephrectomized animal, B: SNX, C: SNX+Q, D: SNX+R, E: SNX+Q+R, F: negative control. Magnification x400.

4.2 RESULTS B (LUPUS NEPHRITIS)

4.2.1. Survival and kidney function

Pregnancy modifies the systemic cytokine expression favouring the production of anti-inflammatory cytokines [143]. As in murine lupus IFN- γ is thought to be a main contributor of the disease [118, 155], we expected an improvement of renal pathology and survival in multiparous animals due to a continuous shift towards anti-inflammatory cytokine production as a consequence of repeated pregnancies [139]. In contrast to our expectations, the life span of multiparous (M) females was significantly shortened to 20 weeks. Only 30% of M mice were alive at the age of 20 weeks compared to 78% of virgin (V) mice (Figure 10). In this first study, 60% of M animals showed uremic symptoms (such as: subcutaneous water retention, fuzzy hair, tremors, and severely reduced activity) preterminally, at 20 weeks of age, with blood urea levels exceeding 20 mmol/l.

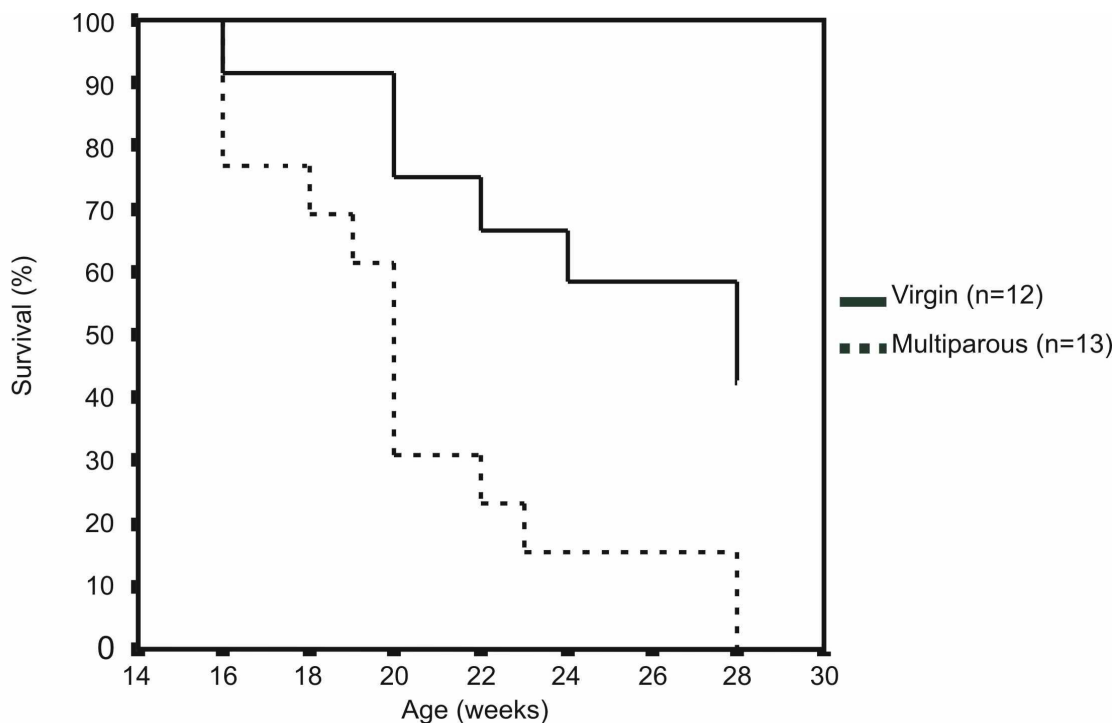


Figure 10. Survival curves. Life span of multiparous mice (dotted line) was significantly shortened compared to virgin animals ($p=0.038$, Kaplan-Meier, Log rank test, V vs M).

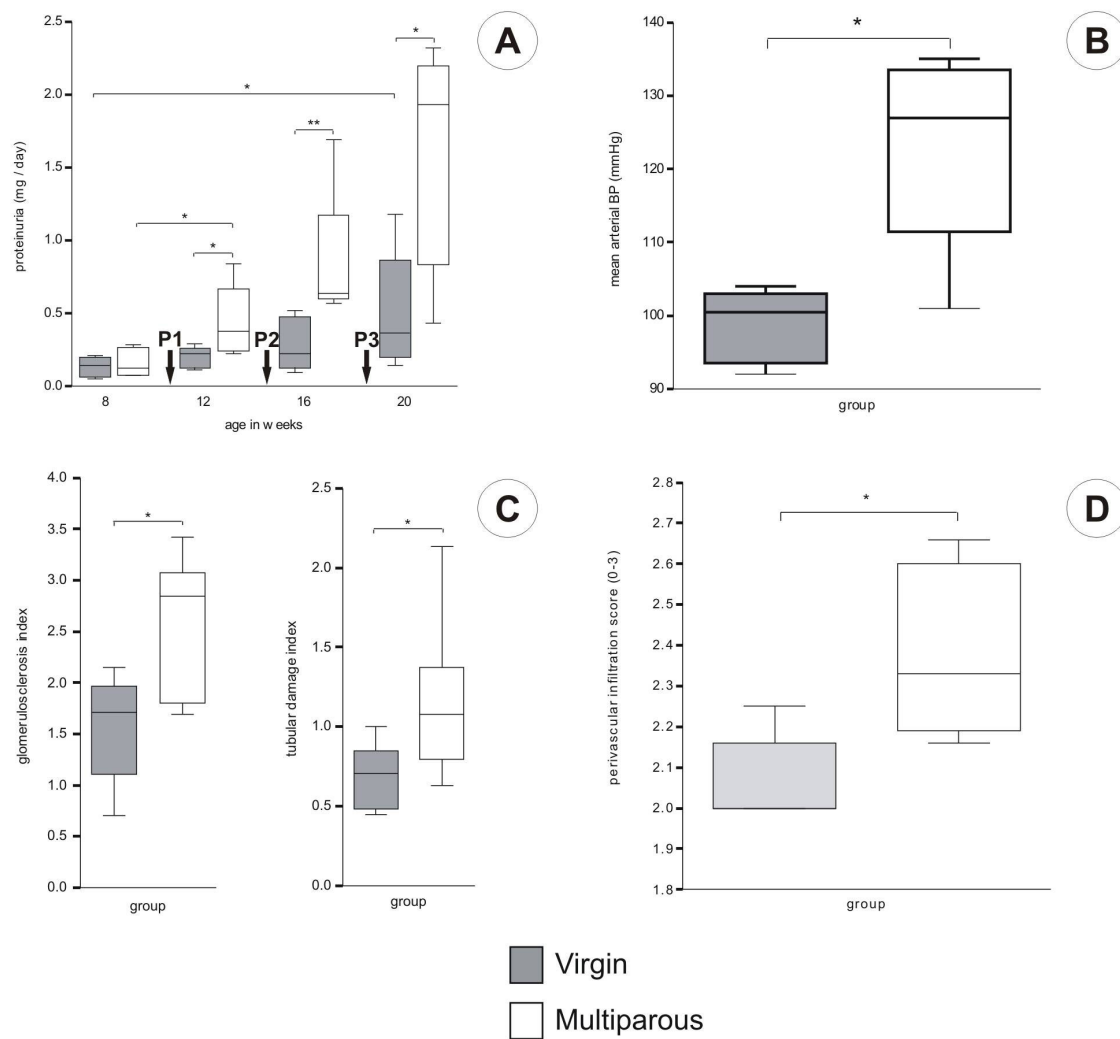


Figure 11. Kidney function and histology scores. A: Proteinuria (n=5-8/group, Mann-Whitney-test) B: Mean arterial blood pressure at harvest (t-test, p=0.019, M:n=4, V:n=6). C: Glomerulosclerosis (V vs M p=0.037) and tubular damage (V vs M p=0.028) indices (n=9/group, Mann-Whitney-U test). D: Perivascular infiltration index (n=9/group, V vs M p=0.01, Mann-Whitney-U test). Data are presented as median \pm 75% quartiles, *: p<0.05 V vs M, **: p<0.05 M 12 weeks vs M 8 weeks. P1-P3: number of respective pregnancy.

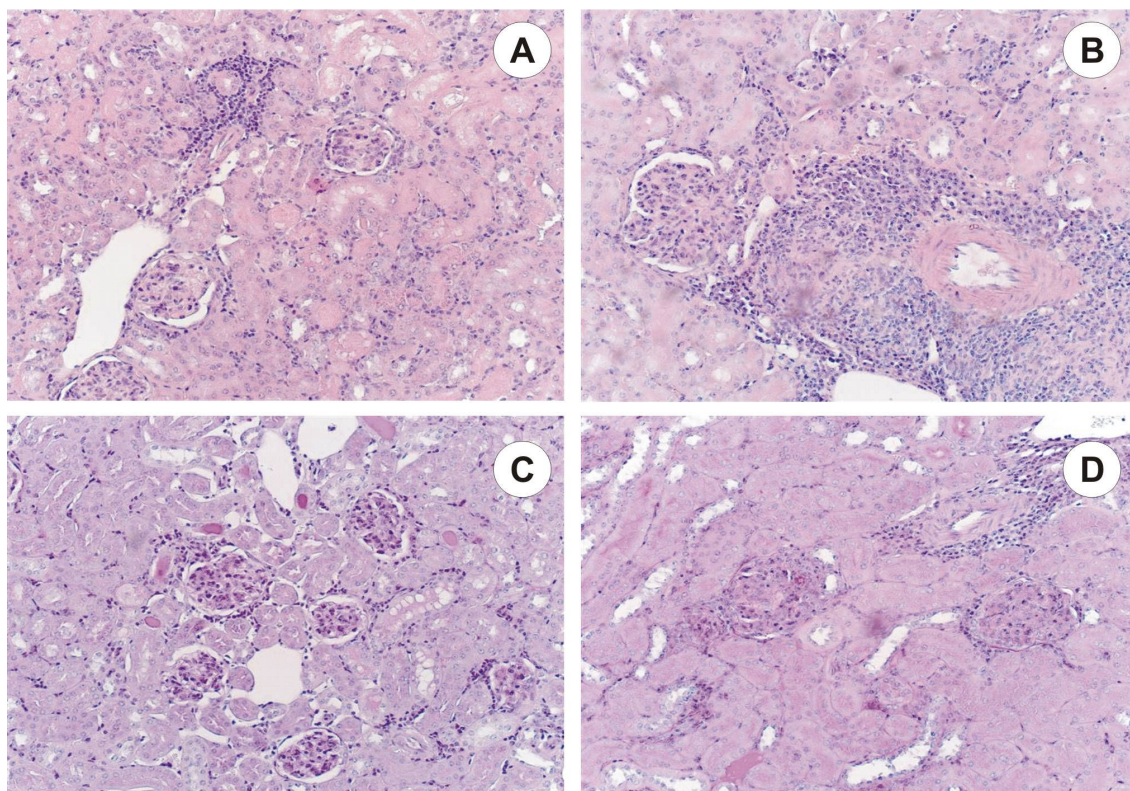


Figure 12. Representative photomicrographs of kidney histology. Vasculitis (A) and normal glomerular structure (A,C) of virgin kidneys, multiparous kidney with massive mononuclear infiltrate (B) and sclerotic glomeruli (D). (A,C: H&E stain; B,D: PAS stain).

Proteinuria levels started to increase at 12 weeks of age (median 0.22 ± 0.07 mg/24h vs 0.38 ± 0.2 , V vs M, $p=0.029$, $n=5-8$ /group) and reached 2.0 mg/day at week 20 in multiparous animals ($n=5$), while virgin mice ($n=8$) showed only mild increase in proteinuria (Figure 11.A). Proteinuria of multiparous mice after the first pregnancy was significantly higher than before pregnancy ($p=0.029$, compared to 8 weeks of age, $n=5-8$ /group). In addition, surviving multiparous animals showed significantly worsened kidney function and 70% of M mice died with uremic symptoms during follow up. BUN levels closely paralleled proteinuria.

The severe kidney dysfunction was accompanied by elevated mean arterial blood pressure (Figure 11.B) in multiparous mice compared to virgin animals.

Histological evaluation of the kidneys showed that renal lesions were markedly increased in multiparous mice according to the functional data. Both glomerulosclerosis

and tubulointerstitial damage indices (Figure 11.C) as well as perivascular infiltration were more severe in the multiparous group (Figure 12). However, there was no difference in the extent of periglomerular infiltration (median score: V:0.76 vs M:0.74, ns, n=9/group) and vascular damage indices between the groups (median score: V:1.49 vs M:1.71, ns, n=9/group).

The number of CD3⁺ infiltrating cells in the kidneys did not differ between the two groups (median: V:320 vs M:384 cells/mm², ns, n=8/group). Evaluation of IgG (Figure 13.A,B) and C3 (Figure 13.C,D) in cryostat kidney sections showed an increased deposition of both IgG (median fluorescence intensity: V:31.1 vs M:47.1, p=0.02, n=4/group) and C3 (median score: V:2.04 vs M:2.76, p=0.033, n=4/group) in multiparous mice.

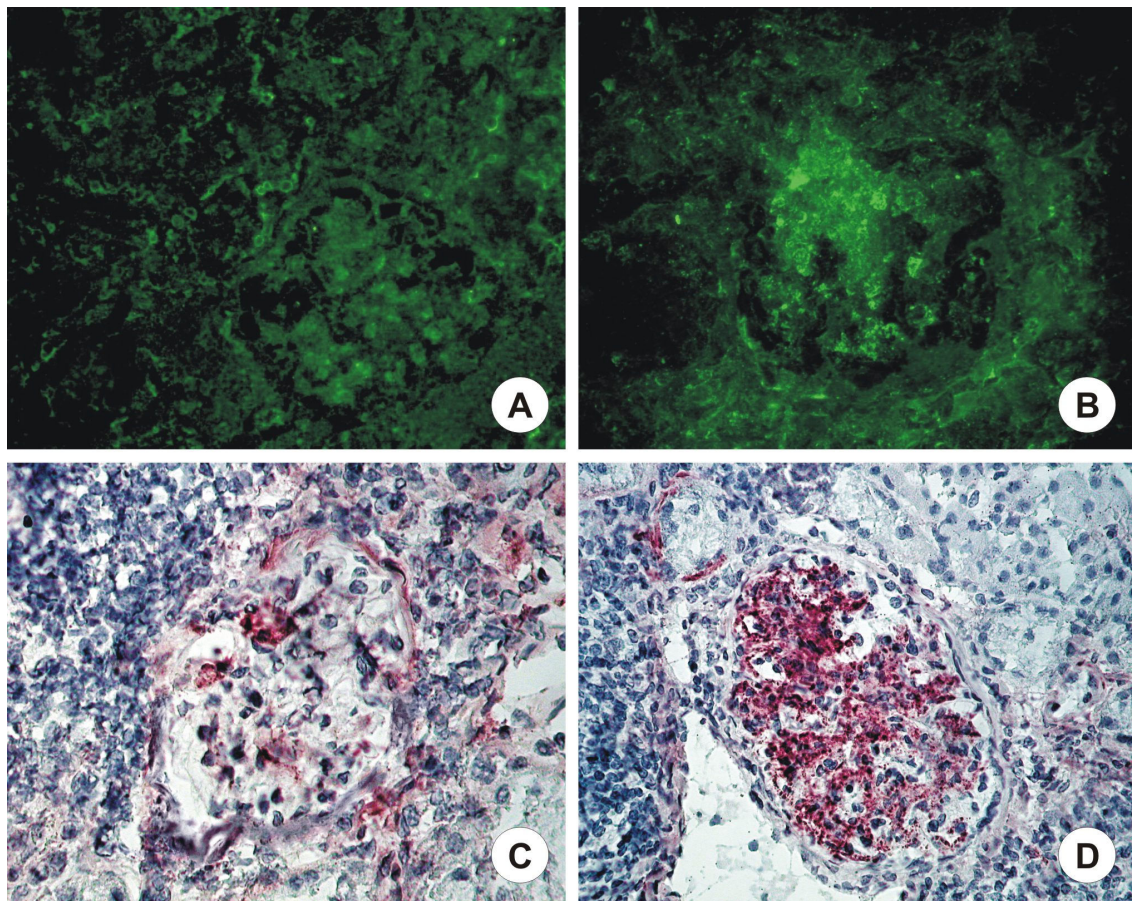


Figure 13. Representative photomicrographs of IgG and C3 deposition in the kidneys. A,B: Direct immunofluorescence of IgG deposits (A: Virgin, B: Multiparous). C, D: Immunohistochemistry of C3 (C: Virgin, D: Multiparous). Magnification x400.

4.2.2. Lymphoproliferation and anti-dsDNA levels

Systemic change in cytokine balance during pregnancy can possibly affect lymphoproliferation, B-cell activity and/or autoantibody levels, both systemic characteristics of SLE in MRL/lpr mice. Despite the fact that the proportion of CD8⁺ T-cells was consistently lower in blood samples of multiparous mice (V: 6.48 ± 0.94 vs. M: 4.8 ± 1.16 , mean percent of total lymphocytes \pm SD), there was no difference in the percentage of CD4⁺ CD8⁻ B220⁺ DN cells (V: 67 ± 9.3 vs. M: 62.1 ± 18.3) or CD19⁺ B-cells (V: 1.86 ± 1.48 vs. M: 1.43 ± 1.15) between the groups. Anti-dsDNA antibody levels in the plasma of multiparous animals were similar to those of virgin mice (median OD₄₅₀ at 12 weeks: V:0.226 vs M:0.232; at 20 weeks: V:0.317 vs M:0.294, ns, n=10/group). There was no significant difference in spleen or lymph node enlargement between the groups (data not shown).

4.2.3. IFN- γ production in the blood and the kidney

We observed significantly diminished plasma IFN- γ levels in multiparous mice when compared to virgin animals at the time of harvest (Figure 14.A), supporting the idea that pregnancy is accompanied by a diminished systemic production of proinflammatory cytokines [143, 156]. To evaluate whether altered cytokine production at the organ level could contribute to the changes seen in the kidney, IFN- γ , IL-10 and IL-4 mRNA levels were measured in the kidneys. Interestingly, in the kidneys of multiparous mice, expression of IFN- γ , IL-10 and IL-4 were significantly higher compared to virgins (Figure 14.B,C).

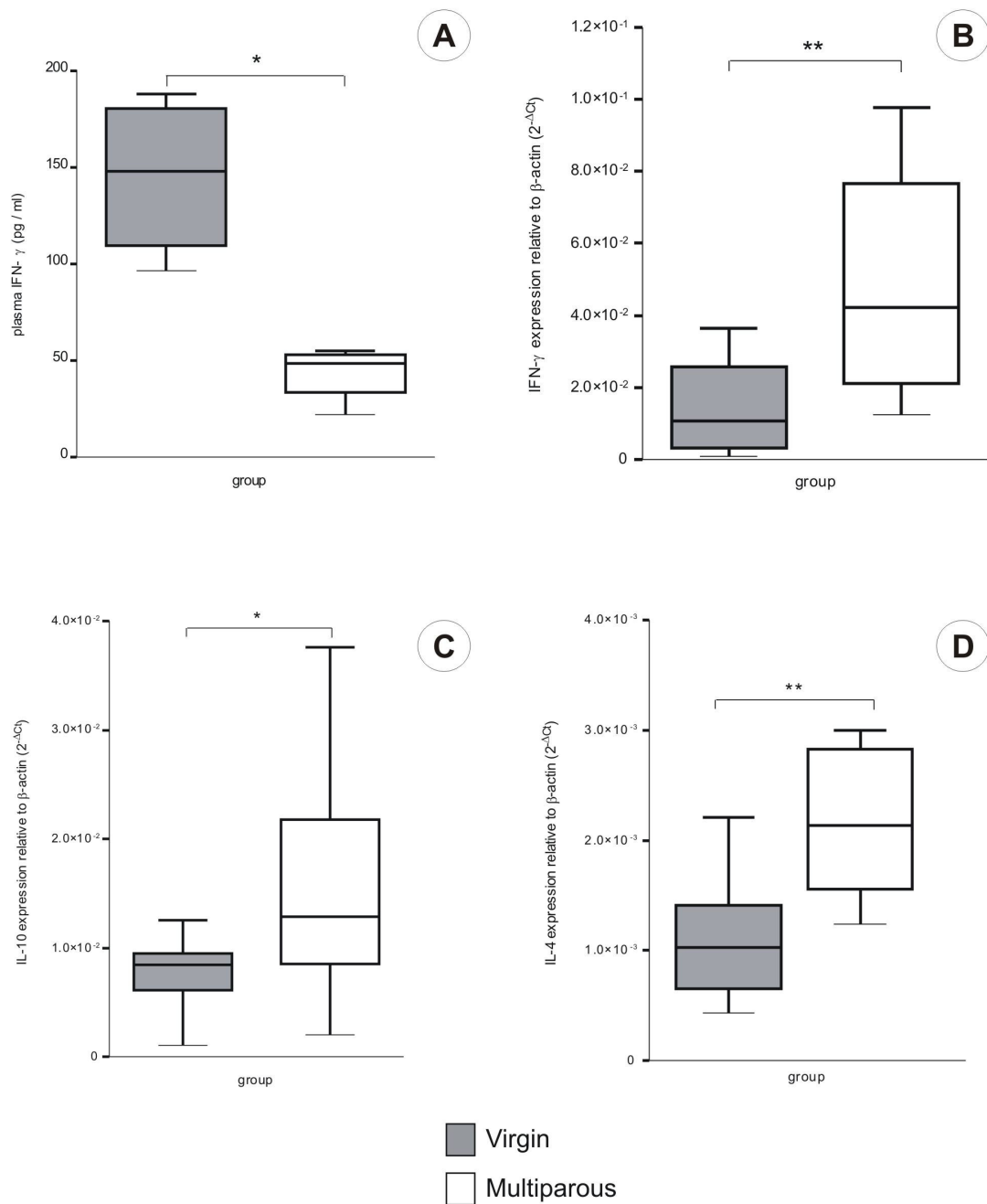


Figure 14. Cytokine expression in blood and kidneys. A: Plasma IFN- γ levels were significantly lower in multiparous mice at the time of harvest, compared to virgins ($p=0.028$, $n=4/\text{group}$, Mann-Whitney-U test). B-D: Renal cytokine mRNA expression analysis showed upregulation of both IFN- γ (B, $p=0.005$, V:n=11, M:n=9), IL-10 (C, $p=0.033$, V:n=11, M:n=9) and IL-4 (D, $p=0.009$, V:n=8, M:n=7) in multiparous animals. Data are presented as medians \pm 75% quartiles, *: $p<0.05$, **: $p<0.01$ V vs M, Mann-Whitney-U test.

5. DISCUSSION

5.1 DISCUSSION A (RENAL FIBROSIS)

Surgical 5/6 nephrectomy (subtotal nephrectomy, SNX) in the rat is a widely used model for experimentally induced progressive GS. In 1981, Brenner and Hostetter demonstrated more than two decades ago that the hyperfiltration of the remnant nephrons act as progressive factor for GS [157]. Experimental renal failure by surgical ablation leads to marked structural alterations of the remaining renal tissue, i.e. glomerular hypertrophy, glomerulosclerosis, vascular lesions and tubulointerstitial damage [158, 159]. The outcome of glomerular remodelling depends on the balance between healing and scarring influences. Resolution of microinflammation, return of glomerular cells to a mature phenotype, halting the excessive ECM synthesis, and the breakdown of the deposited ECM favour healing. By contrast, persistent and continuing activation damage of the glomerular endothelial-mesangial-epithelial axis will lead to cell death through apoptosis as well as their replacement by ECM (Figure 15).

Apart from hypertension, several non-haemodynamic factors are thought to play a role in the development of such renal changes, e.g. glomerular growth, activation of the local renin-angiotensin systems, inappropriate activation of the sympathetic nervous system, elevated levels of parathyroid hormone, to name only a few. It is well known that systemic hypertension accelerates progression of renal failure [160]. Conversely, antihypertensive treatment prevents progression [161]. Several studies [162, 163] demonstrated class-specific effects of different antihypertensive agents, particularly ACE inhibitors. Such actions can possibly be dissociated from lowering of (casual) blood pressure [161, 162]. This observation supports the notion that non-hemodynamic actions are involved.

We deliberately used a model of moderate ablation of cortical mass by surgical resection causing reproducible reduction of the number of glomeruli (table 4). Resection involved the outer cortex, so that the kidney remnant contained a disproportionate number of juxtamedullary glomeruli, which are known to have higher glomerular capillary pressure [164] and to be more susceptible to injury.

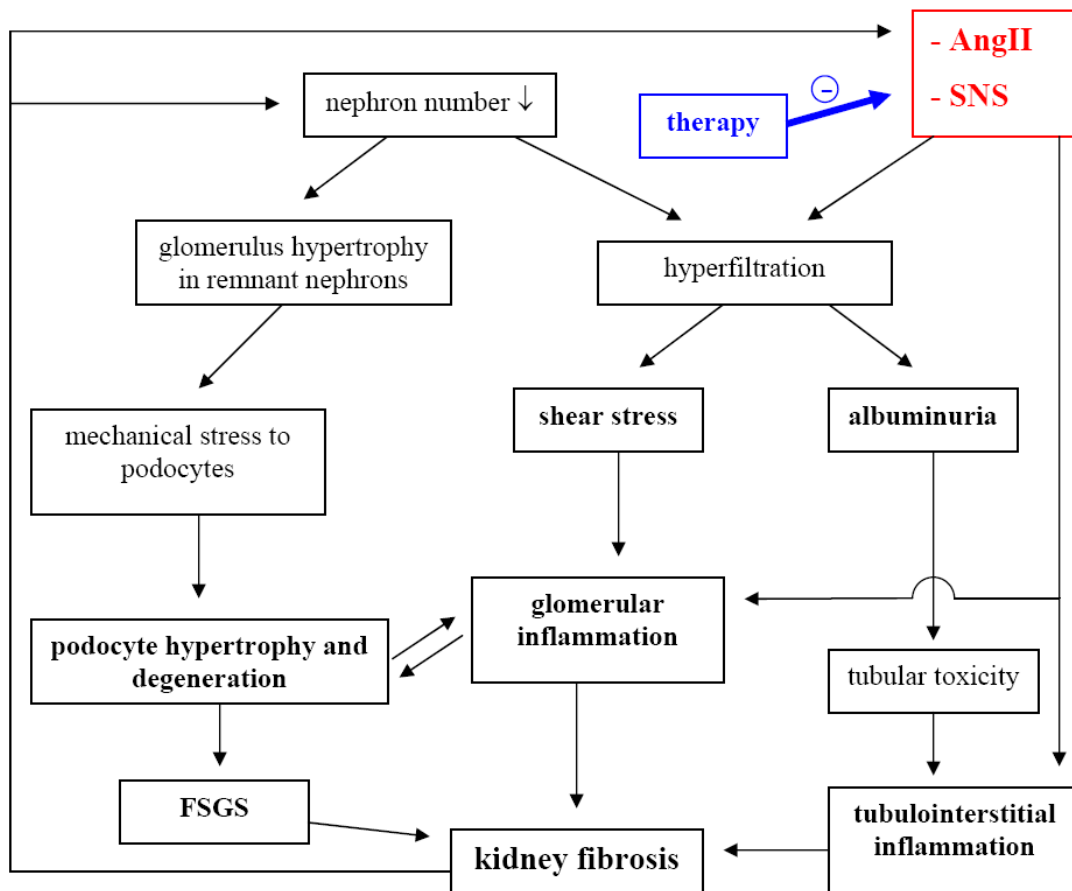


Figure 15. Possible pathomechanism of progressive renal fibrosis. The applied therapies in our experiment (blue box with blue arrow) inhibited the overactivation of the sympathetic nervous system (SNS) and the overproduction of angiotensin II (AngII), the two major contributors of progression (red box).

From the large scale of available ACE-inhibitors we deliberately used Quinapril, as it has been reported, that this formulation can reach the highest tissue concentrations in the kidney, and thus would best inhibit local tissue RAS [165].

High dose ACE inhibitor strikingly attenuated the development of glomerulosclerosis as well as tubular and interstitial damage, confirming previous results. In ACE inhibitor treated animals podocyte volume and mesangial cell numbers were strikingly lower. Furthermore we saw diminished TGF- β_1 expression and less staining for nitrotyrosine in podocytes. These results further support the importance of non-hemodynamic actions of AngII, as it is capable of inducing the production of oxgene radicals, cytokines, stimulation of ECM synthesis, apoptosis, proliferation and hypertrophy [37, 166].

Hypertension in chronic renal disease is to a large part due to sympathetic overactivity triggered by afferent signals emanating from the kidney and resetting sympathetic tone by stimulation of hypothalamic centres [167]. Sympathetic overactivity not only elevates blood pressure but accelerates progression of renal failure. Renal sympathetic nerves are a critical link between the sympathetic nervous system and long-term arterial pressure control [168]. We did not intend to eliminate efferent renal sympathetics as this may increase renal resistance [70] and cause denervation natriuresis [71] leading to a rebound activation of RAS. Such stimulation of RAS synthesis might have obscured the findings in the rhizotomy single intervention group. Thus, we preferred a more selective surgical ablation of sympathetic afferentation from the diseased kidney, leaving the rest of the sympathetic nervous system intact.

One of the main effects of the SNS in the kidney is activation of the juxtaglomerular apparatus [169]. General sympathetic inhibition has been shown to be nephroprotective: in SNX rats moxonidine or metoprolol reduced glomerular damage and blood pressure independently [67, 68]. Also in patients, the general inhibition of the SNS by moxonidine proved beneficial on top of RAS inhibition in progressive renal disease [170, 171]. In their paper, Vonend et al conclude, that the idea of a sympatholytic drug to be renoprotective is appealing but needs further evaluation. Finally, in diabetic patients reduction of sympathetic activity by moxonidine lowered albumin excretion independent of blood pressure [172].

Elimination of sympathetic activity by rhizotomy, i.e. through the interruption of the afferent sympathicostimulatory signals emanating from the kidney, had strikingly beneficial effects on glomerulosclerosis and indices of interstitial damage. Rhizotomy also led to greater length density and total length of glomerular capillaries. This finding is consistent with the observation that sympathetic activity suppresses capillary formation in the heart [173]. These findings were accompanied by markedly lower albuminuria. SNS inhibition proved to be more protective than RAS inhibition in prevention of interstitial collagen deposition and preserving GFR as demonstrated by retention parameters (serum creatinine, BUN).

In addition, rhizotomy amplified the beneficial effects of ACE inhibitor. Albuminuria was significantly lower in SNX rats with Quinapril plus rhizotomy. Tubular and interstitial damage indices were also significantly lower than in SNX on Quinapril monotherapy. Additional benefit of SNS inhibition over maximal RAAS inhibition suggests RAS independent beneficial effects of SNS inhibition.

Systolic blood pressure by tail pletysmography and telemetry was lowered, but not normalized, by rhizotomy alone, confirming results of Campese [65]. Modest further reduction in systolic blood pressure was seen in SNX treated with Quinapril plus rhizotomy. Although tail pletysmography showed significant differences in blood pressure between groups, these differences were minimal by telemetry, the more reliable method. It is unlikely that such small blood pressure differences account, for instance, for the marked differences of nitrosoxidative stress in podocytes.

Paradoxically, but in line with our previous experiments Quinapril treated animals consistently had higher serum creatinine and urea concentrations, possibly because of lower glomerular capillary pressures and filtration rates secondary to diminished efferent resistance [67, 174]. The serum creatinine concentration was significantly ($p < 0.05$) lower in animals with rhizotomy, either alone or in combination with Quinapril, possibly pointing to an independent beneficial effect of reduced sympathetic activation on intrarenal hemodynamics. Sympathetic signals are a potent stimulus for renin transcription and secretion [75, 169], but in animals with RAS blockade it is unlikely that the effect of abrogation of sympathetic activity was mediated by changes in renin secretion, since the high dose of the ACE inhibitor had already caused major inhibition of the juxtaglomerular RAS. In animals with rhizotomy, but not on Quinapril, the length density per glomerulus was largely preserved. It had previously been shown that in SNX rhizotomy normalized the reduced capillary length density in glomeruli [68] and the same had previously been noted in the heart [173]. Rhizotomy failed to affect glomerular capillary length density in sham operated animals, but it apparently modulated the effect of nephron loss on glomerular capillarogenesis. Interestingly, changes in capillary length density were not accompanied by commensurate changes in endothelial cell number and endothelial cell volume: the

endothelial cell number was influenced by Quinapril, but not by rhizotomy. Angiotensin II is known to be an agonist for mesangial cell proliferation; it is therefore not surprising that in Quinapril treated SNX the mesangial cell number was lower. It was not affected by rhizotomy despite the known role of catecholamines on mesangial cell proliferation [175]. The increase in podocyte volume was partially reversed by Quinapril. This observation is consistent with recent observations that podocytes have a potent local RAS, can produce AngII and express AT1 receptors [15].

Certainly the best established and one of the most investigated profibrotic cytokines in renal scarring is TGF- β 1. Glomerular TGF- β 1 expression was significantly lower in SNX animals treated by combination therapy. It is true that ANGII increases the expression of TGF- β 1 and this is thought to mediate the profibrotic action of ANGII [176, 177], but sympathetic activity also seems to play a role: moxonidine decreased glomerular TGF- β 1 mRNA in SNX rats [67].

Nitrotyrosine is a stable metabolite of oxidatively modified nitrogen monoxide (NO), a result and a marker of nitros-oxidative stress. A 10-fold elevation of nitrotyrosine staining despite reduced expression of nitrogen monoxide synthases (eNOS), suggests massive oxidative stress in untreated SNX animals. Nitrotyrosine was mainly localized to podocytes, and the oxidative injury in podocytes could significantly contribute to progression of GS in our model. Double intervention preserved both eNOS expression, and normalized nitrotyrosine staining to sham-control levels.

Experimental evidence suggests that proteinuria has also an important role in the initiation of tubulointerstitial inflammation [178]. Proteinuria, for example, is a potent stimulator of the RAS in proximal tubular cells [179]. Excessive reabsorption of albumin by proximal-tubule cells in vitro stimulates the release of various proinflammatory mediators including chemokines. These agents in turn could attract inflammatory cells to the renal interstitium and initiate interactions with interstitial fibroblasts. Activation and proliferation of fibroblasts and myofibroblasts and the associated excessive synthesis of ECM could culminate in interstitial fibrosis [180, 181].

Injured tubules undergo programmed cell death (apoptosis) leading to tubular atrophy and the formation of atubular glomeruli. Under the influence of TGF- β_1 , some tubular cells become transformed into an embryonic phenotype, thus acquiring mesenchymal properties similar to those of fibroblasts and myofibroblasts [12, 181, 182]. Tubular cells could therefore contribute to the pool of cells directly involved in renal fibrogenesis. The outcome of tubulointerstitial injury depends on the capacity of inflammation to regress, tubules to regenerate, fibroblasts to die, and ECM to be broken down. Continuing injury, inflammation, and fibroblast activation and proliferation will lead to irreversible fibrosis. In our study, tubular damage was markedly reduced by Quinapril treatment. But more importantly, Quinapril plus rhizotomy could completely normalize tubular and interstitial damage scores, further supporting the beneficial effect of combination therapy over monotherapies.

5.2 DISCUSSION B (LUPUS NEPHRITIS)

The design of our study deserves some comment. Allogeneic matings (with NMRI males) were performed primarily for their relevance to humans, as the clinical case is generally the combination of a healthy, allogeneic male + lupus patient mother. Secondly, congenic MRL/lpr males have low testosterone level [183] and low fertility. Thus, the rate of matings can not be calculated exactly, which does not allow the exact timing of parturition required in our study. Therefore, we could not include a syngeneic control group. It has to be noted, that in our MRL/lpr breeder colony, we have observed similar amelioration of skin disease, but a shortened life span compared to non-breeder females. This suggests that the observed alterations in disease activity are rather a consequence of pregnancy per se and not of the repeated allogeneic exposure. In conclusion, although the present study cannot dissect the effects of repeated allo-exposures from the effects of repeated pregnancies, the two cannot be separated in the clinical situation either, as human pregnancies are always allogeneic.

In multiparous mice, a faster deterioration of kidney function was manifested in elevated blood pressure and a shortened survival period. Although 7 month (28 weeks) 50% survival in control MRL/lpr mice suggests an unusual mild disease, similar results with even longer (33 weeks) 50% survival had been observed by Robey *et al* [184]. Factors possibly contributing to long survival are, that animals at our facility are housed in an individually ventilated cage (IVC) system, which provides a strong protection from pathogens – a possible stimulus to the immune system inducing or exacerbating the autoimmune pathology. Furthermore, for the present experiment, animals were housed two per cage (in large cages), further reducing disease promotion by fighting behavior.

Renal flare and pre-eclampsia are sometimes hard to distinguish in human SLE pregnancy. This clinical observation rise the possibility of pre-eclamptic effects in our experiment. Despite we found elevated blood pressure in multiparous mice after the third pregnancy (130-140 mmHg), this hypertension did not reach the typically high levels of the murine model of pre-eclampsia (220-250 mmHg [185]). Moreover, we did not see the typical glomerular hypercellularity and increased periglomerular infiltration

described in the murine pre-eclampsia model, but found no difference in periglomerular infiltration between multiparous and virgin mice. Furthermore, the timing of death in the multiparous group was not associated with third trimester of pregnancy, but death was always accompanied by symptoms of renal failure. These observations suggests that pregnancy itself did not lead to pre-eclampsia in MRL/lpr mice, and we interpret the rise in blood pressure as a symptom of diminishing renal function.

In murine experiments, as well as in normal human pregnancy, there is a systemic cytokine profile change during gestation including increased production of IL-4 and IL-10 [139, 142, 143, 156] accompanied by decreased IFN- γ expression [186].

Lupus nephritis in the MRL/lpr mice and other murine lupus models [118, 119], as well as in humans, has been strongly associated with a predominant proinflammatory cytokine [187] and IFN- γ overproduction [188, 189]. Elevated IFN- γ production has been demonstrated in MRL/lpr mice, compared to MRL controls [118] and IFN- γ knockout MRL/lpr [190] mice had dramatically ameliorated nephritis [119] and improved survival time. The induction of IFN- γ production (by administration of IL-12 [191]), worsened the progression of glomerulonephritis [192, 193] and decreased intrarenal IFN- γ production (in IL-12p40 knockout mice) delayed the onset of nephritis in MRL/lpr mice [194]. In NZBxNZW F1 mice, administration of IFN- γ exacerbated lupus nephritis while the administration of a monoclonal anti-IFN- γ antibody ameliorated the progression of lupus nephritis [195]. Lupus patients with diffuse proliferative nephritis showed increased IFN- γ expression levels both in blood and kidney biopsy samples [187, 196]. In summary, IFN- γ seems to be a key exacerbating cytokine in lupus nephritis. These data support our observation that, in renal samples of the M group with more severe nephritis, IFN- γ production was enhanced, despite lower serum IFN- γ levels in these animals.

Whether IL-10 and IL-4 are beneficial or deleterious in lupus is still a point of discussion. IL-10 is an important anti-inflammatory cytokine which inhibits mononuclear cell infiltration [123, 124]. On the other hand, IL-10 acts as a potent activator of B-cells, promoting antibody production [122]. In the MRL/lpr model, IL-10 knock-out mice had accelerated glomerulonephritis with shortened survival time,

compared to wild type MRL/lpr. Administration of recombinant IL-10 to MRL/lpr mice ameliorated the disease [127], suggesting a protective role of IL-10 [127].

Surprisingly, not only IFN- γ but the anti-inflammatory cytokines IL-10 and IL-4 were also augmented in multiparous kidneys. There is evidence that treatment of mice with both anti-IL-4 [197] and anti-IL-10 [198] antibodies ameliorated lupus nephritis, thus supporting our hypothesis that high IL-10 levels in the kidney may worsen nephritis via promoting B-cells to produce autoantibodies, leading to increased glomerular IgG deposition. In a recent study, Enghard *et al.* described a positive correlation between both IL-4 and IL-10 production and kidney damage of lupus prone NZB/W F1 mice, supporting our results [199]. A recent study on human kidney biopsies also described high glomerular IFN- γ and IL-10 mRNA expression [200], and the expression of these cytokines correlated with disease activity. These findings are supported by the study of Lit and colleagues as well. They found significantly higher relative IFN- γ /IL-4 mRNA expression in kidneys of lupus patients, compared to healthy controls [201]. All these clinical observations further support our findings in pregnant MRL/lpr mice.

The high IFN- γ expression in spite of IL-10 overexpression in multiparous kidneys seem to be surprising. A possible explanation could be that, at the age of the first pregnancy (8 weeks) young females already had detectable circulating autoantibodies, thus possibly had glomerular immune deposits also. Deposited immune complexes might have activated mesangial cells and recruited macrophages to produce IFN- γ . Elevated IL-10 production during gestation may result in B-cell activation and further immune complex deposition, thus enhancing local inflammation and IFN- γ production, leading to a self-sustained propagation of nephritis (Figure 16). Indeed, we found a deterioration in kidney function in our experiments beginning right after the first pregnancy, at 12 weeks of age. Moreover, we investigated the cytokine mRNA expression in MRL/lpr as well as MRL wild type mouse kidneys on day 14 of the first pregnancy, and found not only significantly higher IFN- γ and IL-10 expression compared to age-matched non-pregnant mice, but pregnancy increased glomerular IgG and C3 deposition as well (unpublished data). Recent studies in the autoimmune

NZB/W F1 mice suggest that cellular infiltration into the kidneys is a process regulated by local chemokine production [202].

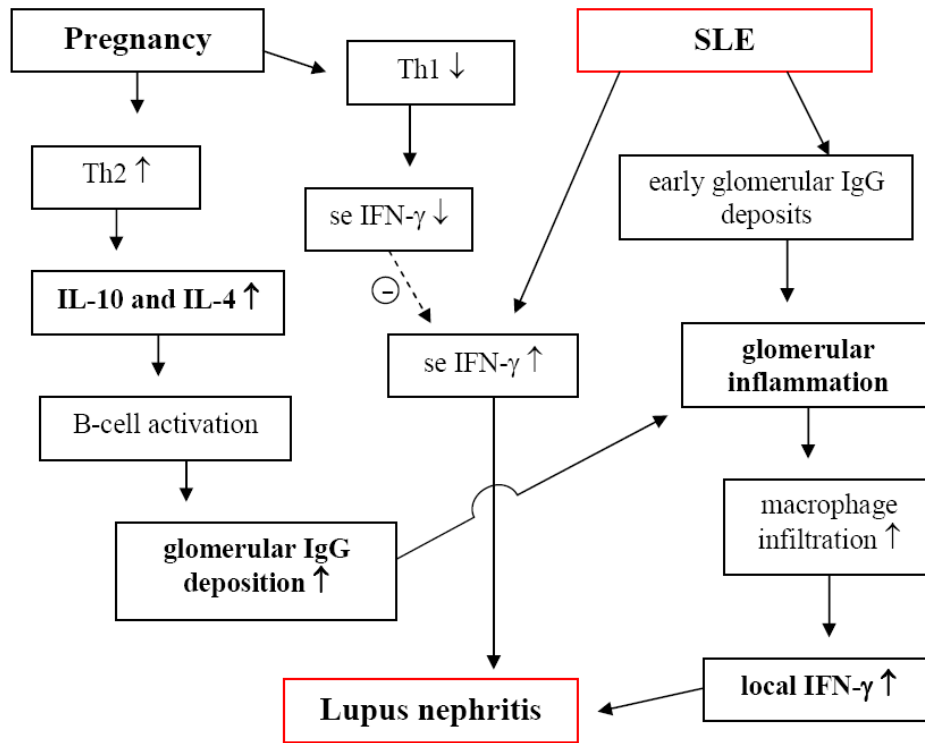


Figure 16. Possible role of cytokines on the pathomechanism of lupus nephritis in pregnant MRL/lpr mice. (Black arrow: activation, dotted arrow: inhibition.)

Renal blood flow increases about 30% in pregnancy, which leads to elevated intraglomerular pressure and elevated proteinuria. The higher intraglomerular pressure could activate endothelial cells, thus enhance the inflammatory phenotype. In our study, we found a mild proteinuria in virgin mice, but multiparous animals had markedly higher levels right after the first pregnancy. These results suggest that the hemodynamic changes could partly explain the high local IFN- γ expression, despite high IL-10 levels in multiparous kidneys. However, there is also evidence that pregnancy did not exacerbate proteinuria or histology in the rat models of renal mass reduction and Heymann nephritis [203, 204].

Hormonal changes during gestation are further issues that possibly affect the progression of SLE during pregnancy. Estrogens and progesterone have immunomodulatory effects. Estrogens may both stimulate or inhibit immune responses (reviewed in: [205]). Estrogens markedly enhance IL-10 production in human Th cells [206], raising the possibility of lupus nephritis exacerbation during pregnancy. Indeed, acceleration of glomerulonephritis was reported in MRL/lpr mice after estrogen administration [207, 208]. Another study showed an opposite effect of estrogen in MRL/lpr mice [209]. Lupus of NZB/W F1 mice was ameliorated after high estrogen treatment [210], but Verheul and colleagues reported that physiological doses of ethynilestradiol did not significantly affect lupus symptoms in NZB/W F1 mice [211]. We have previously demonstrated the nephroprotective effect of physiological doses of estrogens in the rat model of renal mass reduction [212]. In that study, estrogen administration markedly decreased proteinuria and the local production of TGF- β . However, these beneficial effects were abolished when estrogen was co-administered with progesterone [212]. Elevation of serum estradiol is often found in female patients with SLE, and sometimes is linked to active disease [213]. Progesterone favors a shift to Th2 type immune response [214], increases IL-4 production by T-cells [215], thus it may worsen lupus nephritis. However, it has also been recently suggested that the deleterious effect of estrogens is caused by the upregulation of prolactin. Prolactin alone is known to have deleterious effects on autoimmune disease [153], and to avoid this confounding factor pups were weaned immediately after birth in our study to avoid lactation, and prolactin production of M mice. Based on literature data, we can conclude that the role of sex-hormones in pregnancy-associated changes of lupus activity is controversial. A possible background of this controversy could be the organ-dichotomy we observed.

There was no difference in anti-dsDNA levels between multiparous and virgin mice, although serum IFN- γ levels were significantly lower in pregnant mice. We interpret the systemic change in IFN- γ as a cause of the systemic immune regulatory effect of pregnancy. Our finding of unchanged autoantibody levels seem to contradict the theory of Th2 shift in pregnancy, as an elevated anti-dsDNA level would be expected. However, the MRL/lpr mice have a genetic defect on Fas molecule, therefore

an uncontrolled systemic lymphoproliferation. The percentage of B-cells amongst PBMCs as well as splenocytes were similar in both groups, and this could explain the similar autoantibody levels observed, suggesting that systemic autoantibody production is not influenced by hormonal changes in pregnant MRL/lpr mice. Our observation of accelerated kidney disease suggest that local immune regulation could be at least partly independent of systemic changes.

Our findings suggest an important role of local immune regulation of lupus nephritis during pregnancy, independent of systemic changes of the cytokine profile. Moreover, pregnancy markedly aggravated lupus nephritis in our study, according to recent human data. In a retrospective clinical study of 61 pregnant lupus patients, Cavallasca *et al.* found a high rate of disease exacerbation during pregnancy, as well as 46% of preterm deliveries [216]. Thus, better understanding of the pathophysiology in lupus pregnancies might lead to more effective clinical management of these patients.

6. CONCLUSIONS

6.1 CONCLUSIONS A (RENAL FIBROSIS)

In subtotaly nephrectomized rats, concomitant abrogation of sympathetic activity strikingly augments the effect of ACE inhibition. Besides lowering sympathetic RAS stimulation, rhizotomy has RAS and blood pressure independent beneficial effects. Combined intervention prevented oxidative stress of podocytes, ameliorated hyperfiltration induced podocyte injury, and both glomerular and tubulointerstitial fibrosis. Hemodynamic independent effects of ACE inhibition / SNS inhibition strikingly ameliorated glomerular and tubulointerstitial inflammatory damage. This observation provides a rationale for combination treatment.

6.2 CONCLUSIONS B (LUPUS NEPHRITIS)

We first demonstrated a dramatic aggravation of lupus nephritis in mice undergoing multiple pregnancies, accompanied by significantly shortened lifespan. Our data suggest that systemic autoimmunity and kidney disease may be regulated differently from each other during pregnancy in MRL/lpr mice, and both IFN- γ and IL-10 may be important regulatory cytokines at the organ level. Thus, our data support the hypothesis that the kidney is not simply an “innocent bystander” in SLE, but local - possibly cytokine driven – mechanisms determine the faith of the kidney in this systemic disease.

7. ABSTRACT

Progressive renal fibrosis due to ongoing inflammation is the final common pathway of chronic renal failure (CRF), regardless of the etiology. The renin-angiotensin system is a key mediator of kidney fibrosis, and ACE inhibitors are widely used in the treatment of CRF patients. Blood pressure independent blockade of the sympathetic nervous system (SNS) also ameliorated kidney fibrosis in experimental and clinical studies. Although these therapeutic modalities have non-hemodynamic anti-inflammatory effects, monotherapies failed to halt disease progression. We investigated whether combined inhibition of the two systems provides additive renoprotection in experimental progressive glomerulosclerosis. In our model of subtotal nephrectomy (SNX), SNS blockade was achieved by dorsal rhizotomy and ACE was inhibited using Quinapril for 3 months. Blood pressure was not significantly influenced, but combination therapy markedly reduced both glomerulosclerosis and albuminuria. In the combination group, hypertrophy and oxidative stress of podocytes as well as glomerular TGF- β production was reduced to sham levels. In conclusion, combination of ACE inhibitor plus SNS blockade provided additional renoprotection to single interventions, demonstrating the independent contribution of these systems to progressive renal fibrosis.

Glomerulonephritis in systemic lupus erythematosus (SLE) may also lead to CRF. As the majority of patients are young women, the possible effect of pregnancy on progression is of great importance. Clinical data are contradictory, and little is known about the pathophysiology of nephritis in pregnancy. We investigated the effect of pregnancy on systemic autoimmunity of SLE prone MRL/lpr mice. Multiparous mice underwent 3 consecutive pregnancies. Kidney function, organ pathology and cytokine expression was compared to virgin mice. Survival and kidney function was dramatically reduced and accompanied by hypertension in multiparous group, associated with glomerular IgG and C3 deposition and increased local IFN- γ and IL-10 expression. However, serum IFN- γ level was reduced. We conclude that local cytokine production may play an important role in the aggravation of nephritis due to pregnancy, independently of systemic cytokine response. This study supports the hypothesis, that the extent of renal involvement is influenced by local factors in systemic lupus.

8. MAGYAR NYELVŰ ÖSSZEFOGLALÓ

Krónikus kísérletes gyulladásose vesebetegségek molekuláris mechanizmusai

A gyulladás mediálta progresszív vesefibrózis etiológiától függetlenül számos krónikus vesebetegség (KVB) végső közös útja. A renin-angiotensin rendszer központi szerepet játszik, így az ACE gátlók általánosan használt gyógyszerek KVB esetén. Emellett számos klinikai és kísérletes vizsgálatban nyert bizonyítást, hogy a szimpatikus idegrendszer (SZIR) vérnyomástól független gátlása lassítja a progressziót. Ezen kezelések hemodinamikától független gyulladáscsökkentő hatása ellenére monoterápiában nem képesek megállítani a progressziót. Ezért megvizsgáltuk, vajon e két rendszer együttes gátlása erősebb védő hatással bír-e kísérletes progresszív glomeruloszklerózisban. Szubtotális nefrektómia modellünkben dorzális rizotómia alkalmazásával értük el a SZIR gátlását, míg ACE gátláshoz ivóvízben oldott Quinaprilt adtunk az állatoknak. Egyik kezelés sem befolyásolta a vérnyomást. Ugyanakkor a kombinált kezelés erőteljesen csökkentette mind a glomeruloszklerózis, mind az albuminura mértékét, és az ál-operált állatokban mért szintre szorította vissza a podocitákat ért oxidatív stressz mértékét és a podociták térfogatát, valamint a glomeruláris TGF- β szintet. Mindebből arra következtettünk, hogy ACE-gátló és SZIR gátlás együttes alkalmazása a monoterápiáknál erősebb védelmet biztosít.

A szisztémás lupus erythematosus-ban (SLE) kialakuló glomerulonephritis szintén KVB-hez vezethet. A betegek többsége fiatal nő, ezért fontos lenne tudni a terhesség progresszióra kifejtett hatását, azonban a klinikai vizsgálatok ellentmondóak. Ezért lupusos MRL/lpr egerekben vizsgáltuk a terhesség szisztémás autoimmunitásra gyakorolt hatását. A multipara (M) állatokban 3 egymást követő vemhesség után vizsgáltuk a vesefunkciót, szövettant és citokin termelést, összehasonlítva a virgo (V) egerekkel. Az M csoportban drámai halálozást, beszűkült vesefunkciót és hypertóniát találtunk, melyhez glomeruláris IgG és C3 lerakódás valamint emelkedett renális IFN- γ és IL-10 expresszió társult, szemben az alacsonyabb serum IFN- γ szinttel. Eredményeink alapján feltételezzük, hogy a helyi citokin termelésnek fontos szerepe lehet a nephritis súlyosbodásában terhességben, függetlenül a szisztémás citokin választól. Kísérletünk megerősíti azon hipotézist, mely szerint szisztémás lupusban a vesebetegség kialakulását ill. súlyosságát elsősorban lokális faktorok befolyásolják.

9. REFERENCES

1. K/DOQI clinical practice guidelines for chronic kidney disease: evaluation, classification, and stratification. *Am J Kidney Dis* 39:S1-266, 2002
2. ERA-EDTA Registry 2004 Annual Report, Amsterdam, Academic Medical Center, Department of Medical Informatics, 2006, pp 1-121
3. Collins AJ, Kasiske B, Herzog C, Chen SC, Everson S, Constantini E, Grimm R, McBean M, Xue J, Chavers B, Matas A, Manning W, Louis T, Pan W, Liu J, Li S, Roberts T, Dalleska F, Snyder J, Ebben J, Frazier E, Sheets D, Johnson R, Li S, Dunning S, Berrini D, Guo H, Solid C, Arko C, Daniels F, Wang X, Forrest B, Gilbertson D, St Peter W, Frederick P, Eggers P, Agodoa L: Excerpts from the United States Renal Data System 2003 Annual Data Report: atlas of end-stage renal disease in the United States. *Am J Kidney Dis* 42:A5-7, S1-230, 2003
4. Floege J, Alpers CE, Burns MW, Pritzl P, Gordon K, Couser WG, Johnson RJ: Glomerular cells, extracellular matrix accumulation, and the development of glomerulosclerosis in the remnant kidney model. *Lab Invest* 66:485-497, 1992
5. Ebihara I, Suzuki S, Nakamura T, Fukui M, Yaguchi Y, Tomino Y, Koide H: Extracellular matrix component mRNA expression in glomeruli in experimental focal glomerulosclerosis. *J Am Soc Nephrol* 3:1387-1397, 1993
6. Brenner BM, Meyer TW, Hostetter TH: Dietary protein intake and the progressive nature of kidney disease: the role of hemodynamically mediated glomerular injury in the pathogenesis of progressive glomerular sclerosis in aging, renal ablation, and intrinsic renal disease. *N Engl J Med* 307:652-659, 1982
7. Anderson S, Meyer TW, Rennke HG, Brenner BM: Control of glomerular hypertension limits glomerular injury in rats with reduced renal mass. *J Clin Invest* 76:612-619, 1985
8. Fries JW, Sandstrom DJ, Meyer TW, Rennke HG: Glomerular hypertrophy and epithelial cell injury modulate progressive glomerulosclerosis in the rat. *Lab Invest* 60:205-218, 1989

9. Nagata M, Kriz W: Glomerular damage after uninephrectomy in young rats. II. Mechanical stress on podocytes as a pathway to sclerosis. *Kidney Int* 42:148-160, 1992
10. Remuzzi G, Bertani T: Is glomerulosclerosis a consequence of altered glomerular permeability to macromolecules? *Kidney Int* 38:384-394, 1990
11. Cybulsky AV: Growth factor pathways in proliferative glomerulonephritis. *Curr Opin Nephrol Hypertens* 9:217-223, 2000
12. El-Nahas AM: Plasticity of kidney cells: role in kidney remodeling and scarring. *Kidney Int* 64:1553-1563, 2003
13. Pavenstadt H, Kriz W, Kretzler M: Cell biology of the glomerular podocyte. *Physiol Rev* 83:253-307, 2003
14. Kriz W, Gretz N, Lemley KV: Progression of glomerular diseases: is the podocyte the culprit? *Kidney Int* 54:687-697, 1998
15. Durvasula RV, Petermann AT, Hiromura K, Blonski M, Pippin J, Mundel P, Pichler R, Griffin S, Couser WG, Shankland SJ: Activation of a local tissue angiotensin system in podocytes by mechanical strain. *Kidney Int* 65:30-39, 2004
16. Abbate M, Zoja C, Morigi M, Rottoli D, Angioletti S, Tomasoni S, Zanchi C, Longaretti L, Donadelli R, Remuzzi G: Transforming growth factor-beta1 is up-regulated by podocytes in response to excess intraglomerular passage of proteins: a central pathway in progressive glomerulosclerosis. *Am J Pathol* 161:2179-2193, 2002
17. Olson JL, Hostetter TH, Rennke HG, Brenner BM, Venkatachalam MA: Altered glomerular permselectivity and progressive sclerosis following extreme ablation of renal mass. *Kidney Int* 22:112-126, 1982
18. Shimojo H: Adaptation and distortion of podocytes in rat remnant kidney. *Pathol Int* 48:368-383, 1998
19. Hostetter TH, Meyer TW, Rennke HG, Brenner BM: Chronic effects of dietary protein in the rat with intact and reduced renal mass. *Kidney Int* 30:509-517, 1986
20. Riser BL, Ladson-Wofford S, Sharba A, Cortes P, Drake K, Guerin CJ, Yee J, Choi ME, Segarini PR, Narins RG: TGF-beta receptor expression and binding in

- rat mesangial cells: modulation by glucose and cyclic mechanical strain. *Kidney Int* 56:428-439, 1999
21. Ketteler M, Noble NA, Border WA: Transforming growth factor-beta and angiotensin II: the missing link from glomerular hyperfiltration to glomerulosclerosis? *Annu Rev Physiol* 57:279-295, 1995
 22. Wolf G: Renal injury due to renin-angiotensin-aldosterone system activation of the transforming growth factor-beta pathway. *Kidney Int* 70:1914-1919, 2006
 23. Vaziri ND, Dicus M, Ho ND, Boroujerdi-Rad L, Sindhu RK: Oxidative stress and dysregulation of superoxide dismutase and NADPH oxidase in renal insufficiency. *Kidney Int* 63:179-185, 2003
 24. Kumar U, Chen J, Sapoznikhov V, Canteros G, White BH, Sidhu A: Overexpression of inducible nitric oxide synthase in the kidney of the spontaneously hypertensive rat. *Clin Exp Hypertens* 27:17-31, 2005
 25. Satoh M, Fujimoto S, Haruna Y, Arakawa S, Horike H, Komai N, Sasaki T, Tsujioka K, Makino H, Kashihara N: NAD(P)H oxidase and uncoupled nitric oxide synthase are major sources of glomerular superoxide in rats with experimental diabetic nephropathy. *Am J Physiol Renal Physiol* 288:F1144-1152, 2005
 26. Rodriguez-Iturbe B, Vaziri ND, Herrera-Acosta J, Johnson RJ: Oxidative stress, renal infiltration of immune cells, and salt-sensitive hypertension: all for one and one for all. *Am J Physiol Renal Physiol* 286:F606-616, 2004
 27. Vaziri ND, Ni Z, Oveisi F, Liang K, Pandian R: Enhanced nitric oxide inactivation and protein nitration by reactive oxygen species in renal insufficiency. *Hypertension* 39:135-141, 2002
 28. MacAllister RJ, Whitley GS, Vallance P: Effects of guanidino and uremic compounds on nitric oxide pathways. *Kidney Int* 45:737-742, 1994
 29. Vallance P, Leone A, Calver A, Collier J, Moncada S: Accumulation of an endogenous inhibitor of nitric oxide synthesis in chronic renal failure. *Lancet* 339:572-575, 1992
 30. Aiello S, Noris M, Todeschini M, Zappella S, Foglieni C, Benigni A, Corna D, Zoja C, Cavallotti D, Remuzzi G: Renal and systemic nitric oxide synthesis in rats with renal mass reduction. *Kidney Int* 52:171-181, 1997

31. Remuzzi G, Bertani T: Pathophysiology of progressive nephropathies. *N Engl J Med* 339:1448-1456, 1998
32. Rennke HG, Klein PS: Pathogenesis and significance of nonprimary focal and segmental glomerulosclerosis. *Am J Kidney Dis* 13:443-456, 1989
33. Peach MJ: Renin-angiotensin system: biochemistry and mechanisms of action. *Physiol Rev* 57:313-370, 1977
34. Soubrier F, Wei L, Hubert C, Clauser E, Alhenc-Gelas F, Corvol P: Molecular biology of the angiotensin I converting enzyme: II. Structure-function. Gene polymorphism and clinical implications. *J Hypertens* 11:599-604, 1993
35. Blantz RC, Konnen KS, Tucker BJ: Angiotensin II effects upon the glomerular microcirculation and ultrafiltration coefficient of the rat. *J Clin Invest* 57:419-434, 1976
36. Inagami T: Molecular biology and signaling of angiotensin receptors: an overview. *J Am Soc Nephrol* 10 Suppl 11:S2-7, 1999
37. Wolf G, Butzmann U, Wenzel UO: The renin-angiotensin system and progression of renal disease: from hemodynamics to cell biology. *Nephron Physiol* 93:P3-13, 2003
38. Bonnet F, Cao Z, Cooper ME: Apoptosis and angiotensin II: yet another renal regulatory system? *Exp Nephrol* 9:295-300, 2001
39. Volpe M, Savoia C, De Paolis P, Ostrowska B, Tarasi D, Rubattu S: The renin-angiotensin system as a risk factor and therapeutic target for cardiovascular and renal disease. *J Am Soc Nephrol* 13 Suppl 3:S173-178, 2002
40. Nishiyama A, Seth DM, Navar LG: Renal interstitial fluid concentrations of angiotensins I and II in anesthetized rats. *Hypertension* 39:129-134, 2002
41. Liebau MC, Lang D, Bohm J, Endlich N, Bek MJ, Witherden I, Mathieson PW, Saleem MA, Pavenstadt H, Fischer KG: Functional expression of the renin-angiotensin system in human podocytes. *Am J Physiol Renal Physiol* 290:F710-719, 2006
42. Mahmood J, Khan F, Okada S, Kumagai N, Morioka T, Oite T: Local delivery of angiotensin receptor blocker into the kidney ameliorates progression of experimental glomerulonephritis. *Kidney Int* 70:1591-1598, 2006

43. Shirazi M, Noorafshan A, Bahri MA, Tanideh N: Captopril reduces interstitial renal fibrosis and preserves more normal renal tubules in neonatal dogs with partial urethral obstruction: a preliminary study. *Urol Int* 78:173-177, 2007
44. Ding G, Reddy K, Kapasi AA, Franki N, Gibbons N, Kasinath BS, Singhal PC: Angiotensin II induces apoptosis in rat glomerular epithelial cells. *Am J Physiol Renal Physiol* 283:F173-180, 2002
45. Kriz W: Podocytes as a target for treatment with ACE inhibitors and/or angiotensin-receptor blockers. *Kidney Int* 65:333-334, 2004
46. Smeets B, Steenbergen ML, Dijkman HB, Verrijp KN, te Loeke NA, Aten J, Steenbergen EJ, Wetzels JF: Angiotensin converting enzyme inhibition prevents development of collapsing focal segmental glomerulosclerosis in Thy-1.1 transgenic mice. *Nephrol Dial Transplant* 21:3087-3097, 2006
47. Kelly JG, O'Malley K: Clinical pharmacokinetics of the newer ACE inhibitors. A review. *Clin Pharmacokinet* 19:177-196, 1990
48. Lewis EJ, Hunsicker LG, Bain RP, Rohde RD: The effect of angiotensin-converting-enzyme inhibition on diabetic nephropathy. The Collaborative Study Group. *N Engl J Med* 329:1456-1462, 1993
49. Lewis EJ, Hunsicker LG, Clarke WR, Berl T, Pohl MA, Lewis JB, Ritz E, Atkins RC, Rohde R, Raz I: Renoprotective effect of the angiotensin-receptor antagonist irbesartan in patients with nephropathy due to type 2 diabetes. *N Engl J Med* 345:851-860, 2001
50. Brenner BM, Cooper ME, de Zeeuw D, Keane WF, Mitch WE, Parving HH, Remuzzi G, Snapinn SM, Zhang Z, Shahinfar S: Effects of losartan on renal and cardiovascular outcomes in patients with type 2 diabetes and nephropathy. *N Engl J Med* 345:861-869, 2001
51. Copelovitch L, Guttenberg M, Pollak MR, Kaplan BS: Renin-angiotensin axis blockade reduces proteinuria in presymptomatic patients with familial FSGS. *Pediatr Nephrol*, 2007
52. Kahvecioglu S, Akdag I, Gullulu M, Arabul M, Ersoy A, Dilek K, Yavuz M, Yurtkuran M: Comparison of higher dose of losartan treatment with losartan plus carvedilol and losartan plus ramipril in patients with glomerulonephritis and proteinuria. *Ren Fail* 29:169-175, 2007

53. Fabris B, Candido R, Carraro M, Fior F, Artero M, Zennaro C, Cattin MR, Fiorotto A, Bortoletto M, Millevoi C, Bardelli M, Faccini L, Carretta R: Modulation of incipient glomerular lesions in experimental diabetic nephropathy by hypotensive and subhypotensive dosages of an ACE inhibitor. *Diabetes* 50:2619-2624, 2001
54. Ruggenenti P, Perna A, Gherardi G, Garini G, Zoccali C, Salvadori M, Scolari F, Schena FP, Remuzzi G: Renoprotective properties of ACE-inhibition in non-diabetic nephropathies with non-nephrotic proteinuria. *Lancet* 354:359-364, 1999
55. Adamczak M, Gross ML, Krtil J, Koch A, Tyralla K, Amann K, Ritz E: Reversal of glomerulosclerosis after high-dose enalapril treatment in subtotally nephrectomized rats. *J Am Soc Nephrol* 14:2833-2842, 2003
56. Bernard C: *Lecons sur les proprietes physiologiques et les alterations pathologiques des liquides de l'organisme*. Paris, Bailliere et Fils, 1859
57. DiBona GF: Neural control of renal function: role of renal alpha adrenoceptors. *J Cardiovasc Pharmacol* 7 Suppl 8:S18-23, 1985
58. Osborn JL, Holdaas H, Thames MD, DiBona GF: Renal adrenoceptor mediation of antinatriuretic and renin secretion responses to low frequency renal nerve stimulation in the dog. *Circ Res* 53:298-305, 1983
59. Hesse IF, Johns EJ: The subtype of alpha-adrenoceptor involved in the neural control of renal tubular sodium reabsorption in the rabbit. *J Physiol* 352:527-538, 1984
60. Pawluczyk IZ, Patel SR, Harris KP: The role of the alpha-1 adrenoceptor in modulating human mesangial cell matrix production. *Nephrol Dial Transplant* 21:2417-2424, 2006
61. Recordati GM, Moss NG, Waselkov L: Renal chemoreceptors in the rat. *Circ Res* 43:534-543, 1978
62. Stella A, Golin R, Zanchetti A: Effects of reversible renal denervation on haemodynamic and excretory functions of the ipsilateral and contralateral kidney in the cat. *J Hypertens* 4:181-188, 1986
63. Campese VM: Is hypertension in chronic renal failure neurogenic in nature? *Nephrol Dial Transplant* 9:741-742, 1994

64. Converse RL, Jr., Jacobsen TN, Toto RD, Jost CM, Cosentino F, Fouad-Tarazi F, Victor RG: Sympathetic overactivity in patients with chronic renal failure. *N Engl J Med* 327:1912-1918, 1992
65. Campese VM, Kogosov E: Renal afferent denervation prevents hypertension in rats with chronic renal failure. *Hypertension* 25:878-882, 1995
66. Ye S, Zhong H, Yanamadala V, Campese VM: Renal injury caused by intrarenal injection of phenol increases afferent and efferent renal sympathetic nerve activity. *Am J Hypertens* 15:717-724, 2002
67. Amann K, Rump LC, Simonaviciene A, Oberhauser V, Wessels S, Orth SR, Gross ML, Koch A, Bielenberg GW, Van Kats JP, Ehmke H, Mall G, Ritz E: Effects of low dose sympathetic inhibition on glomerulosclerosis and albuminuria in subtotaly nephrectomized rats. *J Am Soc Nephrol* 11:1469-1478, 2000
68. Amann K, Koch A, Hofstetter J, Gross ML, Haas C, Orth SR, Ehmke H, Rump LC, Ritz E: Glomerulosclerosis and progression: effect of subantihypertensive doses of alpha and beta blockers. *Kidney Int* 60:1309-1323, 2001
69. Bakris GL, Hart P, Ritz E: Beta blockers in the management of chronic kidney disease. *Kidney Int* 70:1905-1913, 2006
70. LeNoble LM, Lappe RW, Brody MJ, Struyker Boudier HA, Smits JF: Selective efferent chemical sympathectomy of rat kidneys. *Am J Physiol* 249:R496-501, 1985
71. Szenasi G, Bencsath P, Szalay L, Takacs L: Fasting induces denervation natriuresis in the conscious rat. *Am J Physiol* 249:F753-758, 1985
72. Hendel MD, Collister JP: Renal denervation attenuates long-term hypertensive effects of Angiotensin ii in the rat. *Clin Exp Pharmacol Physiol* 33:1225-1230, 2006
73. Neumann J, Ligtenberg G, Klein IH, Boer P, Oey PL, Koomans HA, Blankestijn PJ: Sympathetic hyperactivity in hypertensive chronic kidney disease patients is reduced during standard treatment. *Hypertension* 49:506-510, 2007
74. Mena-Martin FJ, Martin-Escudero JC, Simal-Blanco F, Carretero-Ares JL, Arzua-Mouronte D, Castrodeza Sanz JJ: Influence of sympathetic activity on

- blood pressure and vascular damage evaluated by means of urinary albumin excretion. *J Clin Hypertens (Greenwich)* 8:619-624, 2006
75. DiBona GF: Neural control of the kidney: past, present, and future. *Hypertension* 41:621-624, 2003
 76. Imig JD, Navar GL, Zou LX, O'Reilly KC, Allen PL, Kaysen JH, Hammond TG, Navar LG: Renal endosomes contain angiotensin peptides, converting enzyme, and AT(1A) receptors. *Am J Physiol* 277:F303-311, 1999
 77. Califf RM, Cohn JN: Cardiac protection: evolving role of angiotensin receptor blockers. *Am Heart J* 139:S15-22, 2000
 78. Juillerat L, Nussberger J, Menard J, Mooser V, Christen Y, Waeber B, Graf P, Brunner HR: Determinants of angiotensin II generation during converting enzyme inhibition. *Hypertension* 16:564-572, 1990
 79. Lee AF, MacFadyen RJ, Struthers AD: Neurohormonal reactivation in heart failure patients on chronic ACE inhibitor therapy: a longitudinal study. *Eur J Heart Fail* 1:401-406, 1999
 80. Petrie MC, Padmanabhan N, McDonald JE, Hillier C, Connell JM, McMurray JJ: Angiotensin converting enzyme (ACE) and non-ACE dependent angiotensin II generation in resistance arteries from patients with heart failure and coronary heart disease. *J Am Coll Cardiol* 37:1056-1061, 2001
 81. Huang XR, Chen WY, Truong LD, Lan HY: Chymase is upregulated in diabetic nephropathy: implications for an alternative pathway of angiotensin II-mediated diabetic renal and vascular disease. *J Am Soc Nephrol* 14:1738-1747, 2003
 82. Onozato ML, Tojo A, Kobayashi N, Goto A, Matsuoka H, Fujita T: Dual blockade of aldosterone and angiotensin II additively suppresses TGF-beta and NADPH oxidase in the hypertensive kidney. *Nephrol Dial Transplant* 22:1314-1322, 2007
 83. Kramer AB, van der Meulen EF, Hamming I, van Goor H, Navis G: Effect of combining ACE inhibition with aldosterone blockade on proteinuria and renal damage in experimental nephrosis. *Kidney Int* 71:417-424, 2007
 84. Klinman DM, Steinberg AD: Inquiry into murine and human lupus. *Immunol Rev* 144:157-193, 1995
 85. Hahn BH: Antibodies to DNA. *N Engl J Med* 338:1359-1368, 1998

86. Petri M: Epidemiology of systemic lupus erythematosus. *Best.Pract.Res Clin Rheumatol* 16:847-858, 2002
87. Uramoto KM, Michet CJ, Jr., Thumboo J, Sunku J, O'Fallon WM, Gabriel SE: Trends in the incidence and mortality of systemic lupus erythematosus, 1950-1992. *Arthritis Rheum* 42:46-50, 1999
88. D'Cruz DP, Khamashta MA, Hughes GR: Systemic lupus erythematosus. *Lancet* 369:587-596, 2007
89. Cooper GS, Dooley MA, Treadwell EL, St Clair EW, Parks CG, Gilkeson GS: Hormonal, environmental, and infectious risk factors for developing systemic lupus erythematosus. *Arthritis Rheum* 41:1714-1724, 1998
90. Lahita RG: The role of sex hormones in systemic lupus erythematosus. *Curr Opin Rheumatol* 11:352-356, 1999
91. Asanuma Y, Oeser A, Shintani AK, Turner E, Olsen N, Fazio S, Linton MF, Raggi P, Stein CM: Premature coronary-artery atherosclerosis in systemic lupus erythematosus. *N Engl J Med* 349:2407-2415, 2003
92. Cameron JS: Lupus nephritis. *J Am Soc Nephrol* 10:413-424, 1999
93. Bono L, Cameron JS, Hicks JA: The very long-term prognosis and complications of lupus nephritis and its treatment. *Qjm* 92:211-218, 1999
94. Cohen PL, Eisenberg RA: Lpr and gld: single gene models of systemic autoimmunity and lymphoproliferative disease. *Annu.Rev.Immunol* 9:243-269, 1991
95. Wu J, Zhou T, He J, Mountz JD: Autoimmune disease in mice due to integration of an endogenous retrovirus in an apoptosis gene. *J Exp.Med* 178:461-468, 1993
96. Theofilopoulos AN, Balderas RS, Shawler DL, Lee S, Dixon FJ: Influence of thymic genotype on the systemic lupus erythematosus-like disease and T cell proliferation of MRL/Mp-lpr/lpr mice. *J Exp.Med* 153:1405-1414, 1981
97. Wofsy D, Murphy ED, Roths JB, Dauphinee MJ, Kipper SB, Talal N: Deficient interleukin 2 activity in MRL/Mp and C57BL/6J mice bearing the lpr gene. *J Exp.Med* 154:1671-1680, 1981
98. Pisetsky DS, McCarty GA, Peters DV: Mechanisms of autoantibody production in autoimmune MRL mice. *J Exp.Med* 152:1302-1310, 1980

99. Pisetsky DS, Caster SA, Roths JB, Murphy ED: Ipr gene control of the anti-DNA antibody response. *J Immunol* 128:2322-2325, 1982
100. Kyttaris VC, Juang YT, Tsokos GC: Immune cells and cytokines in systemic lupus erythematosus: an update. *Curr Opin Rheumatol* 17:518-522, 2005
101. Diaz GC, Jevnikar AM, Brennan DC, Florquin S, Pacheco-Silva A, Kelley VR: Autoreactive kidney-infiltrating T-cell clones in murine lupus nephritis. *Kidney Int* 42:851-859, 1992
102. Hoffman RW, Alspaugh MA, Waggle KS, Durham JB, Walker SE: Sjogren's syndrome in MRL/l and MRL/n mice. *Arthritis Rheum* 27:157-165, 1984
103. Hayashi Y, Haneji N, Hamano H: Pathogenesis of Sjogren's syndrome-like autoimmune lesions in MRL/lpr mice. *Pathol Int* 44:559-568, 1994
104. Humphreys-Beher MG: Animal models for autoimmune disease-associated xerostomia and xerophthalmia. *Adv Dent Res* 10:73-75, 1996
105. Green LM, LaBue M, Lazarus JP, Colburn KK: Characterization of autoimmune thyroiditis in MRL-lpr/lpr mice. *Lupus* 4:187-196, 1995
106. Kanauchi H, Furukawa F, Imamura S: Characterization of cutaneous infiltrates in MRL/lpr mice monitored from onset to the full development of lupus erythematosus-like skin lesions. *J Invest Dermatol* 96:478-483, 1991
107. Shan H, Shlomchik MJ, Marshak-Rothstein A, Pisetsky DS, Litwin S, Weigert MG: The mechanism of autoantibody production in an autoimmune MRL/lpr mouse. *J Immunol* 153:5104-5120, 1994
108. Kolaja GJ, Fast PE: Renal lesions in MRL mice. *Vet. Pathol.* 19:663-668, 1982
109. Bond A, Cooke A, Hay FC: Glycosylation of IgG, immune complexes and IgG subclasses in the MRL-lpr/lpr mouse model of rheumatoid arthritis. *Eur J Immunol* 20:2229-2233, 1990
110. Furukawa F, Tanaka H, Sekita K, Nakamura T, Horiguchi Y, Hamashima Y: Dermatopathological studies on skin lesions of MRL mice. *Arch Dermatol Res* 276:186-194, 1984
111. Agnello V, Koffler D, Kunkel HG: Immune complex systems in the nephritis of systemic lupus erythematosus. *Kidney Int* 3:90-99, 1973

112. Koffler D, Carr R, Agnello V, Thoburn R, Kunkel HG: Antibodies to polynucleotides in human sera: antigenic specificity and relation to disease. *J Exp Med* 134:294-312, 1971
113. Sesin CA, Yin X, Esmon CT, Buyon JP, Clancy RM: Shedding of endothelial protein C receptor contributes to vasculopathy and renal injury in lupus: in vivo and in vitro evidence. *Kidney Int* 68:110-120, 2005
114. Bagavant H, Deshmukh US, Gaskin F, Fu SM: Lupus glomerulonephritis revisited 2004: autoimmunity and end-organ damage. *Scand J Immunol* 60:52-63, 2004
115. Chan OT, Hannum LG, Haberman AM, Madaio MP, Shlomchik MJ: A novel mouse with B cells but lacking serum antibody reveals an antibody-independent role for B cells in murine lupus. *J Exp Med* 189:1639-1648, 1999
116. Bloom RD, O'Connor T, Cizman B, Kalluri R, Naji A, Madaio MP: Intrathymic kidney cells delay the onset of lupus nephritis in MRL-lpr/lpr mice. *Int Immunol* 14:867-871, 2002
117. Kraft SW, Schwartz MM, Korbet SM, Lewis EJ: Glomerular podocytopathy in patients with systemic lupus erythematosus. *J Am Soc Nephrol* 16:175-179, 2005
118. Takahashi S, Fossati L, Iwamoto M, Merino R, Motta R, Kobayakawa T, Izui S: Imbalance towards Th1 predominance is associated with acceleration of lupus-like autoimmune syndrome in MRL mice. *J Clin Invest* 97:1597-1604, 1996
119. Balomenos D, Rumold R, Theofilopoulos AN: Interferon-gamma is required for lupus-like disease and lymphoaccumulation in MRL-lpr mice. *J Clin Invest* 101:364-371, 1998
120. Gomez D, Correa PA, Gomez LM, Cadena J, Molina JF, Anaya JM: Th1/Th2 cytokines in patients with systemic lupus erythematosus: is tumor necrosis factor alpha protective? *Semin Arthritis Rheum* 33:404-413, 2004
121. Chan RW, Lai FM, Li EK, Tam LS, Chow KM, Li PK, Szeto CC: Imbalance of Th1/Th2 transcription factors in patients with lupus nephritis. *Rheumatology (Oxford)* 45:951-957, 2006
122. Rousset F, Garcia E, Defrance T, Peronne C, Vezzio N, Hsu DH, Kastelein R, Moore KW, Banchereau J: Interleukin 10 is a potent growth and differentiation

- factor for activated human B lymphocytes. *Proc Natl Acad Sci U.S.A* 89:1890-1893, 1992
123. Huang XR, Kitching AR, Tipping PG, Holdsworth SR: Interleukin-10 inhibits macrophage-induced glomerular injury. *J Am Soc Nephrol* 11:262-269, 2000
 124. Li L, Elliott JF, Mosmann TR: IL-10 inhibits cytokine production, vascular leakage, and swelling during T helper 1 cell-induced delayed-type hypersensitivity. *J Immunol* 153:3967-3978, 1994
 125. Llorente L, Zou W, Levy Y, Richaud-Patin Y, Wijdenes J, Alcocer-Varela J, Morel-Fourrier B, Brouet JC, Alarcon-Segovia D, Galanaud P: Role of interleukin 10 in the B lymphocyte hyperactivity and autoantibody production of human systemic lupus erythematosus. *J Exp Med* 181:839-844, 1995
 126. Park YB, Lee SK, Kim DS, Lee J, Lee CH, Song CH: Elevated interleukin-10 levels correlated with disease activity in systemic lupus erythematosus. *Clin Exp Rheumatol* 16:283-288, 1998
 127. Yin Z, Bahtiyar G, Zhang N, Liu L, Zhu P, Robert ME, McNiff J, Madaio MP, Craft J: IL-10 regulates murine lupus. *J Immunol* 169:2148-2155, 2002
 128. McCarty DJ, Manzi S, Medsger TA, Jr., Ramsey-Goldman R, LaPorte RE, Kwoh CK: Incidence of systemic lupus erythematosus. Race and gender differences. *Arthritis Rheum* 38:1260-1270, 1995
 129. Ruiz-Irastorza G, Khamashta MA: Evaluation of systemic lupus erythematosus activity during pregnancy. *Lupus* 13:679-682, 2004
 130. Mintz G, Niz J, Gutierrez G, Garcia-Alonso A, Karchmer S: Prospective study of pregnancy in systemic lupus erythematosus. Results of a multidisciplinary approach. *J Rheumatol* 13:732-739, 1986
 131. Moroni G, Quaglini S, Banfi G, Caloni M, Finazzi S, Ambroso G, Como G, Ponticelli C: Pregnancy in lupus nephritis. *Am J Kidney Dis* 40:713-720, 2002
 132. Georgiou PE, Politi EN, Katsimbri P, Sakka V, Drosos AA: Outcome of lupus pregnancy: a controlled study. *Rheumatology.(Oxford)* 39:1014-1019, 2000
 133. Doria A, Ghirardello A, Iaccarino L, Zampieri S, Punzi L, Tarricone E, Ruffatti A, Sulli A, Sarzi-Puttini PC, Gambari PF, Cutolo M: Pregnancy, cytokines, and disease activity in systemic lupus erythematosus. *Arthritis Rheum* 51:989-995, 2004

134. Lockshin MD: Pregnancy does not cause systemic lupus erythematosus to worsen *Arthritis Rheum.* 32:665-670, 1989
135. Tandon A, Ibanez D, Gladman DD, Urowitz MB: The effect of pregnancy on lupus nephritis. *Arthritis Rheum* 50:3941-3946, 2004
136. Molad Y, Borkowski T, Monselise A, Ben-Haroush A, Sulkes J, Hod M, Feldberg D, Bar J: Maternal and fetal outcome of lupus pregnancy: a prospective study of 29 pregnancies. *Lupus* 14:145-151, 2005
137. Johnston C, Russell AS: The effect of pregnancy on disease development and mortality in B/W F1 mice. *J Rheumatol* 14:922-923, 1987
138. McMurray RW, Keisler D, Izui S, Walker SE: Effects of parturition, suckling and pseudopregnancy on variables of disease activity in the B/W mouse model of systemic lupus erythematosus. *J Rheumatol* 20:1143-1151, 1993
139. Lin H, Mosmann TR, Guilbert L, Tuntipopipat S, Wegmann TG: Synthesis of T helper 2-type cytokines at the maternal-fetal interface. *J Immunol* 151:4562-4573, 1993
140. Margni RA, Zenclussen AC: During pregnancy, in the context of a Th2-type cytokine profile, serum IL-6 levels might condition the quality of the synthesized antibodies. *Am J Reprod Immunol* 46:181-187, 2001
141. Wegmann TG, Lin H, Guilbert L, Mosmann TR: Bidirectional cytokine interactions in the maternal-fetal relationship: is successful pregnancy a TH2 phenomenon? *Immunol Today* 14:353-356, 1993
142. Athanassakis I, Iconomidou B: Cytokine production in the serum and spleen of mice from day 6 to 14 of gestation: cytokines/placenta/spleen/serum. *Dev.Immunol* 4:247-255, 1996
143. Marzi M, Vigano A, Trabattoni D, Villa ML, Salvaggio A, Clerici E, Clerici M: Characterization of type 1 and type 2 cytokine production profile in physiologic and pathologic human pregnancy. *Clin Exp Immunol* 106:127-133, 1996
144. Stimson WH: Oestrogen and human T lymphocytes: presence of specific receptors in the T-suppressor/cytotoxic subset. *Scand J Immunol* 28:345-350, 1988
145. Whitacre CC, Reingold SC, O'Looney PA: A gender gap in autoimmunity. *Science* 283:1277-1278, 1999

146. Amann K, Nichols C, Tornig J, Schwarz U, Zeier M, Mall G, Ritz E: Effect of ramipril, nifedipine, and moxonidine on glomerular morphology and podocyte structure in experimental renal failure. *Nephrol Dial Transplant* 11:1003-1011, 1996
147. Fitzgibbon WR, Greene EL, Grewal JS, Hutchison FN, Self SE, Latten SY, Ullian ME: Resistance to remnant nephropathy in the Wistar-Furth rat. *J Am Soc Nephrol* 10:814-821, 1999
148. Magnotti RA, Jr., Stephens GW, Rogers RK, Pesce AJ: Microplate measurement of urinary albumin and creatinine. *Clin Chem* 35:1371-1375, 1989
149. Schwarz U, Amann K, Orth SR, Simonaviciene A, Wessels S, Ritz E: Effect of 1,25 (OH)₂ vitamin D₃ on glomerulosclerosis in subtotally nephrectomized rats. *Kidney Int* 53:1696-1705, 1998
150. Bunag RD: Validation in awake rats of a tail-cuff method for measuring systolic pressure. *J Appl Physiol* 34:279-282, 1973
151. el Nahas AM, Zoob SN, Evans DJ, Rees AJ: Chronic renal failure after nephrotoxic nephritis in rats: contributions to progression. *Kidney Int* 32:173-180, 1987
152. Veniant M, Heudes D, Clozel JP, Bruneval P, Menard J: Calcium blockade versus ACE inhibition in clipped and unclipped kidneys of 2K-1C rats. *Kidney Int* 46:421-429, 1994
153. Ratkay LG, Weinberg J, Waterfield JD: The effect of lactation in the postpartum arthritis of MRL-lpr/fasmice. *Rheumatology.(Oxford)* 39:646-651, 2000
154. Girardi G, Berman J, Redecha P, Spruce L, Thurman JM, Kraus D, Hollmann TJ, Casali P, Carroll MC, Wetsel RA, Lambris JD, Holers VM, Salmon JE: Complement C5a receptors and neutrophils mediate fetal injury in the antiphospholipid syndrome. *J Clin Invest* 112:1644-1654, 2003
155. Csiszar A, Nagy G, Gergely P, Pozsonyi T, Pocsik E: Increased interferon-gamma (IFN-gamma), IL-10 and decreased IL-4 mRNA expression in peripheral blood mononuclear cells (PBMC) from patients with systemic lupus erythematosus (SLE). *Clin Exp Immunol* 122:464-470, 2000

156. Hegde UC, Nainan R: T helper-2 type of interleukins with de novo germinal center formation in the spleen during murine pregnancy. *Am J Reprod.Immunol* 40:424-430, 1998
157. Hostetter TH, Olson JL, Rennke HG, Venkatachalam MA, Brenner BM: Hyperfiltration in remnant nephrons: a potentially adverse response to renal ablation. *Am J Physiol* 241:F85-93, 1981
158. Bohle A, Mackensen-Haen S, von Gise H: Significance of tubulointerstitial changes in the renal cortex for the excretory function and concentration ability of the kidney: a morphometric contribution. *Am J Nephrol* 7:421-433, 1987
159. Shea SM, Raskova J, Morrison AB: A stereologic study of glomerular hypertrophy in the subtotal nephrectomized rat. *Am J Pathol* 90:201-210, 1978
160. Fogo A, Yoshida Y, Glick AD, Homma T, Ichikawa I: Serial micropuncture analysis of glomerular function in two rat models of glomerular sclerosis. *J Clin Invest* 82:322-330, 1988
161. Yoshida Y, Fogo A, Ichikawa I: Glomerular hemodynamic changes vs. hypertrophy in experimental glomerular sclerosis. *Kidney Int* 35:654-660, 1989
162. Anderson S, Rennke HG, Brenner BM: Therapeutic advantage of converting enzyme inhibitors in arresting progressive renal disease associated with systemic hypertension in the rat. *J Clin Invest* 77:1993-2000, 1986
163. Amann K, Irzyniec T, Mall G, Ritz E: The effect of enalapril on glomerular growth and glomerular lesions after subtotal nephrectomy in the rat: a stereological analysis. *J Hypertens* 11:969-975, 1993
164. Skov K, Nyengaard JR, Patwardan A, Mulvany MJ: Large juxtamedullary glomeruli and afferent arterioles in healthy primates. *Kidney Int* 55:1462-1469, 1999
165. Culy CR, Jarvis B: Quinapril: a further update of its pharmacology and therapeutic use in cardiovascular disorders. *Drugs* 62:339-385, 2002
166. Kim S, Iwao H: Molecular and cellular mechanisms of angiotensin II-mediated cardiovascular and renal diseases. *Pharmacol Rev* 52:11-34, 2000
167. Orth SR, Amann K, Strojek K, Ritz E: Sympathetic overactivity and arterial hypertension in renal failure. *Nephrol Dial Transplant* 16 Suppl 1:67-69, 2001

168. Lohmeier TE: The sympathetic nervous system and long-term blood pressure regulation. *Am J Hypertens* 14:147S-154S, 2001
169. DiBona GF: The sympathetic nervous system and hypertension: recent developments. *Hypertension* 43:147-150, 2004
170. Neumann J, Ligtenberg G, Oey L, Koomans HA, Blankestijn PJ: Moxonidine normalizes sympathetic hyperactivity in patients with eprosartan-treated chronic renal failure. *J Am Soc Nephrol* 15:2902-2907, 2004
171. Vonend O, Marsalek P, Russ H, Wulkow R, Oberhauser V, Rump LC: Moxonidine treatment of hypertensive patients with advanced renal failure. *J Hypertens* 21:1709-1717, 2003
172. Strojek K, Grzeszczak W, Gorska J, Leschinger MI, Ritz E: Lowering of microalbuminuria in diabetic patients by a sympathicoplegic agent: novel approach to prevent progression of diabetic nephropathy? *J Am Soc Nephrol* 12:602-605, 2001
173. Torry RJ, Connell PM, O'Brien DM, Chilian WM, Tomanek RJ: Sympathectomy stimulates capillary but not precapillary growth in hypertrophic hearts. *Am J Physiol* 260:H1515-1521, 1991
174. Rosenberg ME, Hostetter TH: Comparative effects of antihypertensives on proteinuria: angiotensin-converting enzyme inhibitor versus alpha 1-antagonist. *Am J Kidney Dis* 18:472-482, 1991
175. Boivin V, Jahns R, Gambaryan S, Ness W, Boege F, Lohse MJ: Immunofluorescent imaging of beta 1- and beta 2-adrenergic receptors in rat kidney. *Kidney Int* 59:515-531, 2001
176. Wolf G, Mueller E, Stahl RA, Ziyadeh FN: Angiotensin II-induced hypertrophy of cultured murine proximal tubular cells is mediated by endogenous transforming growth factor-beta. *J Clin Invest* 92:1366-1372, 1993
177. Kagami S, Border WA, Miller DE, Noble NA: Angiotensin II stimulates extracellular matrix protein synthesis through induction of transforming growth factor-beta expression in rat glomerular mesangial cells. *J Clin Invest* 93:2431-2437, 1994
178. Schieppati A, Remuzzi G: Proteinuria and its consequences in renal disease. *Acta Paediatr Suppl* 92:9-13; discussion 15, 2003

179. Gomez-Garre D, Largo R, Tejera N, Fortes J, Manzarbeitia F, Egido J: Activation of NF-kappaB in tubular epithelial cells of rats with intense proteinuria: role of angiotensin II and endothelin-1. *Hypertension* 37:1171-1178, 2001
180. Zeisberg M, Strutz F, Muller GA: Renal fibrosis: an update. *Curr Opin Nephrol Hypertens* 10:315-320, 2001
181. Iwano M, Neilson EG: Mechanisms of tubulointerstitial fibrosis. *Curr Opin Nephrol Hypertens* 13:279-284, 2004
182. Fan JM, Ng YY, Hill PA, Nikolic-Paterson DJ, Mu W, Atkins RC, Lan HY: Transforming growth factor-beta regulates tubular epithelial-myofibroblast transdifferentiation in vitro. *Kidney Int* 56:1455-1467, 1999
183. Sakic B, Gurunlian L, Denburg SD: Reduced aggressiveness and low testosterone levels in autoimmune MRL-lpr males. *Physiol Behav* 63:305-309, 1998
184. Robey IF, Peterson M, Horwitz MS, Kono DH, Stratmann T, Theofilopoulos AN, Sarvetnick N, Teyton L, Feeney AJ: Terminal deoxynucleotidyltransferase deficiency decreases autoimmune disease in diabetes-prone nonobese diabetic mice and lupus-prone MRL-Fas(lpr) mice. *J Immunol* 172:4624-4629, 2004
185. Zenclussen AC, Fest S, Joachim R, Klapp BF, Arck PC: Introducing a mouse model for pre-eclampsia: adoptive transfer of activated Th1 cells leads to pre-eclampsia-like symptoms exclusively in pregnant mice. *Eur J Immunol* 34:377-387, 2004
186. Munoz-Valle JF, Vazquez-Del Mercado M, Garcia-Iglesias T, Orozco-Barocio G, Bernard-Medina G, Martinez-Bonilla G, Bastidas-Ramirez BE, Navarro AD, Bueno M, Martinez-Lopez E, Best-Aguilera CR, Kamachi M, Armendariz-Borunda J: T(H)1/T(H)2 cytokine profile, metalloprotease-9 activity and hormonal status in pregnant rheumatoid arthritis and systemic lupus erythematosus patients. *Clin Exp Immunol* 131:377-384, 2003
187. Akahoshi M, Nakashima H, Tanaka Y, Kohsaka T, Nagano S, Ohgami E, Arinobu Y, Yamaoka K, Niuro H, Shinozaki M, Hirakata H, Horiuchi T, Otsuka T, Niho Y: Th1/Th2 balance of peripheral T helper cells in systemic lupus erythematosus. *Arthritis Rheum* 42:1644-1648, 1999

188. Prud'homme GJ, Kono DH, Theofilopoulos AN: Quantitative polymerase chain reaction analysis reveals marked overexpression of interleukin-1 beta, interleukin-1 and interferon-gamma mRNA in the lymph nodes of lupus-prone mice. *Mol.Immunol* 32:495-503, 1995
189. Murray LJ, Lee R, Martens C: In vivo cytokine gene expression in T cell subsets of the autoimmune MRL/Mp-lpr/lpr mouse. *Eur J Immunol* 20:163-170, 1990
190. Peng SL, Moslehi J, Craft J: Roles of interferon-gamma and interleukin-4 in murine lupus. *J Clin Invest* 99:1936-1946, 1997
191. Trinchieri G, Gerosa F: Immunoregulation by interleukin-12. *J Leukoc.Biol* 59:505-511, 1996
192. Huang FP, Feng GJ, Lindop G, Stott DI, Liew FY: The role of interleukin 12 and nitric oxide in the development of spontaneous autoimmune disease in MRL inverted question markMP-lpr inverted question marklpr mice. *J Exp Med* 183:1447-1459, 1996
193. Schwarting A, Tesch G, Kinoshita K, Maron R, Weiner HL, Kelley VR: IL-12 drives IFN-gamma-dependent autoimmune kidney disease in MRL-Fas(lpr) mice. *J Immunol* 163:6884-6891, 1999
194. Kikawada E, Lenda DM, Kelley VR: IL-12 deficiency in MRL-Fas(lpr) mice delays nephritis and intrarenal IFN-gamma expression, and diminishes systemic pathology. *J Immunol* 170:3915-3925, 2003
195. Jacob CO, van der Meide PH, McDevitt HO: In vivo treatment of (NZB X NZW)F1 lupus-like nephritis with monoclonal antibody to gamma interferon. *J Exp Med* 166:798-803, 1987
196. Calvani N, Richards HB, Tucci M, Pannarale G, Silvestris F: Up-regulation of IL-18 and predominance of a Th1 immune response is a hallmark of lupus nephritis. *Clin Exp Immunol* 138:171-178, 2004
197. Nakajima A, Hirose S, Yagita H, Okumura K: Roles of IL-4 and IL-12 in the development of lupus in NZB/W F1 mice. *J Immunol* 158:1466-1472, 1997
198. Ishida H, Muchamuel T, Sakaguchi S, Andrade S, Menon S, Howard M: Continuous administration of anti-interleukin 10 antibodies delays onset of autoimmunity in NZB/W F1 mice. *J Exp Med* 179:305-310, 1994

199. Enghard P, Langnickel D, Riemekasten G: T cell cytokine imbalance towards production of IFN-gamma and IL-10 in NZB/W F1 lupus-prone mice is associated with autoantibody levels and nephritis. *Scand J Rheumatol* 35:209-216, 2006
200. Chan RW, Lai FM, Li EK, Tam LS, Chow KM, Lai KB, Li PK, Szeto CC: Intra-renal cytokine gene expression in lupus nephritis. *Ann Rheum Dis*, 2007
201. Lit LC, Wong CK, Li EK, Tam LS, Lam CW, Lo YM: Elevated gene expression of Th1/Th2 associated transcription factors is correlated with disease activity in patients with systemic lupus erythematosus. *J Rheumatol* 34:89-96, 2007
202. Schiffer L, Sinha J, Wang X, Huang W, von Gersdorff G, Schiffer M, Madaio MP, Davidson A: Short term administration of costimulatory blockade and cyclophosphamide induces remission of systemic lupus erythematosus nephritis in NZB/W F1 mice by a mechanism downstream of renal immune complex deposition. *J Immunol* 171:489-497, 2003
203. Baylis C, Deng A, Couser WG: Glomerular hemodynamic effects of late pregnancy in rats with experimental membranous glomerulonephropathy. *J Am Soc Nephrol* 6:1197-1201, 1995
204. Deng A, Baylis C: Glomerular hemodynamic responses to pregnancy in rats with severe reduction of renal mass. *Kidney Int* 48:39-44, 1995
205. McMurray RW: Estrogen, prolactin, and autoimmunity: actions and interactions. *Int Immunopharmacol* 1:995-1008, 2001
206. Correale J, Arias M, Gilmore W: Steroid hormone regulation of cytokine secretion by proteolipid protein-specific CD4+ T cell clones isolated from multiple sclerosis patients and normal control subjects. *J Immunol* 161:3365-3374, 1998
207. Carlsten H, Tarkowski A, Holmdahl R, Nilsson LA: Oestrogen is a potent disease accelerator in SLE-prone MRL lpr/lpr mice. *Clin Exp Immunol* 80:467-473, 1990
208. Carlsten H, Nilsson N, Jonsson R, Backman K, Holmdahl R, Tarkowski A: Estrogen accelerates immune complex glomerulonephritis but ameliorates T cell-mediated vasculitis and sialadenitis in autoimmune MRL lpr/lpr mice. *Cell Immunol* 144:190-202, 1992

209. Apelgren LD, Bailey DL, Fouts RL, Short L, Bryan N, Evans GF, Sandusky GE, Zuckerman SH, Glasebrook A, Bumol TF: The effect of a selective estrogen receptor modulator on the progression of spontaneous autoimmune disease in MRL lpr/lpr mice. *Cell Immunol* 173:55-63, 1996
210. Elbourne KB, Keisler D, McMurray RW: Differential effects of estrogen and prolactin on autoimmune disease in the NZB/NZW F1 mouse model of systemic lupus erythematosus. *Lupus* 7:420-427, 1998
211. Verheul HA, Verveld M, Hoefakker S, Schuurs AH: Effects of ethinylestradiol on the course of spontaneous autoimmune disease in NZB/W and NOD mice. *Immunopharmacol Immunotoxicol* 17:163-180, 1995
212. Antus B, Hamar P, Kokeny G, Szollosi Z, Mucsi I, Nemes Z, Rosivall L: Estradiol is nephroprotective in the rat remnant kidney. *Nephrol Dial Transplant* 18:54-61, 2003
213. Folomeev M, Dougados M, Beaune J, Kouyoumdjian JC, Nahoul K, Amor B, Alekberova Z: Plasma sex hormones and aromatase activity in tissues of patients with systemic lupus erythematosus. *Lupus* 1:191-195, 1992
214. Szekeres-Bartho J, Barakonyi A, Par G, Polgar B, Palkovics T, Szereday L: Progesterone as an immunomodulatory molecule. *Int Immunopharmacol* 1:1037-1048, 2001
215. Piccinni MP, Giudizi MG, Biagiotti R, Beloni L, Giannarini L, Sampognaro S, Parronchi P, Manetti R, Annunziato F, Livi C, et al.: Progesterone favors the development of human T helper cells producing Th2-type cytokines and promotes both IL-4 production and membrane CD30 expression in established Th1 cell clones. *J Immunol* 155:128-133, 1995
216. Cavallasca JA, Laborde HA, Ruda-Vega H, Nasswetter GG: Maternal and fetal outcomes of 72 pregnancies in Argentine patients with systemic lupus erythematosus (SLE). *Clin Rheumatol* (Epub May 22), 2007

10. LIST OF PUBLICATIONS

Publications related to present thesis:

- 1) Hamar P*, **Kökény G.***, Liptak P.*, Krtíl J., Adamczak M., Amann K., Ritz E., Gross ML. The combination of ACE inhibition plus sympathetic denervation is superior to ACE inhibitor monotherapy in the rat renal ablation model. *Nephron Exp Nephrol.* 2007; 105: e124-e136. (* equal contribution)
IF(2005): 1.394
- 2) **Kökény G**, Godó M, Nagy E, Kardos M, Kotsch K, Casalis P, Bodor Cs, Rosivall L, Volk HD, Zenclussen AC, Hamar P. Skin disease is prevented but nephritis is accelerated by multiple pregnancies in autoimmune MRL/lpr mice. *Lupus* 2007; 16: 465-477
IF(2005): 2.4
- 3) Antus B, Hamar P, **Kökény G**, Szollosi Z, Mucsi I, Nemes Z, Rosivall L. Estradiol is nephroprotective in the rat remnant kidney. *Nephrol Dial Transplant.* 2003;18(1):54-61.
IF: 2.607

Other publications in peer-reviewed journals:

- 1) Hamar P, Song E, **Kökény G**, Chen A, Ouyang N, Lieberman J. Small interfering RNA targeting Fas protects mice against renal ischemia-reperfusion injury. *Proc Natl Acad Sci USA.* 2004;101(41):14883-8.
IF: 10.5

Publications in hungarian journals:

- 1) Hamar P, Szabó A, Kovács G, **Kökény G**, Heeman UW, Rosivall L: Az interleukin-2 által közvetített mechanizmusok szerepet játszanak a transzplantált patkányvese chronicus kilöködésében. *Hypertonia és Nephrologia*, 1999; 3(2): 93-100.

Abstracts:

- 1) **G Kökény**, Z Nemeth, E Ritz, ML Gross, P Hamar. Podocyte loss is prevented by combined therapy with RAS inhibition and aldosterone antagonism in the rat experimental model of glomerulosclerosis. *Nephrol Dial Transplant* 2007; 22 (S6): 3-463 (FP254)
- 2) D Gero, **G Kökény**, L Rosivall, M Mozes. C57Bl6 genetic background reduced the progression of renal fibrosis in Alb/TGF-beta1 transgenic mice. *Nephrol Dial Transplant* 2007; 22 (S6): 3-463 (FP255)
- 3) **G Kökény**, P Hamar, P Liptak, J Krttil, M Adamczak, K Amann, E Ritz, ML Gross. Podocyte damage is attenuated after sympathetic denervation plus ACE-inhibition in rats with renal mass reduction. *Nephrol Dial Transplant* 2006; 21 (S4): 3-609 (MP256)
- 4) **G Kökény**, P Hamar, M Godo, E Pallinger, L Rosivall: The absence of mature T-cells results in less severe remnant nephropathy in rats. *J Am Soc Nephrol.* 2005 Oct; 16 (TH-PO400)
- 5) **G Kökény**, K Neumann, P Hamar, K Amann, E Ritz, ML Gross: High dietary phosphate accelerates the progression of kidney damage in uninephrectomized ApoE^{-/-} mice. *J Am Soc Nephrol.* 2005 Oct; 16 (SA-PO447)
- 6) **G Kökény**, P Hamar, P Liptak, J Krttil, M Adameczak, K Amann, E Ritz, ML Gross: Sympathetic denervation causes further attenuation of progression in subtotaly nephrectomised animals on ACE inhibitors. *J Am Soc Nephrol.* 2005 Oct; 16 (SA-PO446)
- 7) **G Kökény**, Z Nemeth, E Ritz, ML Gross, P Hamar: Aldosterone inhibition further improves glomerular morphology in subtotaly nephrectomized rats with RAS blockade. *J Am Soc Nephrol.* 2005 Oct; 16 (SA-PO445)
- 8) **G Kökény**, P Hamar, A Sollwedel, P Casalis, A Zambon Bertoja, S Ritschel, M Godó, C Bodor, E Nagy, L Rosivall, HD Volk, AC Zenclussen. Pregnancy worsen kidney function while improving skin pathology in a murine model of systemic lupus erythematosus: role of IL-10 and IFN- γ . *Am J Reprod Immunol* 2005; 53 (6): 288 (ASRI05-27)

- 9) P Hamar, Zs Bagi, **G Kökény**, Á Koller. Arteriolar Dysfunction in Mice with Systemic Autoimmune Disease. *Nephrol Dial Transplant* 2003; 18 (S4): 593-607 (W146)
- 10) P Hamar, A Regos, **G Kökény**, B Antus, L Rosivall: Injury caused by kidney perfusion significantly impairs graft function in rats. *J Am Soc Nephrol* 2001; 12 858: A4492
- 11) Hamar P, Antus B, Regős A, G Csóka, **G Kökény**, G Kovács, L Rosivall: Early kidney function following transplantation in rats. *J Physiol-London* 2000; 526 (Suppl S): 178P

11. ACKNOWLEDGEMENTS

I would like to thank Prof. Laszlo Rosivall and Peter Hamar the continuous support (Institute of Pathophysiology, Semmelweis University, Budapest). I thank the support of Ana Claudia Zenclussen (Reproductive immunology Group, Institute of Medical Immunology, Charite Medical School, Berlin) and Marie-Luise Gross (Institute of Pathology, University of Heidelberg, Germany) for allowing me to work in their laboratories and giving me all the assistance needed.

I especially thank Prof. Eberhard Ritz (Department of Nephrology, University of Heidelberg, Germany) for the thoughtful discussions on the projects and for partly financing my stay in Heidelberg.

The substantial technical assistance of Mária Godó (Department of Pathophysiology) and Magdolna Pekár (Department of Pathology, Semmelweis University, Budapest), and also Heike Ziebart, Monika Weckbach and Zlata Antoni (Institute of Pathology, University of Heidelberg, Germany) are gratefully acknowledged, but especially the invaluable help of Peter Rieger (Institute of Pathology, University of Heidelberg, Germany) for teaching me the secrets of perfusion fixation, tissue processing and electron microscopy.

A special thank go to my parents for the patience and continuous support during the course of my studies.

My work in Berlin and Heidelberg was further supported by the intergovernmental collaboration project between Hungary and Germany by the Hungarian Ministry of Education (Project Nr: 6) and the German Academic Exchange Service (DAAD).